REMOTE SENSING BASED AGRICULTURAL WATER PRODUCTIVITY ASSESSMENT

Analysis of FAO-WaPOR measured L1, L2, & L3 water productivity at Gezira Irrigation Scheme in Sudan.

MD JAMAL FARUQUE

Enschede, The Netherlands, July, 2020

SUPERVISORS:

Dr. B. H. P. Maathuis
Dr. Ir. C.M.M. Mannaerts

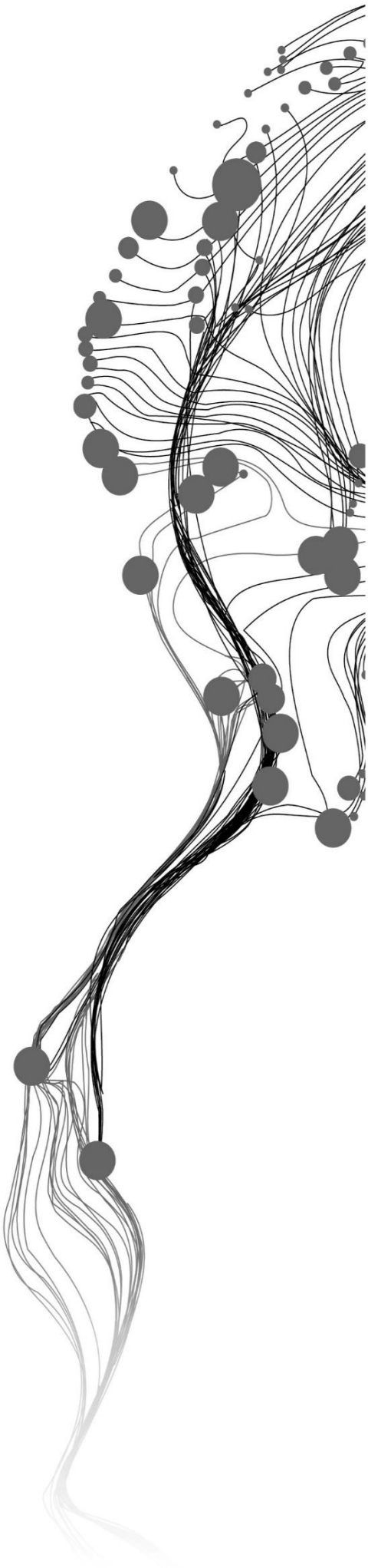

REMOTE SENSING BASED AGRICULTURAL WATER PRODUCTIVITY ASSESSMENT

Analysis of FAO-WaPOR measured L1, L2, & L3 water productivity at Gezira Irrigation Scheme in Sudan.

MD JAMAL FARUQUE
Enschede, The Netherlands, July, 2020

Thesis submitted to the Faculty of Geo-Information Science and Earth Observation of the University of Twente in partial fulfilment of the requirements for the degree of Master of Science in Geo-information Science and Earth Observation.

Specialization: Water Resources and Environmental Management

SUPERVISORS:

Dr. B. H. P. Maathuis
Dr. Ir. C.M.M. Mannaerts

THESIS EXAMINATION BOARD:

Dr. Ir. Christiaan Van der Tol (Chair)
Dr. Michael T Marshall (External Examiner, University of Twente)

DISCLAIMER

This document describes work undertaken as part of a programme of study at the Faculty of Geo-Information Science and Earth Observation of the University of Twente. All views and opinions expressed therein remain the sole responsibility of the author and do not necessarily represent those of the Faculty.

ABSTRACT

Water productivity is a useful indicator to measure how efficiently water is used in crop production. In this study, FAO-WaPOR developed methodology and L1 (250m), L2 (100m), and L3 (30m) remote sensing datasets used to calculate water productivity in the Gezira Irrigation Scheme in Sudan from 2009 to 2020. In the summer season, average evapotranspiration and interception (ETI) of Cotton, Groundnut, and Sorghum were 455mm, 486mm, and 423mm, respectively. In the winter season, average ETI of Onion, Pigeonpea, and Wheat was 436mm, 354mm, and 372mm, respectively. From 2009 to 2014, GBWP and NBWP increased gradually and 2015 to 2018; the productivity was substantially low, whereas, in 2019, the productivity increased significantly. The average GBWP and NBWP of Cotton, Groundnut, and Sorghum was 0.51, 0.56, 0.48 kgm^{-3} and 0.48, 0.54, 0.43 kgm^{-3}, respectively. In the winter season, GBWP and NBWP increased gradually from 2010 and peaked in 2014 then decreased steadily till 2020. The average GBWP and NBWP of Onion, Pigeonpea, and Wheat was 0.60, 0.59, 0.52 kgm^{-3} and 0.51, 0.59, and 0.53 kgm^{-3}, respectively. The overall average water productivity derived from WaPOR datasets results in a lower value than similar types of studies. There might be several reasons or combinations of reasons that are responsible for the low water productivity in the scheme. WaPOR uses the CHIRPS v2 dataset as precipitation, compared with another independent dataset shows that CHIRPS v2 overestimates precipitation. From 2014, there was a transformation of MERRA to the GEOS-5 model for all three levels for the downscaling and retrieving of meteorological inputs, and this might result in inconsistency in the temporal WP assessment (e.g. 2014-15). This comment also holds for other satellite sources input data, e.g. NDVI, and albedo, which underwent sensor changes (e.g. MODIS to PROBA-V) during the 2009-2020 period. In the Gezira scheme, scattered settlements, bare areas as well as fallow lands are observed, which may also influence the aggregated response recorded by the sensor that results in low water productivity. Moreover, long-term political instability was affecting irrigation scheme management, and lack of farmer's trust also might have implications on water productivity. The results show that there is a considerable scope to increase water productivity in the Gezira Irrigation Scheme. The results also point out the need to further analyse and investigate the multiple causes of variations observed in the WP time series in the Gezira scheme. This is required for being able to use WP as a water use efficiency and performance indicator in agricultural water management.

Key Words: Water productivity, FAO, WaPOR, remote sensing, GBWP, NBWP, Sudan, Gezira.

ACKNOWLEDGEMENTS

I am grateful to almighty ALLAH (SWT) for His immense support and guidance in the challenging time. I would like to express my gratitude to the Orange Knowledge Programme (OKP) and my organization, BADC, for granting me the opportunity and fulfilling a dream. I am very much grateful to my supervisors Dr. B. H. P. Maathuis and Dr. Ir. C. M. M. Mannaerts, for their continuous support, courage and guidance. I am also thankful to Dr. Christiaan Van der Tol for his valuable advice and suggestions.

I am thankful to the personnel in Sudan, especially Prof. Hussain and his team's hard work during field campaigns and information about the Gezira Irrigation Scheme.

I would like to extend my gratitude to WREM course director Ir. A. M. Van Lieshout and officers of student affairs of University of Twente, ITC Marie-Chantal and Theresa for encouragement and support in the challenging time. Special thanks to Theresa for enormous support to bring the family in Enschede.

My heartfelt gratitude to my father, sisters and late mother, whose dream helps me to achieve higher education. I am always thankful to my lovely wife, Sayeada Arefin, and three little mom Afra Zabeen, Zinat Zaima, and Afsara Atika for their love and sacrifice. I remember all of my friends and classmates for their unending support.

Faruque
mjfaruque@gmail.com

TABLE OF CONTENTS

1. Introduction 9
   1.1. Background 9
   1.2. Objectives of the study 12
   1.2.1. Objectives 12
   1.2.2. Research questions 12
2. Literature Review 13
   2.1. Agriculture and Water 13
   2.2. Agriculture Water Productivity 14
   2.3. Remote Sensing and Water Productivity 15
   2.4. Remote sensing-based Water Productivity 17
   2.5. Validation of Water Productivity 19
3. Methodology 20
   3.1. Study Area 20
   3.2. Climate 21
   3.3. Irrigation and Cropping System in Gezira Scheme 22
   3.4. Methodological Framework 22
   3.5. Data Description 23
   3.5.1. Field Data Description 24
   3.5.2. CHIRPS v2 and ERA5 Precipitation 25
   3.5.3. NDVI and CHIRPS v2 Precipitation 26
   3.5.4. Evaporation, Transpiration, Interception 26
   3.5.5. Total and Above-ground Biomass Production 28
   3.5.6. Gross Biomass Water Productivity 30
   3.5.7. Net Biomass Water Productivity 31
   3.5.8. Comparison of WaPOR Water Productivity 31
4. Results and Discussions 32
   4.1. General Characteristics of the Gezira Scheme 32
   4.1.1. Land Cover 32
   4.1.2. CHIRPS v2 and ERA5 Precipitation 33
   4.1.3. NDVI and Precipitation 33
   4.2. Evapotranspiration and Interception 34
   4.2.1. Summer Season ETI 34
   4.2.2. Winter Season ETI 37
   4.3. Total Biomass Production 38
   4.3.1. Summer Season TBP 38
   4.3.2. Winter Season TBP 41
   4.4. Gross Biomass Water Productivity 42
   4.4.1. Summer season GBWP_TBP 42
   4.4.2. Winter Season GBWP_TBP 45
   4.5. Net Biomass Water Productivity 46
   4.5.1. Summer Season NBWP_AGBP 46
   4.5.2. Winter Season NBWP_AGBP 49
   4.6. Validation of Evapotranspiration 50
   4.6.1. Summer Season ET 50

4.6.2. Winter Season ET....51
4.6.3. Comparison of Water Productivity....52
4.6.4. Gross Biomass Water Productivity....52
4.6.5. Net Biomass Water Productivity....53
5. Limitations and Opportunities....55
5.1. Limitations....55
5.2. Opportunities....55
6. Conclusions and recommendations....56

LIST OF FIGURES

Figure 3-1: Location of the study area with sample points of summer and winter season. 20
Figure 3-2: Monthly average rainfall, maximum and minimum temperature. 21
Figure 3-3: Monthly average daylight hours in the study area. 21
Figure 3-4: Methodological framework used in the study (Part-I) 23
Figure 3-5: Methodological framework used in the study (Part-II) 23
Figure 3-6: Summer season main crops in the Gezira scheme. 24
Figure 3-7: Winter season main crops in the Gezira scheme. 25
Figure 4-1: Land cover class in the study area. 32
Figure 4-2: Yearly average precipitation from CHIRPS v2 and ERA5 in the study area. 33
Figure 4-3: Monthly average NDVI and precipitation of Cotton, Groundnut, and Sorghum in summer season. 33
Figure 4-4: Standard deviation of ETI calculated from WaPOR L1, L2 and L3 in summer season. 35
Figure 4-5: Summer season yearly average ETI of Cotton, Groundnut, and Sorghum from WaPOR L1, L2 and L3. 35
Figure 4-6: Temporal variation of ETI at 26th dekad of 2009, 2014 and 2019 (left column) in summer season and 4th dekad of 2010, 2015 and 2020 (right column) in winter season. 36
Figure 4-7: Standard deviation of ETI calculated from WaPOR L1, L2 and L3 in winter season. 37
Figure 4-8: Winter season yearly average ETI of Onion, Pigeonpea, and Wheat from WaPOR L1, L2 and L3. 38
Figure 4-9: TBP of Cotton and yearly changes in TBP of WaPOR L1, L2, and L3 in summer season. 39
Figure 4-10: TBP of Groundnut and yearly changes in TBP of WaPOR L1, L2, and L3 in summer season. 39
Figure 4-11: TBP of Sorghum and yearly changes in TBP of WaPOR L1, L2, and L3 in summer season. 39
Figure 4-12: Temporal variations of summer season TBP at 26th dekad of 2009, 2014 and 2019 (left column) and winter season TBP of 4th dekad of 2010, 2015 and 2020 (right column). 40
Figure 4-13: TBP of Onion and yearly changes in TBP of WaPOR L1, L2, and L3 in winter season. 41
Figure 4-14: TBP of Pigeonpea and yearly changes in TBP of WaPOR L1, L2, and L3 in winter season.. 41
Figure 4-15: TBP of Wheat and yearly changes in TBP of WaPOR L1, L2, and L3 in winter season..... 42
Figure 4-16: Dekadal average GBWP_TBP of WaPOR L1, L2, and L3 and monthly precipitation time series for Cotton, Groundnut, and Sorghum. 43
Figure 4-17: Temporal variations GBWP_TBP at 26th dekad of 2009, 2014 & 2019 (left column) in summer season and 4th dekad of 2010, 2015 & 2020 (right column) in winter season. 44
Figure 4-18: WaPOR L1, L2, and L3 dekadal GBWP_TBP time series for Onion, Pigeonpea, and Wheat. 45
Figure 4-19: WaPOR L1, L2, and L3 dekadal NBWP_AGBP and monthly precipitation time series for Cotton, Groundnut, and Sorghum. 47
Figure 4-20: Temporal variations NBWP_AGBP at 26th dekad of 2009, 2014 & 2019 (left column) in summer season and 4th dekad of 2010, 2015 & 2020 (right column) in winter season. 48
Figure 4-21: WaPOR L1, L2, and L3 dekadal NBWP_AGBP time series for Onion, Pigeonpea, and Wheat. 49

Figure 4-22: Summer season dekadal variation (left) and regression (right) of ETI of WaPOR L1, L2, & L3, and DMET of Cotton. 50

Figure 4-23: Summer season dekadal variation (left) and regression (right) of ETI of WaPOR L1, L2, & L3, and DMET of Groundnut. 50

Figure 4-24: Summer season dekadal variation (left) and regression (right) of ETI of WaPOR L1, L2, & L3, and DMET of Sorghum. 51

Figure 4-25: Winter season dekadal variation of ETI of WaPOR L1, L2, & L3, and DMET for Onion (left), and Pigeonpea (right). 51

Figure 4-26: Winter season dekadal variation of ETI of WaPOR L1, L2, & L3, and DMET for Wheat. 52

Figure 4-27: Average dekadal GBWP_TBP from WaPOR L1, L2, and L3 at SOS, MOS, and EOS of summer (Left) and winter (Right) season crops. 53

Figure 4-28: Average dekadal NBWP_AGBP from WaPOR L1, L2, and L3 at SOS, MOS, and EOS of summer (Left) and winter (Right) season crops. 54

LIST OF TABLES

Table 3-1: WaPOR and FRAME data components used in the study. 26
Table 4-1: ETI consumption of Cotton, Groundnut, and Sorghum in the summer season. 34
Table 4-2: Summarize ETI consumption of Onion, Pigeonpea, and Wheat in the winter season. 37

LIST OF ABBREVIATIONS

AWP	Agricultural Water Productivity
AGBP	Above Ground Biomass Production
CHIRPS v2	Climate Hazards Group Infrared Precipitation with Station Data (version 2.0)
DMP	Dry Matter Production
ET	Evapotranspiration
ETI	Evaporation, Transpiration and Interception
ECMWF	European Centre for Medium-Range Weather Forecasts
FRAME	Consortium consisting of eLEAF, VITO, ITC, and the Waterwatch Foundation
FAO	Food and Agriculture Organization
GBWP	Gross Biomass Water Productivity
I	Interception
LAI	Leaf Area Index
NBWP	Net Biomass Water Productivity
NPP	Net Primary Products
R^2	Coefficient of Determination
STD	Standard deviation
TBP	Total Biomass Production
T	Transpiration
WaPOR derived data	FAO portal to monitor Water Productivity through Open access of Remotely sensed

1. INTRODUCTION

1.1. Background

Freshwater, a scarce natural resource, is an essential input in agricultural production systems and plays a vital role in the growth and development of civilization. Global freshwater consumption increased by six times over the last century and continues to grow (Wada et al., 2016). The world population is increasing as well as food demand is also growing, which leads an additional pressure on freshwater resources. World Bank estimated that the world population would reach nine billion in 2050, and agricultural production needs to be increased by seventy percent to feed the expanded population and their associated needs. Moreover, incremental agricultural production is essential to maintain food and nutritional security and income generation of seventy-five percent of the world's poverty-stricken population who lives in rural areas, and they solely rely on agriculture for the livelihoods (Lipper et al., 2014). United Nations (2014) reported that around 1.6 billion people of the world or almost a quarter of the entire population are facing different degrees of water scarcity. Abbott et al. (2019) also reported that eighty percent of the world's population faces water insecurity or severe water scarcity. Alongside global climate change severely impacts on the availability of freshwater resources. Better livelihood requirements of the growing population, changes in consumption patterns of expanding population, the continual industrial revolution, and infrastructure development continuously exaggerating pressure on water resources. Increasing water scarcity competition within agricultural sub-sectors and also with non-agricultural sectors forced to improve agricultural water productivity to ensure adequate food for emerging generations with the same or less water than that is now available for agriculture (Bastiaanssen, Thiruvengadachari, Sakthivadivel, & Molden, 1999).

The agriculture sector accounts for seventy percent of global freshwater withdrawals from both surface and groundwater resources, which is ninety percent more than their consumptive use (FAO, 2012). Appropriate planning and management techniques of irrigated agriculture can be achieved sustainably in two ways-either establishing new irrigation projects or improvement of existing irrigation systems by evaluating their performance (Russo, Alfredo, & Fisher, 2014). Therefore it is essential to adopt a simplified method to the proper evaluation of the agricultural production system globally as well as nationally. Proper identification of the performance-limiting factors of the national and local agricultural production system would be convenient to increase its performance. Performance evaluation of the farming system by using remote sensing applications might be a convenient tool because of its broad spatial coverage and low temporal resolution, which is very handy to evaluate regional, national, scheme, and field levels.

Agricultural Water Productivity (WP) is considered a useful parameter to assess the performance of irrigated and rainfed agriculture. Generally, WP is referred to as biomass production (both above and below ground) by using per unit of water consumption and expressed as kgm^{-3}. Increasing agricultural water productivity means more production can be a practical pathway for poverty reduction, especially in developing countries, where the variability of water productivity within and between fields is very high compared to the developed countries (Zwart & Bastiaanssen, 2004). United Nations also emphasized to increase productivity by setting up a specific target of it's Sustainable Development Goal (SDG) 2.3 "to doubling Agricultural Productivity" and 6.4 –"to substantially increase water-use efficiency" by 2030 (United Nations, 2016).

WP improvement is an often-cited solution for optimal use of limited water resources and also essential to secure the food demand of the growing population. Large scale spatial distribution of water productivity is vital to pin-point low-value areas and to figure out the causes of low values (Zwart, Bastiaanssen, de Fraiture, & Molden, 2010). (Molden et al., 2010) reported that worldwide, there is considerable scope for improvement of water productivity, especially in rainfed areas. Generally, water productivity is assessed at the plot or field level experiment, or calculated from secondary data like crop statistics and water use information (Biradar et al., 2008). Field level experimental approach provides a better understanding of water productivity helps to get the primary knowledge of water productivity. The field-level procedure of water productivity measurement is time-consuming, labor-intensive, and money dependent. The primary constraint of the field-level method, it is applicable only on a small scale, which is not appropriate for policy adaptation.

Recently, several remote sensing methods (SEBAL, METRIC), contributed valuable information on water management in agriculture. They offer the possibility of broader coverage of both spatial and temporal details in mapping water productivity through the use of earth observation techniques with synoptic coverage over large areas at regular time intervals. Time-series analysis of remote sensing data provides an excellent opportunity to understand and mapping of water productivity over large areas (Platonov et al., 2008). Earth observation application in the agricultural water management sector, coarse spatial resolution satellite images (such as AVHRR, MODIS) used as a source of water use and water productivity analysis (Conrad et al., 2007). Spaceborne spatial information of crop production, water consumption, and water productivity variability information will play a useful tool for water managers to assess where scarce resources wasted and where water productivity can be improved (Zwart, 2010).

Food and Agriculture Organization (FAO) has developed an online portal to monitor water productivity through open access of remotely sensed derived data (WaPOR) and provide access to continuous remotely sensed observation data over ten years from 2009 to till today. The spatial datasets include precipitation, biomass production, actual evapotranspiration, land use, land cover classification maps, and others over Africa and the Near East. The First WaPOR database focusing on spatial resolutions of 250m (L1) is covering whole Africa and Near East. The 100m spatial resolution or L2 data set focuses on the national or river basin level, and the final 30m spatial resolution of the L3 data set is focusing on irrigation

schemes and rainfed areas (FAO, 2018a). The aim is to help systematic monitoring of water productivity, identifying water productivity gaps, proposing solutions to reduce these gaps, and contributing to the sustainable development of agricultural production with the help of remote sensing technology. If these datasets are considered acceptable, benefits would be manifold to various stakeholders in their decision making; farmers by providing reliable yields, irrigation authorities by improving access to information, government bodies by promoting and increasing efficient use of water resources.

Optimum water availability is the prerequisite of agriculture to get potential productivity. Climate change continuously altering agricultural water availability, and it has many detrimental effects, which is apparent to all of us. The scenarios are worse in developing with water-scarce countries. Sudan is a water-scarce country, and its food supply largely depends on a few major irrigation schemes. So, the sustainability of these irrigation schemes has great importance for the growth and stability of Sudan. Gezira scheme is the oldest and largest irrigation scheme in Sudan and plays a vital role in the country's economy. Water productivity of the Gezira scheme is comparatively low compared to other similar projects like Rahad and New Halfa (Al Zayed, Elagib, Ribbe, & Heinrich, 2016). Moreover, water productivity within the different sections of the Gezira scheme is not also even. Therefore, it is essential to specify the areas of low water productivity and figure out the causes of low productivity for further improvement.

Water productivity estimation at coarse spatial resolution is helpful for the national and river basin level information but may not suitable for scheme or field level. Coarse-resolution derived water productivity is useful to get an overview of a large area, e.g., for the whole country, which is helpful for policy and planning purposes. Coarse-resolution derived products use average values of spectral responses to represent pixel information, which may not reflect the actual field information. High-resolution satellite-derived products are useful to describe the real field situation and may help to minimize the error in the representation. These products will be beneficial for local farmers, irrigation engineers, and extension workers to get the maximum benefit from their fields.

Additionally, the Gezira irrigation scheme is known as the food silos of Sudan and plays a very significant role in the national economy. Farmers are used to cultivating multiple crops on their farm holdings. So for appropriate representation of water productivity analysis, a high spatial and temporal resolution is required to obtain the actual spectral response of the crops in the field. Continuous monitoring of water productivity with earth observation techniques surely be useful to increase the water productivity of the Gezira irrigation scheme. This study aims to use remote sensing techniques to estimate water productivity at different spatial resolutions (coarse to high) and compares the results and their relations at the Gezira scheme in Sudan.

1.2. Objectives of the study

1.2.1. Objectives

The study aims to use remote sensing applications to assess agricultural water productivity with WaPOR derived different resolution satellite products, and validation of WaPOR measured L3 water productivity at Wad Medani, Gezira scheme, Sudan.

The specific objectives are

1. To assess WaPOR L1, L2, and L3 derived water productivity over the period 2009 to 2020.
2. To validate WaPOR (L3), measured water productivity with field measurements at Wad Medani, Sudan.
3. To compare the WaPOR derived different levels of water productivity at Wad Medani, Sudan.

1.2.2. Research questions

The following research questions have arisen from the objectives

RQ. 1a: What is the WaPOR L1, L2, and L3 water productivity at the Gezira irrigation scheme, Sudan?

RQ1b: How the WaPOR L1, L2, and L3 derived water productivity changes over time in the study area?

RQ. 2: How well WaPOR (L3) is measured water productivity correlated with in-field measurement at Wad Medani, Sudan?

RQ. 3: Which WaPOR level water productivity is suitable to represent water productivity in the study area?

2. LITERATURE REVIEW

2.1. Agriculture and Water

Freshwater, finite resources with experiencing continuous stress due to population growth and concurrently increase in per capita water demand. Though globally, there are adequate water resources to fulfill the present and future requirements, until now, many regions and localities are experiencing various levels of water scarcity (FAO, 2012). Future food security mostly depends on the sustainable use of water resources, and this will be the major challenge of current and future generations. There are increasing population, economic advancement, and climate change, altogether adding additional pressure on the available resources (FAO, 2018a). Agriculture is the most significant land-use sector, which covers a third of the planet's ice-free land area. Agriculture also providing food, fibers, biofuels, and other products to the present 7.7 billion people around the globe with their diverse consumption pattern though yet 80 million people remain undernourished. Forty percent of the world's population depends on agriculture for their livelihood, and this sector contributes about thirty percent of gross domestic production (GDP) in low-income generation countries (Ramankutty et al., 2011). Medium population growth projection estimates that the world population to grow from 7.7 billion at present to nearly 10 billion by 2050 and more than 11 billion by 2100. World average per capita calorie consumption will also increase to 2960 in 2030 and 3070 in 2050 from the 2005-07 value of 2772 Kcal/person/day (Alexandratos & Bruinsma, 2012). Moreover global per capita arable land will be 0.25 ha in 2010 to 0.21 ha in 2030 and 0.19 ha in 2050 respectively. To feed the expanded population the agriculture sector needs to respond in two ways, firstly to increase the cultivable land 1620 million hectares at present to 1690 million hectares in 2050 and secondly increase the productivity from 3.2 tonnes/ha at present to 4.3 tonnes/ha by 2050 (Bruinsma, 2009).

Globally, freshwater consumption increased by a factor of six over the last century and continues to grow gradually about one percent per year to fulfill the additional requirements of increasing population, industrial, economic development, and changing consumption patterns as their buying capacity will increase (FAO, 2011a). FAO (2015) projected that in 2050 agriculture sector will remain to be the largest freshwater user in most of the countries and accounting for 70 percent or more water withdrawals from rivers, lakes, and reservoirs around the world. Farmers need to adopt smart and more efficient technologies to grow the crop with less available water for irrigation due to competition with other unavoidable sectors like industries and cities demand. Globally, irrigation water withdrawal will increase from 2.6 thousand km^3 in 2005-07 to 2.9 thousand km^3 in 2050, and most of the net increase will come from lower-income countries (FAO, 2011b). The net irrigation requirement will increase from 1.27 thousand km^3 to 1.34 thousand km^3 for the same period. Available freshwater resources are sufficient to

fulfill this modest increase, though there will be substantial water scarcity that will persist in the Near East and North Africa and South Asia. Alexandratos & Bruinsma (2012) projected that growing water resources scarcities have manifold detrimental effects on the agricultural sector. Increased competition on water resources might trigger overexploitation, and unjustifiable use of the resources leads to a continual degradation of environmental cohorts and creates a vicious loop where finite resources degradation foster competition on the remaining resources that further leads to degradation of the resource. So a large number of farmers, pastoralists, foresters, and fishers are facing numerous difficulties in improving their living conditions to escape from the poverty circle.

de Fraiture & Wichelns (2010) suggest several options for sustainable crop production pathways to satisfy future food demand while protecting the environment by reducing poverty. They projected four possible scenarios, including a focus on investments in irrigation and rainfed agriculture. Productivity enhancement in rainfed agriculture has considerable potential, but it deserves adequate mechanisms to minimize inherent associated risks—expansion of potential irrigation areas where irrigation infrastructure is underutilized or invested like sub-Saharan Africa. In South Asia, there is a considerable scope to increase irrigation performance and water productivity enhancement by pointing out low score areas. They also projected that in a 'business as usual,' scenario that an additional 80 percent water requirement is needed to meet food demands by 2050. They concluded that if we manage our water resources appropriately and effectively in agriculture, presently available land and water resources can satisfy global food demands during the next 50 years. The scenarios, as mentioned above, accomplished that it is urgently necessary to improve the present productivity level through the judicial use of available resources in agriculture to get the potential benefit from these finite resources.

2.2. Agriculture Water Productivity

Agriculture is the primary user of water resources and draws attention to careful monitoring of water productivity in agriculture, and it is crucial to explore the opportunities to increase water productivity where it is possible. Improvement of water productivity is often cited as the most important pathway to ease with the increased water demand in agriculture (FAO, 2018a). Water productivity is generally defined as crop biomass production per unit water consumption though the definition of water productivity depends on the stakeholder involved in the process of calculation (Molden et al., 2010). Some examples are:

- An agronomist when analyzing irrigation performance at the field level where soil evaporation and transpiration is challenging to differentiate define WP as harvested yield to the evapotranspiration.
- At the farm level, a farmer typically considers WP as harvester yield to the irrigation water supply.
- An irrigation network engineer usually expressed WP as farm yield to the canal water supply.
- In basin level, a policymaker interested in the economic value of water, and usually, WP defines as gain USD per unit water consumed.

The term WP derived from the concept "more crop per drop" to evaluate the water use in agriculture usually defined as value or benefit obtained by the use of a unit amount of water (Kijne, Barker, & Molden, 2003). WP can be increased mainly in three-ways, firstly by increasing crop yield by manipulating other inputs and maintaining constant water-use level. Secondly, maintaining crop yield by reducing water consumption and finally, both increasing crop yield and reducing water consumption by better management of resources (Cai & Rosegrant, 2009). Several factors affected WP, such as crop cultivar type, water availability and weather condition, soil characteristics, and management practices (Ali & Talukder, 2008). Doorebos & Kassam (1979) first compiled various crops WP values around the globe, which were published in FAO drainage paper 33. Steduto, P., Raes, D., Hsiao, T. C., Fereres (2012) also published WP values based on the review of the field experimental measurement result reported in international literature published on FAO drainage paper 66. They also reported that the WP values of most crops increased considerably compared to the values of the 1970s, which were achieved by the development of improved crop varieties that helped to produce higher yields, drought, and pest/disease-resistant crops, improved soil fertility, and a better understanding of the land, and water management practices.

Globally, in the last few decades, agricultural water productivity concepts have been used as an established performance indicator in the agricultural production system to measure the performance of the crop production system. Continuous use, field applicability, and widely accepted performance indicators of the agricultural production system by the scientific community make agricultural productivity a vital indicator in the development agenda of United Nations Sustainable Development Goals (SDGs). United Nations emphasized to increase productivity by setting up a specific target of it's Sustainable Development Goal (SDG) 2.3 "to doubling Agricultural Productivity" and 6.4 –"to substantially increase water-use efficiency" and "Combat desertification, restore degraded land and soil, including land degraded by desertification, drought, and floods, and strive to achieve a land degradation-neutral world" by 2030 (United Nations, 2016).

2.3. Remote Sensing and Water Productivity

Remote sensing applications in agriculture based on electromagnetic radiation interaction with plant or soil materials. In agriculture, remote sensing uses the technique of reflected radiation measurement from the plants and soil surface rather than the transmitted or absorbed radiation. In the early 1970s, Landsat 1 satellite (known initially as Earth Resources Technology Satellite 1) used first multispectral scanner system (MSS) imagery of green, red and two infrared bands with a spatial resolution of 80 m and 18 days temporal resolution to classify Midwestern agricultural landscapes in the USA into maize or soybean field with 83% overall accuracy (Mulla, 2013). Remote sensing offers a wide range of monitoring and measurement approach in the agricultural production system (Blatchford, Mannaerts, Zeng, Nouri, & Karimi, 2019) includes crop yield and biomass estimation (Shanahan et al., 2001; Yang, Everitt, Bradford, & Escobar, 2000), crop nutrient and water stress effect on the crop (Bastiaanssen, Molden, & Makin,

2000; Clay, Kim, Chang, Clay, & Dalsted, 2006; Cohen, Alchanatis, Meron, Saranga, & Tsipris, 2005; Tilling et al., 2007), weed infestations (Lamb & Brown, 2001; Thorp & Tian, 2004), plant diseases and insects management (Seelan, Laguette, Casady, & Seielstad, 2003), and soil properties estimation like soil organic matter, moisture content, and pH (Christy, 2008), or salinity (Corwin & Lesch, 2003). A remote sensing-based approach to systematic monitoring of water productivity is useful to point out spatial water productivity gaps and useful to provide an appropriate measure to reduce these gaps (FAO, 2018b). Better management and potential utilization of scarce water resources spatial information on crop production, water use, and water productivity are crucial for the water managers to identify low productive areas for further improvement of the crop production system (Zwart, 2010).

Continuous improvement of the human capacity to explore the earth from space creates an enormous opportunity for the scientific community. This improvement opens tremendous scope to monitor the global agricultural production system more precisely. Over the period, both the spatial and spectral resolution of satellite imagery improved considerably. At present, both open sources and paid satellite imagery from coarse to high resolutions are available for the user community. Open access remotely sensed multispectral imagery now provides near real-time data with different spatial and temporal resolutions. Open access high, medium, and coarse resolutions images are Sentinel-2 with 10 m resolution within tandem mode having a revisit period of five days, Landsat with 30m resolution, and 16 days revisit period, PROBA-V 100m resolution with daily revisit period and MODIS and Sentinel 3 with 250m resolution with 1-2 days revisit period. High-resolution paid products include GeoEye (1m and <10 days), Pleiades (2m and daily), WorldView (<2m and daily), QuickBird (<3m and <4days), SPOT (6m and daily).

FAO-WaPOR developed an online portal to monitor water productivity through open access of remotely sensed derived data and provide access to continuous remotely sensed observation data, starting from 2009 to today. The spatial datasets include precipitation, biomass production, actual evapotranspiration, land use, land cover classification maps, and others over Africa and the Near East. The first set of WaPOR databases focused on spatial resolutions of 250m (L1) to cover the whole of Africa and the Near East. The second dataset of 100m spatial resolution (L2) focuses on the number of selected countries and several river basins, and the final 30m spatial resolution of (L3) data set is focusing on selected irrigation schemes and rainfed areas. WaPOR used a generic methodology in WP calculation for all three levels considering each pixel as a closed system with adjacent pixels neglecting neighbour pixels influence though, in reality, there is an exchange in energy and matters between pixels. They use two fundamental inputs in the calculation of WP, which is Net Primary Production (NPP) as production and actual Evaporation, Transpiration, and Interception (ETI) as water consumption. The NPP is the conversion of carbon dioxide into biomass through photosynthesis. NPP is derived from Gross Primary Production (GPP) minus autotrophic respiration, losses due to conversion of glucose to higher-level photosynthates (starch, cellulose, fats, and proteins) and respiration. The second one is the ETI, which is the sum of actual soil evaporation (E), canopy transpiration (T), and interception (I). The ETI depends on the climatic factors (radiation, wind speed, and air temperature) and soil conditions (soil moisture content).

WaPOR uses the ETLook model described by Bastiaanssen, Cheema, Immerzeel, & Miltenburg (2012) to calculate E and T. The ETLook model is based on the Penman-Monteith (P-M) equation, adapted with remote sensing input data. Allen, Pereira, Raes, & Smith (2005) described that the Penman-Monteith equation is based on two fundamental approaches one energy balance equation and the aerodynamic equation. The other component interception is the intercepted rainfall by the vegetation leaves, and it depends on vegetation cover, leaf Area Index (LAI), and precipitation.

WaPOR used Moderate-resolution Imaging Spectroradiometer (MODIS) 250m resolution derived optical data for L1, PROBA-V multispectral data from March 2014 and earlier to this MODIS data resampled to 100m used for L2, and Landsat 5, 6, & 7 data used for L3 (30m) in WP calculation. The detailed description of methods (algorithms) used in the derivation of each component is available in the WaPOR database documents (FAO, 2018a; FAO, 2018b; (FAO, 2018c). More information about WaPOR used data products in WP calculation are listed in appendix A&B. The FAO-WaPOR online portal provides free access to various spatial data sets related to land and water use for agricultural production. It allows instant data queries, time series analyses, area statistics, and data download facilities of key variables to measure land and water productivity gaps in the irrigated and rainfed agriculture in Africa and Near East (FAO, 2018c).

2.4. Remote sensing-based Water Productivity

Choudhury & Bhattacharya (2018) used a satellite-based approach to analyse agricultural water productivity in India. They used MODIS GPP, and MODIS ETa derived data in productivity mapping, actual and reference evapotranspiration mapping over India from 2007 to 2012. The result shows that average seasonal agricultural water productivity (AWP) and rainwater productivity (RWP) ranges from 1.10-1.30 kg C m^{-3} and 0.94-1.0 Kg C m^{-3}, respectively. The average AWP over India was 1.41 Kg C m^{-3}. They concluded that there were no significant annual variability values of WP, but the spatial variability was considerable. This spatial variability provides useful information for further improvement to boost crop production.

Patil et al. (2015) assessed agricultural water productivity using remotely sensed products in the desert farming system in Saudi Arabia. They assessed annual crop wheat, barley, and corn and biannual crop alfalfa and Rhodes grass, which were cultivated under a center-pivot irrigation system located in desert areas of the Al-Kharj region. For the evapotranspiration (ET) assessment, they applied the Surface Energy Balance Algorithm for Land (SEBAL) to Advanced Spaceborne Thermal Emission and Reflection Radiometer (ASTER) images to calculate water productivity and irrigation performance. Normalized Difference Vegetation Index (NDVI) used to estimate crop productivity. The observed water productivity was 2.01, 1.07, 0.68, 0.55, and 0.38 kgm^{-3} for Wheat, Rhodes grass, barley, corn, and alfalfa, respectively, with contrast field measurement values of water productivity of 1.63, 0.69, 0.55, 0.51, and 0.43 kgm^{-3} for the same sequence crops.

(Cai & Sharma, 2009) used remote sensing-based applications to assess water productivity of rice and Wheat over large Indo-Gangetic river basins, which cover a large part of Pakistan, India, Nepal, and Bangladesh. MODIS NDVI product was used to compute crop production, and Simplified Surface Energy Balance (SSEB) model was used for actual evapotranspiration estimation. Water productivity was calculated by dividing production with the actual seasonal evapotranspiration. The basin average rice yields for Pakistan, India, Nepal, and Bangladesh were 2.60, 2.53, 3.54, and 2.75 tonnes per hectare, respectively. The average evapotranspiration amount was 416mm, which is 68 percent of potential ET. They found that the average water productivity for rice and Wheat was 0.84 and 1.36 $kgm^{-3,}$ respectively. They suggested that remote sensing-based water productivity assessment over large scale basin (national or river basin) has a significant prospect in development policy and planning sustainably. They also suggested that proper understanding of magnitude and variations of WP results in further improvement, which is useful to ensure future food security.

Platonov et al. (2008) used satellite sensor products with various spatial, spectral, radiometric, and temporal resolutions to derive water productivity maps of Cotton dominated Sry Darya basin in Central Asia. The results showed that water productivity in the basin ranges from 0-0.9 kg/m^{-3} among this 55% area's water productivity is less than 0.30 kgm^{-3}. They suggest that there is an enormous scope to increase water productivity by proper management of land and water resources in low water productivity areas. They also indicate that there is significant scope to increase crop production without further expansion of cropland and irrigated areas to ensure food security. Courault, Seguin, & Olioso (2005) monitored consumptive crop use (evapotranspiration) with remote sensing derived products, which is the crucial element in water productivity and suggests that remote sensing techniques use relatively fewer ground data and provide useful information for further analysis.

Li et al. (2008) used remote sensing technology to estimate water consumption and water productivity of winter wheat of 83 counties in the North China Plain. They computed daily evapotranspiration with NOAA/AVHRR data and SEBAL model and reference ET with the Hargreaves formula. They found minimum and maximum water consumption of winter wheat for the study area 424 and 475 mm, respectively. The highest crop water productivity of the region was 1.67 kgm^{-3}, and the lowest figure was less than 0.5 kgm^{-3}. They suggest that there is a close linear relationship between WP to the crop yield. Generally, WP increases with the increase in crop yield. They also reported that the relationship between WP and ET and found the relationship is a parabola means crop yield increases up to a certain level of ET then decreases with the increase of ET. They concluded that the higher amount of irrigation does not necessarily result in a higher yield. Sun, Liu, Zhang, Shen, & Zhang (2006) also reported similar results that with increasing ET, irrigation requirements also increase as soil evaporation increases. Excessive irrigation may decrease both yields, water-use efficiency. They concluded that to avoid excessive irrigation; a proper irrigation schedule might be helpful to produce a higher yield and better economic benefit.

2.5. Validation of Water Productivity

Validation of remote sensing products is the process that independently assesses the accuracy and precision of the remote sensing products with ground observation data (Ge et al., 2013). Usually, validation of remote sensing is carried out in two ways-with the ground measurements or simulation with the model-generated data. Remote sensing application uses different sensors to acquire ground information, which has a different range that needs further interpretation and analysis for further use depending on the purpose and area of application. Validation is essential to ensure the quality of remote sensing derived products before further use in the decision-making process. Estimation of WP from remote sensing derived products depends on the measurement of evapotranspiration and biomass precisely. Evapotranspiration is the critical component of WP measurement that has to be accurately measured. The most common approach for validation of remote sensing derived evapotranspiration is by direct measurements from lysimeters, Large Aperture Scintillometer (LAS), tower-based energy flux measurement system using Bowen ratio methods and eddy covariance (Xiong et al., 2008). A reliable validation result surely has a valuable contribution to boost confidence in remote sensing derived products that help in the decision making process more positively. Patil et al. (2015), Sun et al. (2012), Allen, Pereira, Howell, & Jensen (2011), Teixeira, Bastiaanssen, Ahmad, & Bos (2009), and Tasumi, Trezza, Allen, & Wright (2005) used ground measurement approach for the validation of evapotranspiration derived from remotely sensed products with various resolutions.

In the pre-COVID stage, the study was designed to validate the water productivity in two ways-crop water consumption (ETI) and biomass production by in-situ measurements. Two field campaigns have been conducted, and crop information such as crop variety, yield, cropping period, plot size of both summer and winter season were collected. On-going Sudan political instability, along with global COVID-19 pandemic outbreak in-situ climate data from nearby weather stations, could not be provided. In this altered situation, another satellite-derived independent evapotranspiration dataset from LSA SAF MSG DMET is used in this study to validate WaPOR data derived ETI for L1, L2, and L3. Blatchford et al. (2020) reported that there are two remote sensing-based open-access evapotranspiration datasets available at the global and continental scale: MOD16 with 250m resolution and 8-day revisit time described by (Mu, Zhao, & Running, 2011) and LSA SAF MSG ET generated daily basis with 3km resolution (Ghilain, Arboleda, & Gellens-Meulenberghs, 2011). MODIS generated 250m resolution data is used in WaPOR ET measurement. LSA SAF MSG generated 3km resolution DMET used in this study to validate WaPOR measured ETI for L1, L2 and L3. LSA-SAF derived evapotranspiration is appropriate for large scale climate assessment; it also provides reasonable estimation for irrigation requirements and water management (Trigo & DeBruin, 2016).

3. METHODOLOGY

3.1. Study Area

The study area, the Gezira Irrigation Scheme, is one of the largest surface water irrigation schemes in Africa and as well as in the world. The total area under the Gezira Irrigation Scheme is 880,000 ha. Gezira scheme accounts for half of the total irrigation area in Sudan. The Gezira scheme played a pioneering role in the history of irrigation scheme development in the region as it became a model of many similar schemes in sub-Saharan Africa (Elshaikh, Yang, Jiao, & Elbashier, 2018). The scheme is located in the triangular tract enclosed with the two branches of the Nile river-The White and the Blue Nile river. The geographical extent of the Gezira irrigation scheme is 13˚52' to 15˚32' North latitude and 32 ˚44' to 33 ˚65' East longitude, respectively.

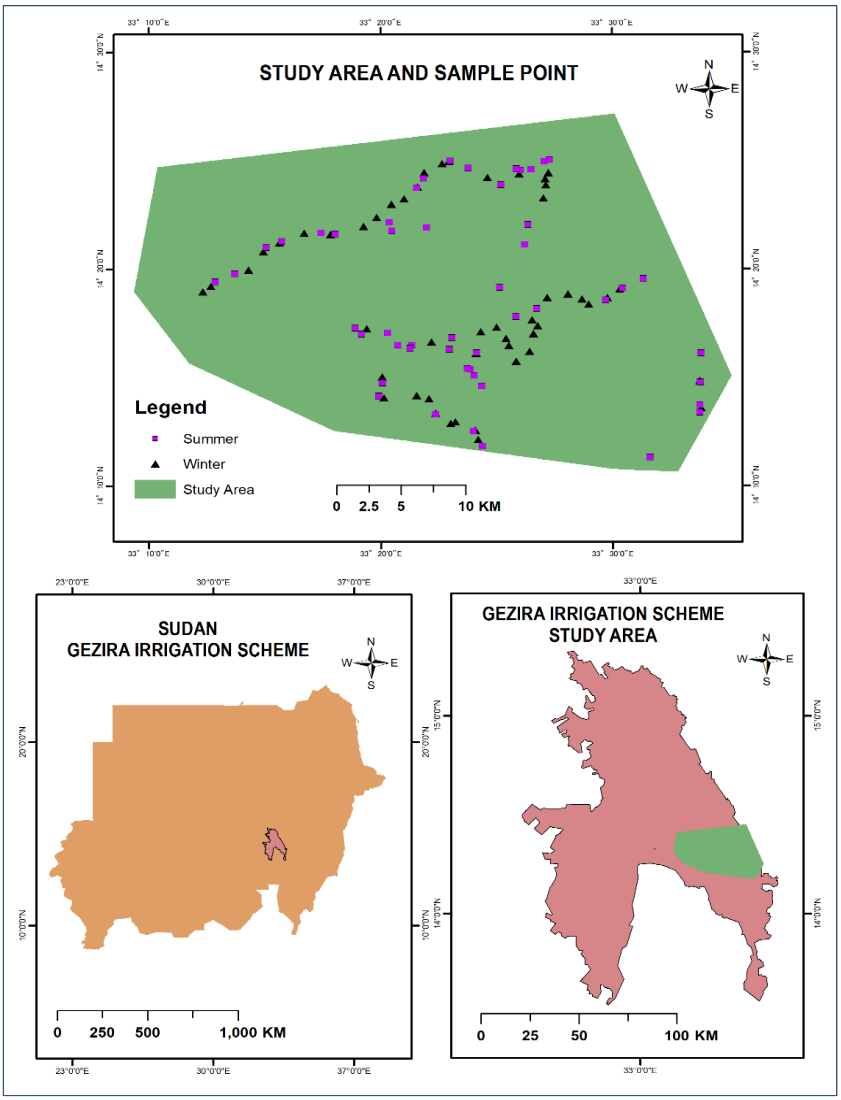

Figure 3-1: Location of the study area with sample points of summer and winter season.

3.2. Climate

The climate in the Gezira scheme is characterized as semi-arid. Figure 3.2 shows the long-term monthly average rainfall, maximum and minimum temperature in the study area. The average long-term rainfall is 354 mm at Wad Medani. Usually, rainfall starts in April, peaks in August and ended in October (Elshaikh et al., 2018). Gezira scheme receives two-third of the total rainfall in July and August. There is no rainfall from November to March. Figure 3.2 also shows that May is the hottest month and January and December the coldest months in the study area (www.weather-atlas.com).

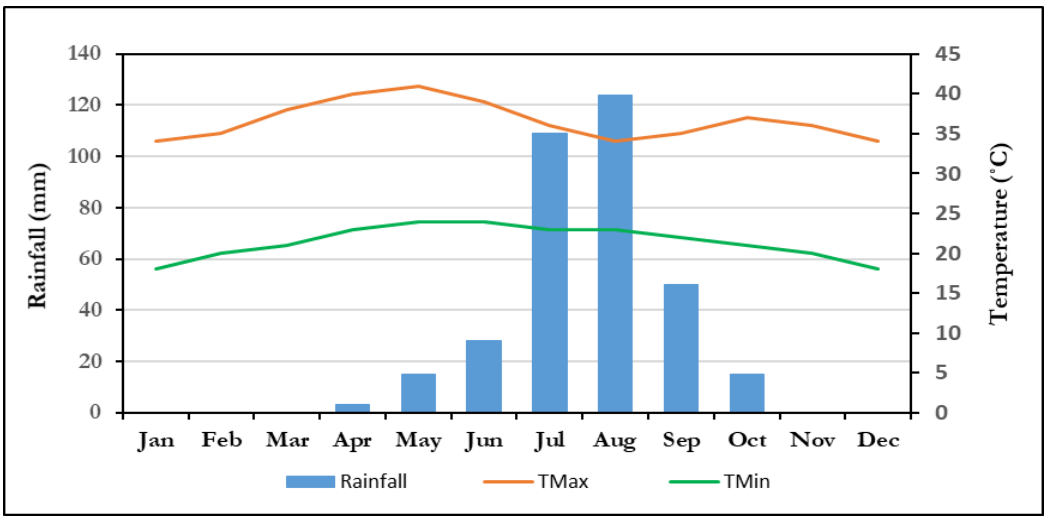

Figure 3-2: Monthly average rainfall, maximum and minimum temperature.

Figure 3.3 shows the monthly average daylight hours in the study area. Jun receives the most prolonged average daylight, 13 hours, and December observes the lowest average daylight 11.6 hours (www.weather-atlas.com.).

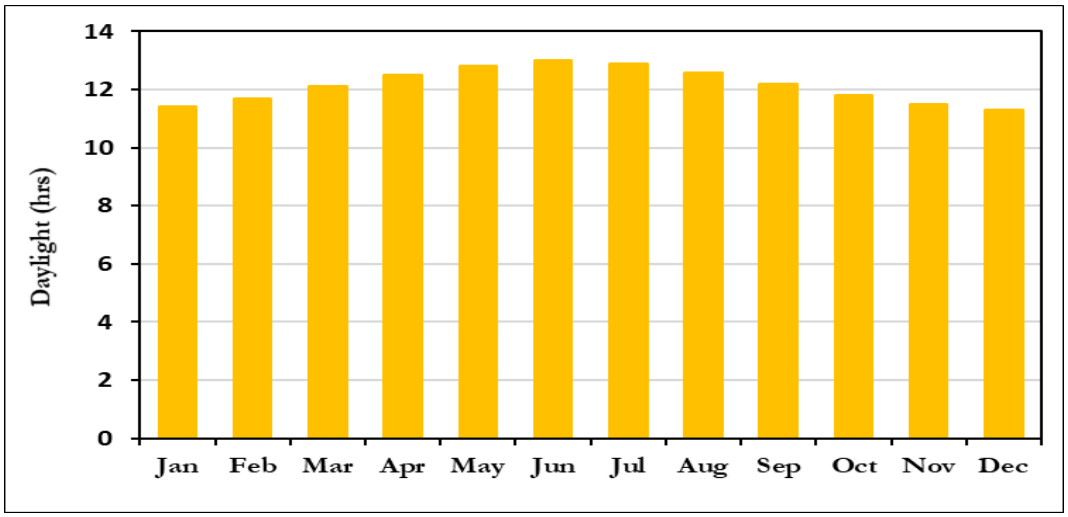

Figure 3-3: Monthly average daylight hours in the study area.

3.3. Irrigation and Cropping System in Gezira Scheme

The irrigation network of the entire Gezira irrigation scheme feeds through two main canals from the Sennar dam named Gezira and Managil extension. The gentle slope from south to north made it suitable for gravity irrigation. The irrigation water source in the Gezira scheme is the Nile river. The distribution of irrigation water is well planned in the scheme after diverting from Senner Dam to the two main canals then distributed secondary, tertiary, and minor channels to the entire irrigation scheme. The carrying capacity of the Gezira and Managil canal 168 m3/sec and 186 m3/sec, respectively. The irrigation plot size in the tail end is about 36 ha, and each farmer has an average of 8.4 ha, which is divided into four plots (Elshaikh et al., 2018). The cultivation season in the Gezira scheme starts in July and ends at the end of March. The period of April to May generally is allocated for maintenance of the hydraulic structures and clearance of the distribution canals. There are mainly two growing seasons- summer (July to November) and winter season (December to March). The summer season's main crops are Cotton, Sorghum, Groundnuts, and in the winter season, the main crops are Wheat, Pigeonpea, and Onion. Also, other crops are grown in the scheme like Chickpea, Okra, White bean, Soybean, and various vegetables. Gezira irrigation scheme supports not only domestic food consumption but also a vital source of foreign currency in Sudan by exporting Cotton (Bushara & Ahmed, 2016).

3.4. Methodological Framework

The methodological framework used in this study to achieve the stated objectives are summarized in Figures 3.1 and 3.2. The first objective of this study is designed to use FAO-WaPOR open-access database products to assess the WP with L1 (250m resolution), L2 (100m resolution), and L3 (30m resolution) products and develop a time-series for the study area at Gezira irrigation scheme in Sudan. There are two options to retrieve the required datasets, one is the FAO-WaPOR database, and the second one is the ITC data repository. The second data source, ITC data repository data products are used in this study for the analysis purpose for the period 2009 to 2019. For the data of the running year, 2020 data is retrieved from the FAO-WaPOR website. Evaporation (E), transpiration (T), interception (I), and net primary productions (NPP) data sets are retrieved from the ITC data archive and extracted for the Sudan national level, Gezira irrigation scheme level and Wad Medani (validation area) for the 250m, 100m, and 30m resolutions, respectively.

The second objective of this study is the validation of WaPOR measured L3 (30m resolution) WP with in-situ measured WP at Wad Medani, Gezira Irrigation scheme. FAO select Wad Medina as one of their validation sites for the L3 measured water productivity. Two crop season, the summer season of 2019, and the winter season of 2019-20 data are used for the validation purpose. Figure 3.5 shows the methodological approach used to achieve the objective. L3 dataset of evaporation (E), transpiration (T), interception (I), and net primary productions (NPP) are retrieved from the ITC repository for the Wad Medina validation area. In-situ measurements of crop data are collected by conducting a field campaign in

both summer and winter seasons. Detailed field measurement data for the two seasons are presented in Appendices C&D.

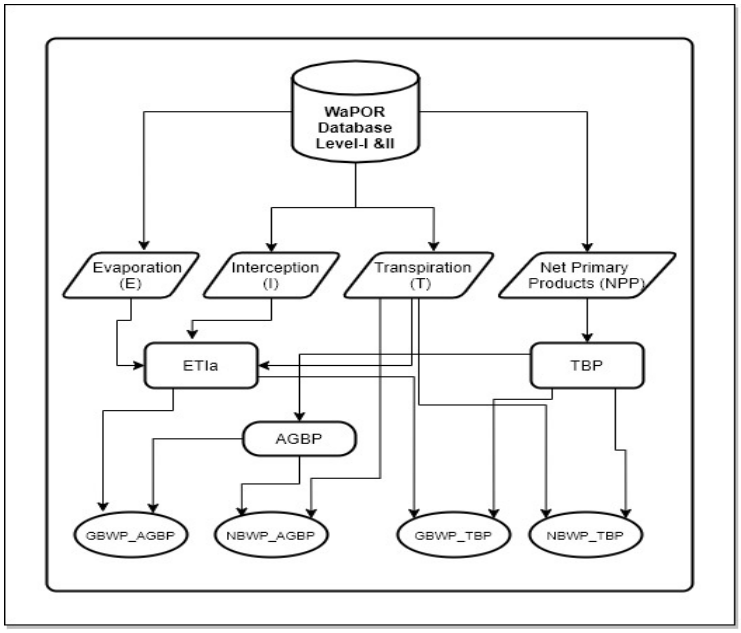

Figure 3-4: Methodological framework used in the study (Part-I)

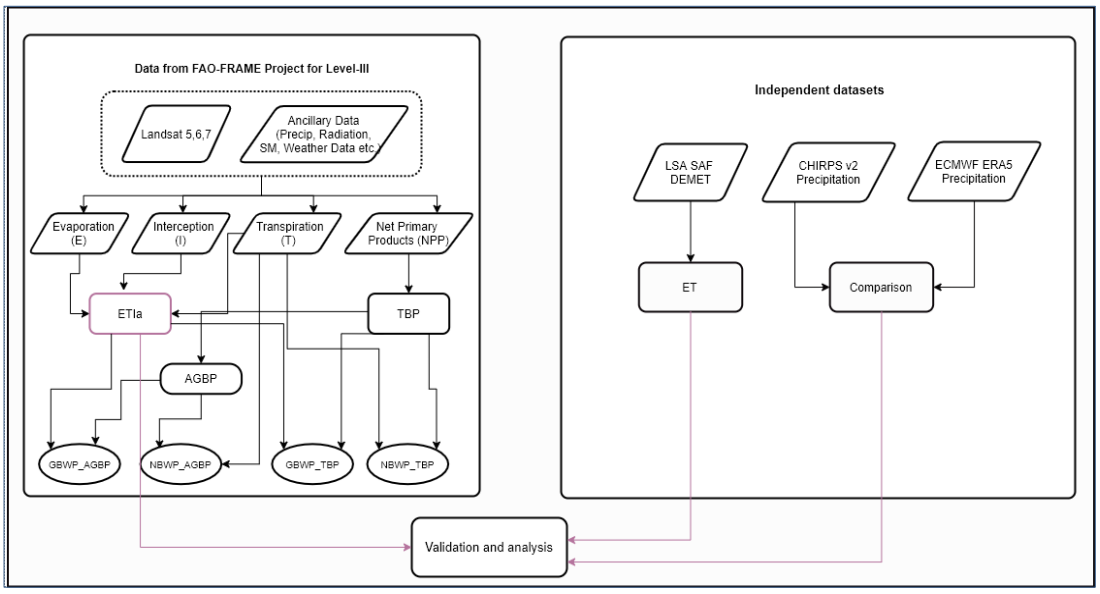

Figure 3-5: Methodological framework used in the study (Part-II)

3.5. Data Description

Several data components, such as the WaPOR database, FRAME project, DMET, ERA5, and field campaign information, are used in this study. Table 3-1 represents the main WaPOR and Frame data component of all three levels with spatial, temporal, period, scaling factor, and respective unit. The

temporal resolution of data components expressed in the dekadal basis—the dekad values calculated as considering the whole year composing of 36 dekad. First, 20 days of a month taken as two dekad's (each of 10 days) and third dekad values considered as the third quarter of a month. The days for the third dekad ranges from 8-11 days. Main data components processing workflow is described below:

3.5.1. Field Data Description

A reconnaissance visit was conducted to the study area from 20-25 October 2019 to by the local partners and expertise to get initial information, to set-up a framework for field campaign, and to get contact with locals, farmers, and authorities. Based on the reconnaissance survey, two field campaign was carried out for the summer and winter season in the study area on 4-9 November 2019 and 10-13 February 2020, respectively. The experts from the Faculty of Agriculture, University of Gezira, inspector working in the scheme, and knowledgeable farmers participated in the field campaign. The main crops cultivated in the summer season are Sorghum, Cotton, and Groundnut. The area cultivated under each of these crops is about 7693 ha, 5607 ha, and 2108 ha, respectively. The other crops cultivated in the summer season are Onion, Pigeonpea, along with other crops such as Okra, Cowpea, Sesame, White bean, and others.

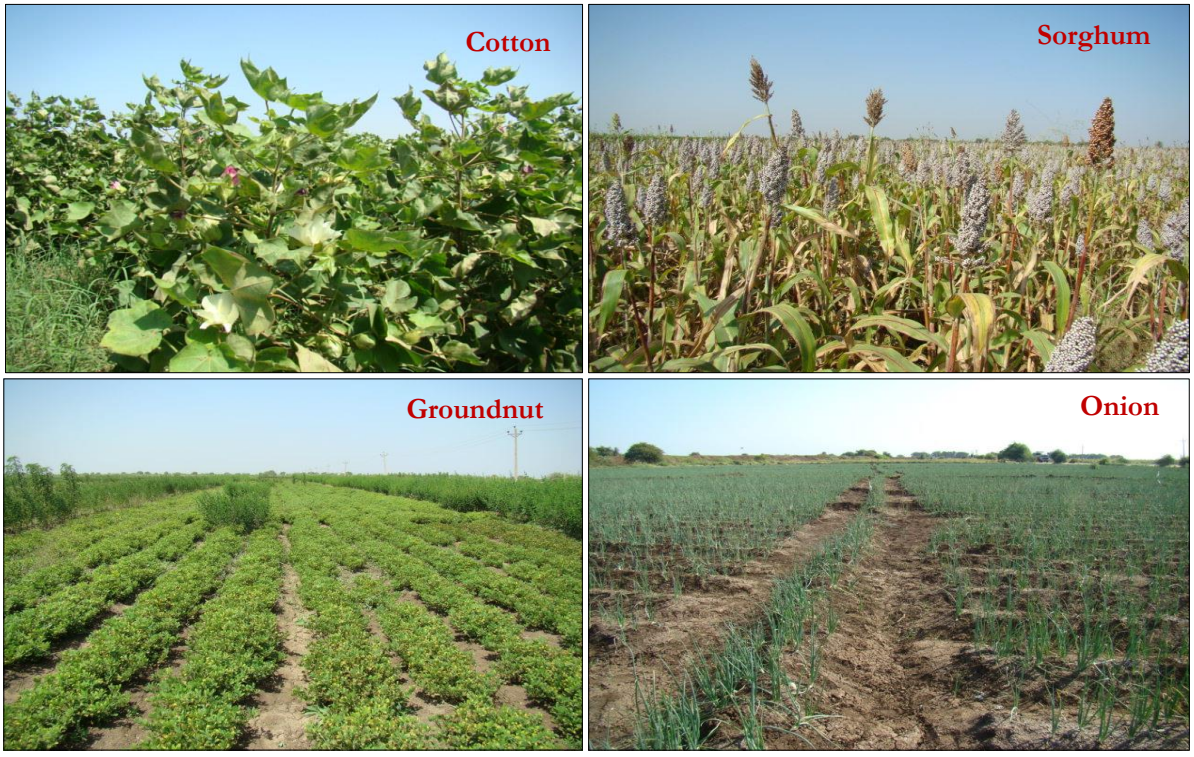

Figure 3-6: Summer season main crops in the Gezira scheme.

During the summer field campaign, a total of 50 ground-truthing samples with XY coordinates are collected. These 51 sample includes 13 samples of both Cotton, and Sorghum, 12 samples of Groundnut, 6 samples of Onion, and Pigeonpea each. The other information, such as sowing and harvesting time, number of irrigations, crop yield, and plot size, were also collected during the campaign—the complied information is attached in appendix-C. Supervised classification is performed to generate landcover

classification maps of the Gezira scheme. Field campaign ground-truthing crop data of summer season also with other permanent classes like bare land, built-up area, evergreen trees, irrigation canal, depression, and water area are selected using Google Earth.

In the winter field campaign, a total of 51 ground-truthing crop samples with XY coordinates are collected. The main crops cultivated in the winter season are Wheat, Onion, and Pigeonpea. The other crops cultivated in the scheme in the winter season are white bean, chickpea, okra, soybean, garlic, among others. There are 17 ground-truthing samples from all three main crops Wheat, Onion, and Pigeonpea were collected. Other information, such as sowing and harvesting time, the number of irrigations, crop yield, and plot size, was also collected during the campaign—the detailed information of the winter season field campaign is attached in appendix D. A supervised classification was also performed to generate a land cover classification map of the Gezira scheme. Field campaign ground-truthing crop data of winter season along with other permanent classes like bare land, built-up area, evergreen trees, irrigation canal, depression, and water are collected using Google Earth. Figure 3-7 shows some field photo's of the main crop collected during the field campaign.

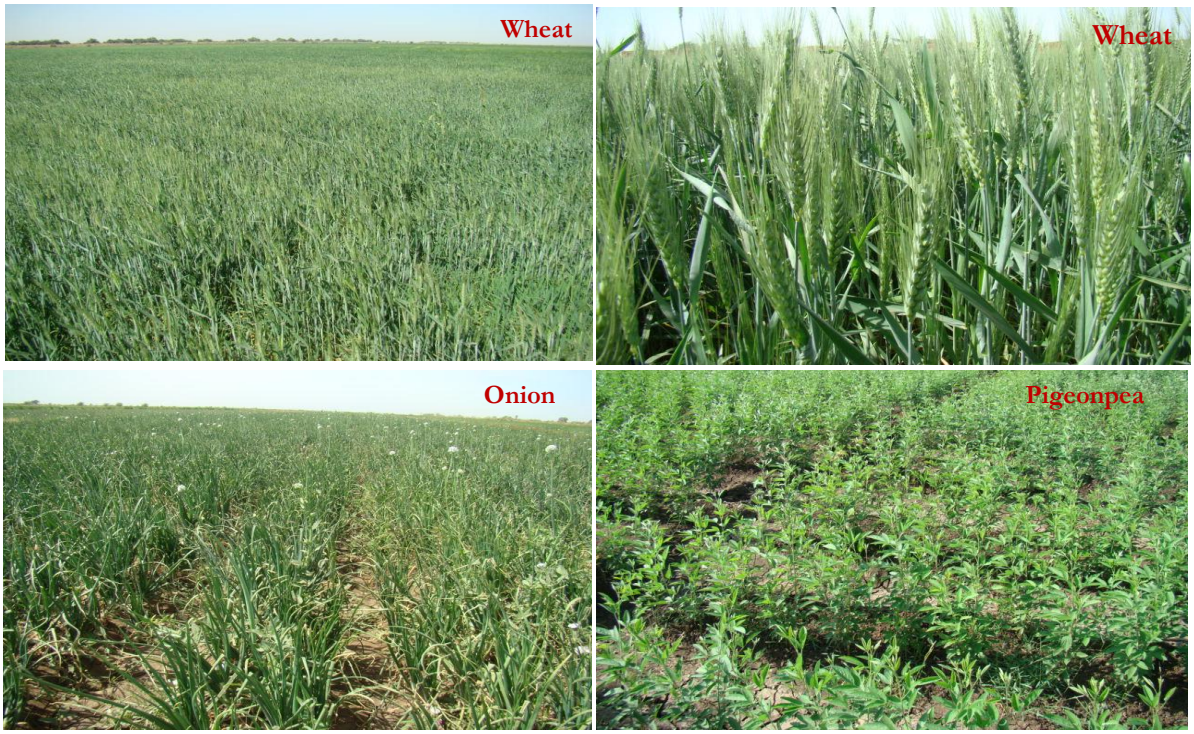

Figure 3-7: Winter season main crops in the Gezira scheme.

3.5.2. CHIRPS v2 and ERA5 Precipitation

To compare the CHIRPS v2 precipitation data, another independent dataset ERA5 precipitation from the European Centre for Medium-Range Weather Forecasts (ECMWF) used in the analysis. Ten selected point average precipitation from both CHIRPS v2 and ERA5 were collected for the period 2009 to 2019. The data were collected daily, then aggregated yearly and used in the analysis.

3.5.3. NDVI and CHIRPS v2 Precipitation

Dekadal Normalized Difference Vegetation Index (NDVI) values were retrieved for the selected points and aggregate monthly in the summer season. Monthly average NDVI response to monthly average precipitation from CHIRPS v2 was analysed for Cotton, Groundnut, and Sorghum in the study area.

3.5.4. Evaporation, Transpiration, Interception

Evapotranspiration and interception (ETI) is the sum of evaporation from the soil surface, transpiration from the crop canopy, and intercepted precipitation and irrigation water on the plant leaves that directly evaporated from the leaves. Climatic factors (radiation, air temperature, precipitation, and wind speed) and soil conditions (soil water content) are the limiting factors of evaporation, transpiration, and interception.

Table 3-1: WaPOR and FRAME data components used in the study.

Data Component	Temporal Resolution	Period*		Spatial Resolution	Scaling Factor	Unit
		From	To			
L1 (Sudan)						
Evaporation	dekad	200901	202009	250 m	10	avg. mm/day
Transpiration	dekad	200901	202009	250 m	10	avg. mm/day
Interception	dekad	200901	202009	250 m	10	avg. mm/day
Net Primary Products	dekad	200901	202009	250 m	1000	avg. gC/m²/day
Soil Moisture Content	dekad	200901	202009		100	0=wilting point, 1= field capacity
L2 (Gezira Scheme)						
Evaporation	dekad	200901	202009	100 m	10	avg. mm/day
Transpiration	dekad	200901	202009	100 m	10	avg. mm/day
Interception	dekad	200901	202009	100 m	10	avg. mm/day
Net Primary Products	dekad	200901	202009	100 m	1000	avg. gC/m²/day
Soil Moisture Content	dekad	200901	202009		100	0=wilting point, 1= field capacity
L3 (Wad Medani, Gezira Scheme)						
Evaporation	dekad	200901	202009	30 m	10	avg. mm/day
Transpiration	dekad	200901	202009	30 m	10	avg. mm/day
Interception	dekad	200901	202009	30 m	10	avg. mm/day
Net Primary Products	dekad	200901	202009	30 m	1000	avg. gC/m²/day
Soil Moisture Content	dekad	200901	202009		100	0=wilting point, 1= field capacity

*First four-digit represents the year, and the last two digits represent the dekad values.

The WaPOR used the ETLook model described in (Bastiaanssen et al., 2012) to calculate evaporation and transpiration. The ETLook model used the Penman-Monteith equation (Monteith, 1965) by adapting remote sensing input data. This method becomes the FAO standard in calculating the reference and actual evapotranspiration. The detailed description of the method is available in FAO irrigation and drainage

paper 56 (Allen, Pereira, Raes, & Smith, 1998). Equation 3-1 is used in the calculation of evapotranspiration. The equation combines the surface energy balance equation and the aerodynamic equation. The Penman-Monteith equation is expressed as:

$$\lambda ET = \frac{\Delta(R_n - G) + \rho_a c_\rho \frac{(e_s - e_a)}{r_a}}{\Delta + \gamma\left(1 + \frac{r_s}{r_a}\right)} \text{----------(3-1)}$$

Where:

λ	latent heat of evaporation [J kg^{-1}]
E	evaporation [kg m^{-2} s^{-1}]
T	transpiration [kg m^{-2} s^{-1}]
R_n	net radiation [W m^{-2}]
G	soil heat flux [W m^{-2}]
ρ_a	air density [kg m^{-3}]
c_ρ	specific heat of dry air [J kg^{-1} k^{-1}]
e_s	saturated vapor pressure [Pa]
e_a	actual vapor pressure of the air [Pa]
Δ	saturation vapor pressure vs. temperature curve slope [PaK^{-1}]
γ	psychrometric constant [Pa K^{-1}]
r_s	bulk surface resistance [s m^{-1}]
r_a	aerodynamic resistance [s m^{-1}]

The ETLook model used the Penman-Monteith equation separately for soil evaporation (E) and canopy transpiration (T) and is expressed as follows:

$$\lambda E = \frac{\Delta\left(R_{n,soil} - G\right) + \rho_a c_p \frac{(e_s - e_a)}{r_{a,soil}}}{\Delta + \gamma\left(1 + \frac{r_{s,soil}}{r_{a,soil}}\right)} \text{----------(3-2)}$$

and

$$\lambda T = \frac{\Delta\left(R_{n,canopy}\right) + \rho_a c_p \frac{(e_s - e_a)}{r_{a,canopy}}}{\Delta + \gamma\left(1 + \frac{r_{s,canopy}}{r_{a,canopy}}\right)} \text{----------(3-3)}$$

The two-equations differ in the accounting of the net radiation ($R_{n,soil}$ and $R_{n,canopy}$) and aerodynamic and surface resistance ($r_{s,soil}, r_{a,soil}$ and $r_{s,canopy}, r_{a,canopy}$). Moreover, for transpiration calculation, the soil heat flux (G) is not taken in to account.

Other parameters, interception (mm day^{-1}) is a function of the vegetation cover, leaf area index (LAI), and precipitation (P). WaPOR measures interception by using the following equation:

$$I_{mm} = 0.2\, l_{LAI} \left(1 - \frac{1}{1 + \frac{c_{veg}\ p}{0.2 l_{LAI}}}\right) \text{----------(3-4)}$$

Where, c_{veg} refers vegetation cover, P is precipitation, and l_{LAI} is the leaf area index.

A small intensity of precipitation results in a higher interception as most of the precipitation is retained by the canopy leaves. With the increase of precipitation, interception decreases quickly as the top of the leaves become thoroughly wetted. The interception amount directly relates to the LAI as LAI also increases interception increases, whereas low LAI results in a small interception.

The output of Penman-Monteith equation λET, λE, λT is converted to mm by using the following equation:

$$E = \lambda E \left(\frac{t_{day}}{\lambda}\right) = \lambda \mathrm{E} \left(\frac{864000}{245780}\right) \approx 0.035 \lambda E \text{ ----------(3-5)}$$

Where, t_{day} is the number of seconds in a day (84,600) and λ is the latent heat of evaporation and is a function of temperature. At 293°K temperature, the value of latent heat λ is equal to 2,453,780. Similarly, λET, λT are converted to mm. The λ is calculated with the following equation:

$$\lambda = \lambda_0 + C * T \text{----------(3-6)}$$

Where, C equals to -2361 J/kg/C and the value of λ_0 is 25,01,000 J/kg.

In this study, evaporation, transpiration, and interception raw dekadal data retrieved from the ITC data repository and clipped to the area of interest. The three different levels of 250m, 100m, and 30m resolution are obtained for the respective areas of interest as Sudan, Gezira irrigation scheme, and specified area of Wad Medina, respectively. Ilwis scripts are used to process the raw dekadal input maps of evaporation, transpiration, and interception to get dekadal ETI and T maps. For the calculation of dekadal ETI, several calculations are performed. First, the input maps are summed, divided by the scaling factor, and multiplied by the length of the dekad. After running the script with inputs maps and dekadal values, two sets of output map of ETI and T are generated with filename extensions representing the map units in mm and m^3ha^{-1}. The output map with mm file name extension is multiplied by a factor of 10 to get m^3ha^{-1}, which represents the amount of water consumption by the crop per hectare.

The procedure is repeated to get the dekadal summed ETI and T maps for the period starting at the first dekad of 2009 to the 9th dekad of 2020. A yearly and seasonal based map list of ETI and T is generated for easing calculations.

3.5.5. Total and Above-ground Biomass Production

The total biomass production (TBP) is the sum of total dry matter production during the growing season. The above-ground biomass production (AGBP) is the sum of above-ground dry matter production during the growing season. Both TBP and AGBP expressed in $kgDMha^{-1}day^{-1}$. The TBP and AGBP steadily increase from the start of the season (SOS) to the end of the season (EOS). AGBP is a useful indicator to estimate crop yield and production forecasting as it integrates the three essential aspects: the current vegetation status, the dry matter production (meteorological influence), and the history of the growing

season (FAO, 2018c). As the TBP and AGBP is the integration of dry matter production over the season, its accuracy largely depends on the accuracy of the net primary production (NPP) estimation.

The NPP is the conversion of carbon dioxide into biomass through photosynthesis. NPP derived from Gross Primary Production (GPP) minus autotrophic respiration, losses due to conversion of glucose to higher-level photosynthates (starch, cellulose, fats, and proteins) and respiration. WaPOR derived NPP by using satellite imagery and meteorological data. WaPOR used Veroustraete, Sabbe, & Eerens (2002) described methods and illustrated the implementation approach to estimate NPP. The methodology furthered improved within the Copernicus Global Land Component, and WaPOR uses these updated methodologies. The NPP computation method based on (Monteith, 1972) that described the ecosystem productivity as a function of solar radiation. The equation is expressed as follows:

$$NPP = Sc\ R_s \varepsilon_p\ fAPAR\ SM\ \varepsilon_{lue}\ \varepsilon_T\ \varepsilon_{co_2}\ \varepsilon_{AR}\ [\varepsilon_{RES}] \text{----------(3-7)}$$

Where,

NPP	Net primary production [gC/m2/day]
Sc	Scaling factor from DMP to NPP [-]
Rs	Total shortwave incoming radiation [GJ/ha/day]
ε_p	Frac. of PAR (0.4-0.7μm) in total shortwave usually taken as 0.48 [JP/JT]
fAPAR	PAR-fraction absorbed by green vegetation [JPA/JP]
SM	Soil moisture stress reduction factor
ε_{lue}	Light use efficiency [kgDM/GJPA]
ε_T	Normalized temperature effect [-]
ε_{co_2}	Normalized CO_2 fertilization effect [-]
ε_{AR}	Fraction kept after autotrophic respiration [-]
ε_{RES}	Fraction kept after residual effects [-]

Veroustraete et al. (2002) described the complex biochemical process involved in the effect of temperature (ε_T), atmospheric carbon dioxide (ε_{co_2}), and autotrophic respiration (ε_{AR}). However, temperature and carbon dioxide acts as a driving force to these biochemical processes. Globally, the yearly concentration of carbon dioxide is assumed as constant. The overall increasing trend of the global carbon dioxide concentration level is resulting in the greenhouse effect. The addition of residual factor (ε_{RES}) emphasizes some important practical factors such as drought effect, nutrient deficiencies, pests and plant diseases that influence the NPP estimation.

$$NPP = Sc.R_s\varepsilon_p fAPAR\ SM\varepsilon_{lue}\ \varepsilon_T\ \varepsilon_{co2}\ \varepsilon_{AR}\ [\varepsilon_{RES}] = s_c.R_s.fAPAR.SM\varepsilon_{LUE}.\varepsilon(T, CO_2).[\varepsilon_{RES}] \text{----------(3-8)}$$

Where, $\varepsilon(T, CO_2) = \varepsilon_P.\varepsilon_T.\varepsilon_{CO2}.\varepsilon_{AR}$

Equation 3-8 shows that the estimation of NPP depends on the six factors such as fAPAR, radiation, soil moisture stress, light use efficiency, temperature, and carbon dioxide. By using meteorological inputs (Rs, T), fAPAR, and soil moisture stress factor, the NPP is estimated on dekadal basis.

Ilwis scripts are used to calculate the dekadal TBP and AGBP using the raw NPP dekadal map, which is retrieved from the ITC data repository for the area of interest. For the generation of dekadal TBP and AGBP map, several calculations are performed. First, the input NPP map is multiplied by 22.222 (conversion factor of $gCm^{-2}day^{-1}$ to $kgDMha^{-1}$), then divided by the scaling factor (1000) and multiplied by the length of the dekad to get the TBP map.

This TBP map subsequently multiplied by 0.65 (root/shoot ratio) to obtain the AGBP map. The unit of both TBP and AGBP maps are $kgDMha^{-1}$. This procedure is repeated for each dekad from the first dekad of 2009 to the 9th dekad of 2020. A map list is created for calculation and analysis.

3.5.6. Gross Biomass Water Productivity

The gross biomass water productivity (GBWP) defined as the quantity of output (above-ground biomass production and total biomass production) to the consumption of the total volume of water in a certain period (FAO, 2016). The GBWP expressed in kgm^{-3}. The consumption of water is the sum of soil evaporation, crop canopy transpiration, and interception expressed as ETI. As previously mentioned, total water consumption (ETI) and biomass production as AGBP and TBP are calculated on dekadal basis. The dekadal GBWP is calculated by relating biomass production to the respective dekad water consumption. In this study, the GBWP calculated in terms of TBP and AGBP. GBWP_AGBP calculated from GBWP_TBP multiplied by 0.65. The equation 3-9 and 3-10 shows the calculation of GBWP.

$$GBWP\_TBP = \frac{TBP}{E+T+I} \text{----------(3-9)}$$

$$GBWP\_AGBP = \frac{AGBP}{E+T+I} \text{----------(3-10)}$$

Where,

TBP Total biomass production [kgDM ha^{-1}]
AGBP Above-ground biomass production [kgDM ha^{-1}]
E Soil evaporation [m^3ha^{-1}]
T Canopy transpiration [m^3ha^{-1}]
I Interception [m^3ha^{-1}]

An Ilwis script is used to calculate the dekadal basis GBWP_TBP and GBWP_AGBP using the dekadal map of TBP, AGBP, and ETI maps. This procedure is repeated for each dekad from the first dekad of 2009 to the 10th dekad of 2020. A map list is created on the yearly and seasonal basis for the easing of calculation and analysis.

3.5.7. Net Biomass Water Productivity

The net biomass water productivity (NBWP) defined as the quantity of output (above-ground biomass production and total biomass production) to the actual volume of water consumption by the crop in the photosynthesis process known as canopy transpiration in a certain period (FAO, 2016). The NBWP also expressed in kgm^{-3}. As mentioned earlier, actual water consumption (T) and biomass production as AGBP and TBP are calculated on dekadal basis. The dekadal NBWP is calculated by relating biomass production to the respective dekadal amount of canopy transpiration. Like GBWP, NBWP is also calculated in terms of TBP and AGBP. NBWP_AGBP is calculated from NBWP_TBP multiplied by 0.65. The equation 3-11 and 3-12 shows the calculation of NBWP.

$$NBWP\_TBP = \frac{TBP}{T} \text{----------(3-11)}$$

$$NBWP\_AGBP = \frac{AGBP}{T} \text{----------(3-12)}$$

Where,

TBP Total biomass production [$kgDMha^{-1}$]

AGBP Above-ground biomass production [$kgDM\ ha^{-1}$]

T Canopy transpiration [m^3ha^{-1}]

An Ilwis script is used to calculate the dekadal NBWP_TBP and NBWP_AGBP using the dekadal map of TBP, AGBP, and T maps. This procedure is repeated for each dekad from the first dekad of 2009 to the 10th dekad of 2020. A map list is created on the yearly and seasonal basis for calculation and interpretation purposes.

3.5.8. Comparison of WaPOR Water Productivity

The comparison of WaPOR data derived water productivity has been carried out on a seasonal basis in the study area. Cotton, Groundnut, and Sorghum of summer season and Onion, Pigeonpea, and Wheat of winter season used in the comparison. Three temporal region SOS, MOS, EOS data used here for this analysis. The SOS, MOS, and EOS were fixed depending on the cropping season. In the summer season, the 22nd, 26th, and 30th dekad are used as SOS, MOS, and EOS, respectively. In the winter season, the 35th dekad of the running year and 2nd and 7th dekad of the next year are used as SOS, MOS, and EOS, respectively. The sample point coordinates from both seasons, which were collected from the field campaign, were used to calculate the respective crop water productivity. Ilwis point cross-function used to calculate the respective point of water productivity. With the point-cross function, water productivity of WaPOR L1, L2, and L3 calculate separately.

4. RESULTS AND DISCUSSIONS

4.1. General Characteristics of the Gezira Scheme

Some general characteristics of the FAO-WaPOR selected focus area (L3) at Wad Medani in the Gezira irrigation scheme, are analysed such as land cover, precipitation, and NDVI. The results are below:

4.1.1. Land Cover

Land cover is useful to observe variations over time, especially for agricultural land that helps in farm design, crop selection, and water budgeting. Supervised classification is performed to generate land cover maps of the Gezira scheme. Two Sentinel-2A images, one from the middle of the summer (25.09.2019) and the other one is in the middle of the winter season (02.02.2020), are used in the classification. Field campaign ground-truthing crop data of summer and winter season along with other permanent classes like bare areas, built-up area, canal, depression, and water are selected by Google Earth, are used in the classification process. Ground truth details are found in the appendix E&F. The maximum likelihood classifier was applied classification process, and Figure 4-1 represents the classified land cover map of the summer and winter season. The overall accuracy in the summer and winter season is 83.33% and 84.62%, respectively. The overall Kappa coefficients of the classification for summer and winter season are 0.817 and 0.821, respectively. The confusion matrix is found in appendix G&H. According to local expert's observation, from 2005, farmers in the Gezira scheme barely practice crop rotation. It is noticeable that both summer and winter season considerable cropland remains fallow in the scheme. Classification also shows scattered built-up areas visible in the irrigation scheme. The classification is also considered valid for all the periods in the study, especially concerning the main crops selected.

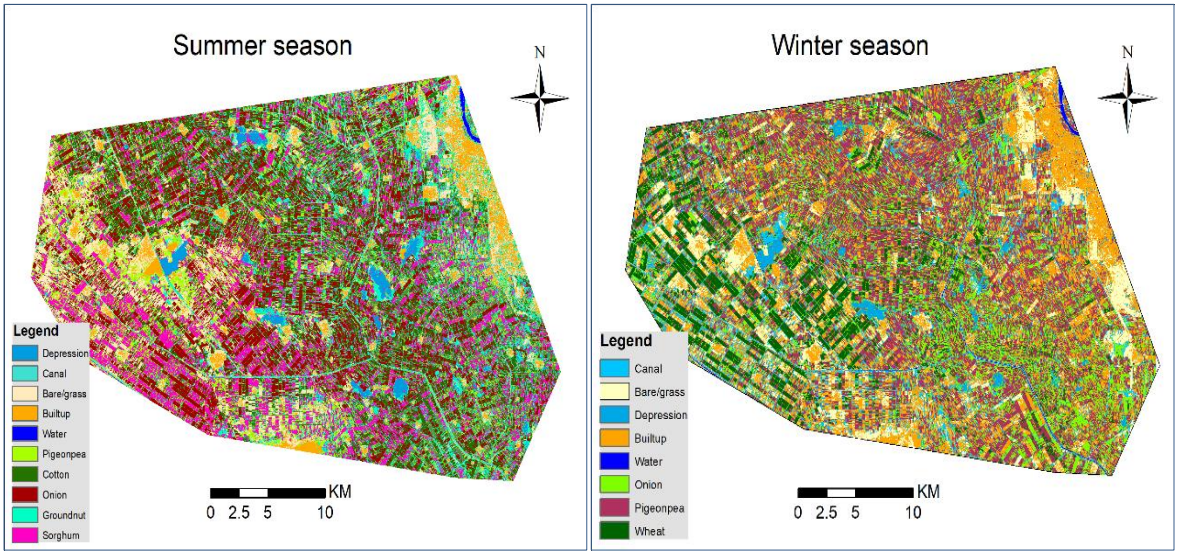

Figure 4-1: Land cover class in the study area.

4.1.2. CHIRPS v2 and ERA5 Precipitation

Google Earth Engine is used to retrieve ten selected points daily precipitation for both CHIRPSv2 and ERA5 for the period 2009 to 2019. The selected points and data retrieve scripts are found in appendix I&J. The average of daily values aggregated to obtain yearly precipitation. Figure 4-2 illustrates the yearly average precipitation from CHIRPS v2, and ECMWF generated ERA5 for the period 2009 to 2019 in the study area. CHIRPS v2 always estimates significantly higher precipitation compared to ERA5 throughout the period. It is visible that in 2013 and 2015, the study area received very low precipitation compared to the average for both datasets result in different degrees of drought in the study area.

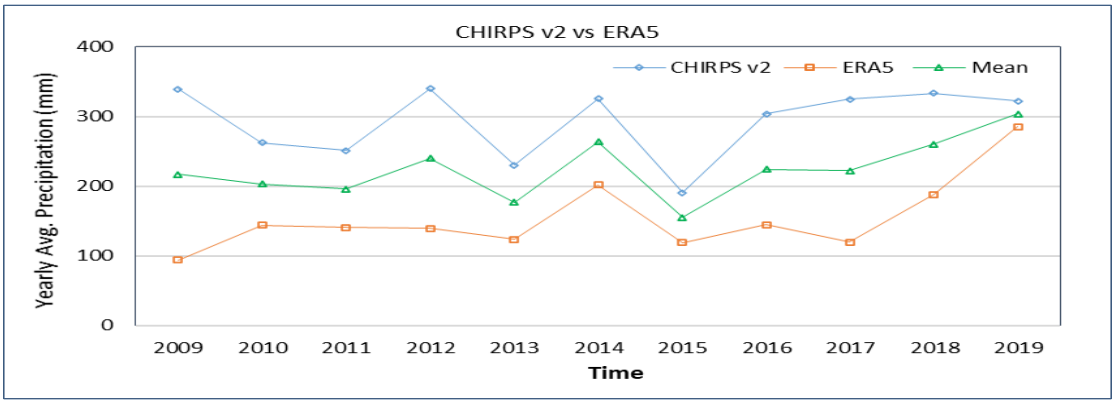

Figure 4-2: Yearly average precipitation from CHIRPS v2 and ERA5 in the study area.

4.1.3. NDVI and Precipitation

WaPOR L3 dekadal Normalized Difference Vegetation Index (NDVI) data is retrieved from the ITC data repository. Ilwis point-cross function and conversion formula is used to obtain pre-selected crops average NDVI value. The figure illustrates the vegetation response to the precipitation in the study area for the period 2009 to 2019. Throughout the period, the highest precipitation occurred in August. In 2009 and 2015, there was considerable low precipitation compared to other years in the study area. NDVI is a well-established indicator of vegetation growth assessment. Figure 4-3 shows the NDVI peak every year follows the peak of precipitation by 2-3 dekads lag. The trend is followed by all three crops in the summer season.

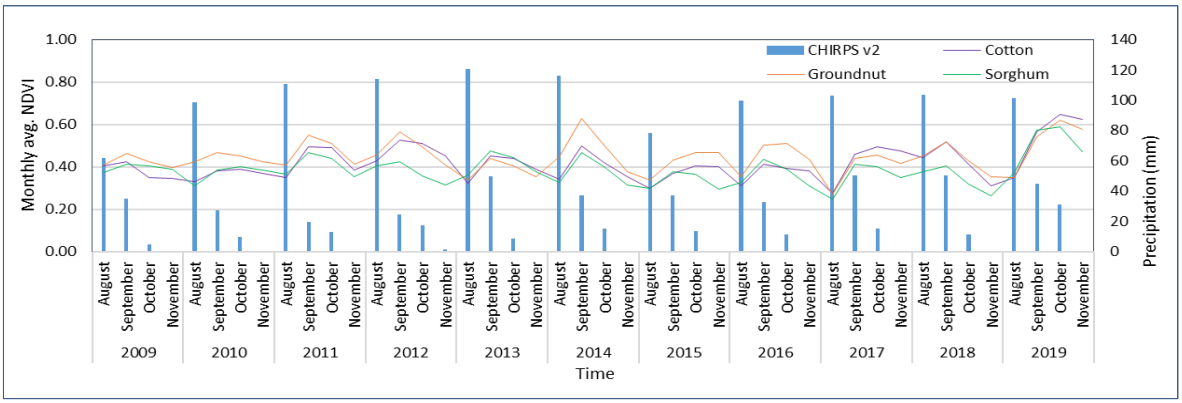

Figure 4-3: Monthly average NDVI and precipitation of Cotton, Groundnut, and Sorghum in summer season.

4.2. Evapotranspiration and Interception

Accuracy of water productivity calculation largely depends on the accuracy of actual evapotranspiration estimation. The water consumption, actual evapotranspiration, and interception is a vital component of the water balance system that accounts upto 90% of the incoming precipitation in the river basin such as Nile river basin (Mul & Bastiaanssen, 2019). Since ETI is not directly measured by satellites, it can be calculated indirectly using other algorithms and models like surface energy balance, which use physical variables that can be observed from the space (Mul & Bastiaanssen, 2019). WaPOR used (Bastiaanssen et al., 2012) ETLook model, which, coupled with remote sensing derived data, is applied to calculate evapotranspiration for all three levels. Remotely sensed WaPOR generated data is used here to derive the actual evapotranspiration and interception component for all three levels. The data processed on dekadal basis and summarized for the summer and winter season from 2009 to 2020.

4.2.1. Summer Season ETI

Summer season ETI analysis derived by the average of twelve sample points of Cotton and Groundnut each, and eleven sample points of Sorghum are used in the computation and analysis in the study. Table 4.1 summarize the summer season average minimum, maximum, and mean consumed ETI of Cotton, Groundnut, and Sorghum derived from WaPOR L1, L2, and L3 data sets. The table shows the minimum and maximum ETI consumption range of WaPOR L1 and L2 are close to each other. However, the ETI consumption range of WaPOR L3 is always higher than the L2, and L3 consumed ETI for all three crops. Calculated yearly detailed water consumption information for Cotton, Groundnut, and Sorghum are shown in appendix K.

Table 4-1: ETI consumption of Cotton, Groundnut, and Sorghum in the summer season.

	Cotton			Groundnut			Sorghum		
Level	L1	L2	L3	L1	L2	L3	L1	L2	L3
Minimum	299	273	204	351	317	234	261	240	191
Maximum	656	635	740	653	644	767	606	589	674
Mean	478	451	435	506	476	476	450	421	397
Std deviation	105	108	170	91	98	176	111	113	154

Figure 4.4 shows the variation of the standard deviation of measured ETI for Cotton, Groundnut, and Sorghum from WaPOR L1, L2, and L3. WaPOR L1 and L2 measured ETI are similarly distributed around the mean for all three crops. WaPOR L3 measured ETI is dispersedly distributed compare to WaPOR L1 and L2 for all crops.

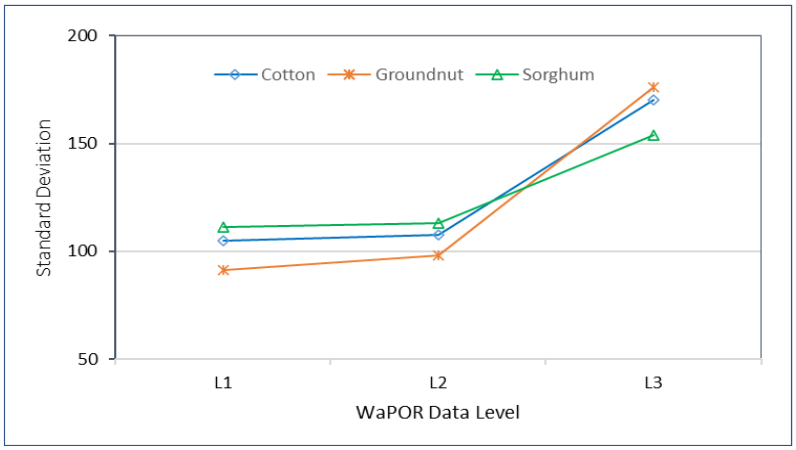

Figure 4-4: Standard deviation of ETI calculated from WaPOR L1, L2 and L3 in summer season.

Figure 4.5 also shows the summer season average ETI of Cotton, Groundnut, and Sorghum for all three level datasets. For all three crops, ETI values decrease with spatial resolution increases. Calculated seasonal average ETI values of Cotton are 478mm, 451mm, and 435mm for 250m, 100m, and 30m resolution, respectively. Singh, Datta, & Dharaiya (2013) also used Landsat TM5 images and reported that spatial distribution of actual evapotranspiration ranges for Cotton from 317mm to 534mm in Sirsa district, Haryana, India. Steduto et al. (2012) also reported that Cotton evapotranspiration varies from 410mm to 780mm on the United States southern high plains depending on the irrigation method. Groundnut seasonal ETI values for 250m, 100m, and 30m resolution are 506mm, 476mm, and 476mm, respectively. Steduto et al. (2012) also reported that the seasonal evapotranspiration of Groundnut ranges from 500mm to 700mm depending on the environment. Calculated seasonal average ETI of Sorghum from WaPOR L1, L2, and L3 are 450mm, 421mm, and 397mm, respectively. The consumptive use (ET) of 110-130 days Sorghum ranges between 450mm to 750mm depending on cultivar and weather Steduto et al. (2012).

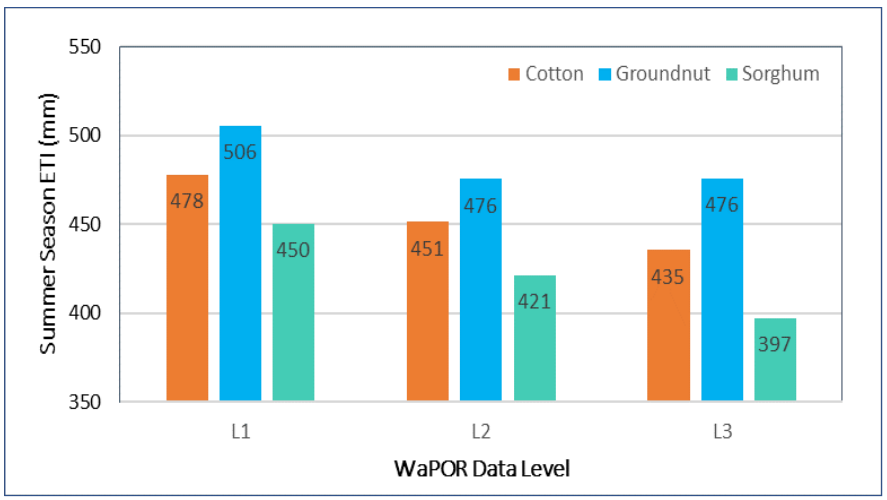

Figure 4-5: Summer season yearly average ETI of Cotton, Groundnut, and Sorghum from WaPOR L1, L2 and L3.

WaPOR L1, L2, and L3 derived ETI were computed on dekadal basis. Every year 36 dekadal maps of each level were generated and used in water productivity calculation from 2009 to 2020. Figures 4.6 represents the sample temporal variation of WaPOR L3 ETI in the summer season and winter season. Figures show ETI variation in the summer season in the entire study area. Cropping areas of both summer and winter season shows higher ETI while bare and built-up areas ETI was significantly low as expected. In the summer season, ETI from bare and built-up areas shows higher amplitude than winter season because of evaporation from the soil, which results from precipitation, whereas winter season precipitation is almost zero.

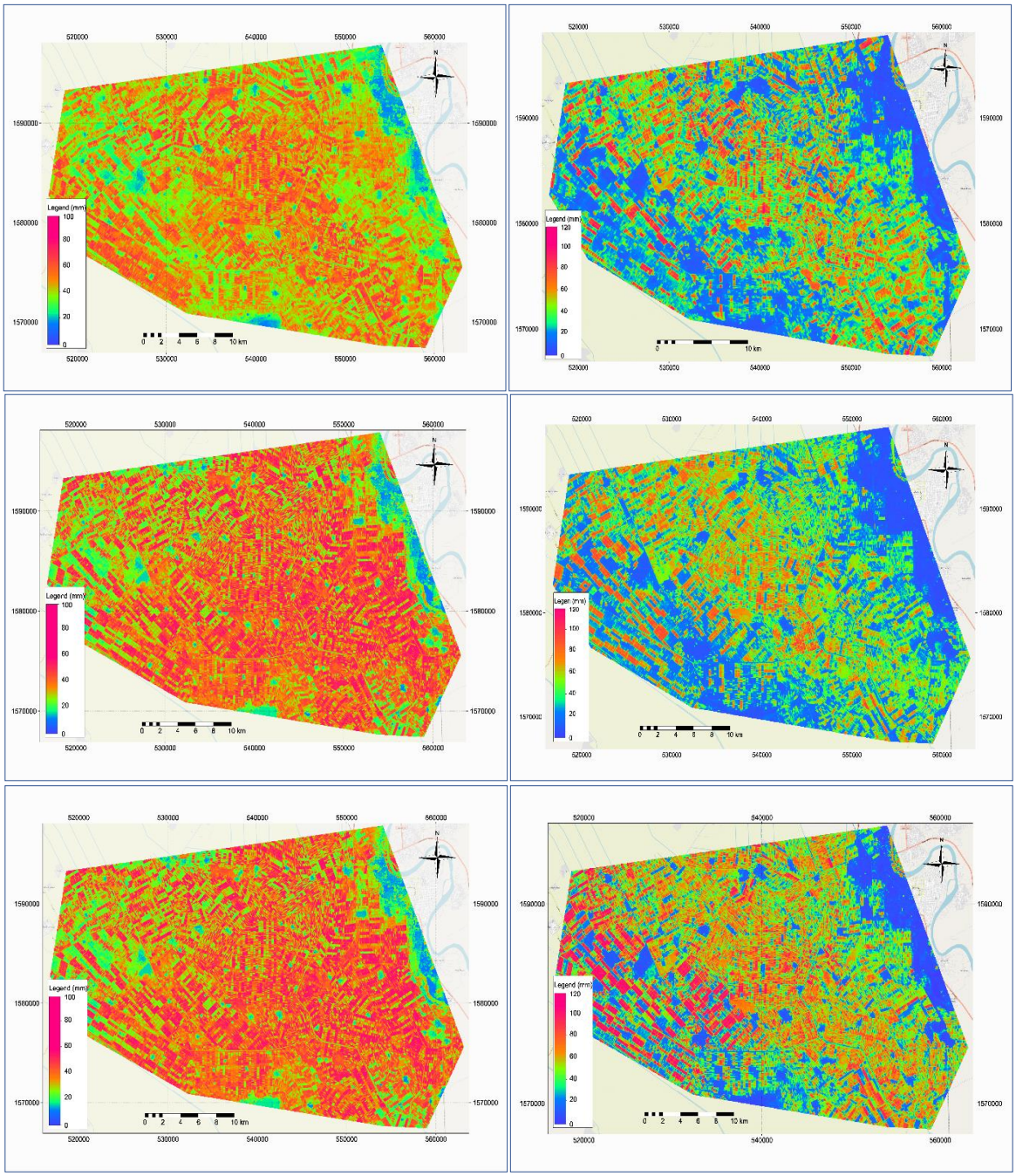

Figure 4-6: Temporal variation of ETI at 26th dekad of 2009, 2014 and 2019 (left column) in summer season and 4th dekad of 2010, 2015 and 2020 (right column) in winter season.

4.2.2. Winter Season ETI

Winter season ETI computation and analysis carried out by using the average of seventeen sample points ETI for Onion, Pigeonpea, and Wheat. Table 4.2 summarizes the winter season average minimum, maximum, and average ETI of Onion, Pigeonpea, and Wheat derived from WaPOR L1, L2, and L3. The table shows that the minimum and maximum ETI consumption ranges of WaPOR L1 and L2 are very close to each other for all three crops. However, the ETI consumption range of WaPOR L3 is always higher than the L2, and L3 consumed ETI for all three crops. Yearly detailed water consumption information of Onion, Pigeonpea, and Wheat are shown in appendix L.

Table 4-2: Summarize ETI consumption of Onion, Pigeonpea, and Wheat in the winter season.

	Onion			Pigeonpea			Wheat		
Level	L1	L2	L3	L1	L2	L3	L1	L2	L3
Minimum	224	215	152	203	184	131	175	154	133
Maximum	666	665	785	635	668	756	652	653	776
Mean	444	423	441	361	351	351	379	355	381
Std deviation	129	128	187	126	138	187	136	142	184

Figure 4.7 shows the variation of the standard deviation of measured ETI for Onion, Pigeonpea, and Wheat from WaPOR L1, L2, and L3. WaPOR L1 and L2 measured ETI are similarly distributed around the mean for all three crops. On the other hand, WaPOR L3 measured ETI is dispersedly distributed around the mean compare to WaPOR L1 and L2 for all three crops.

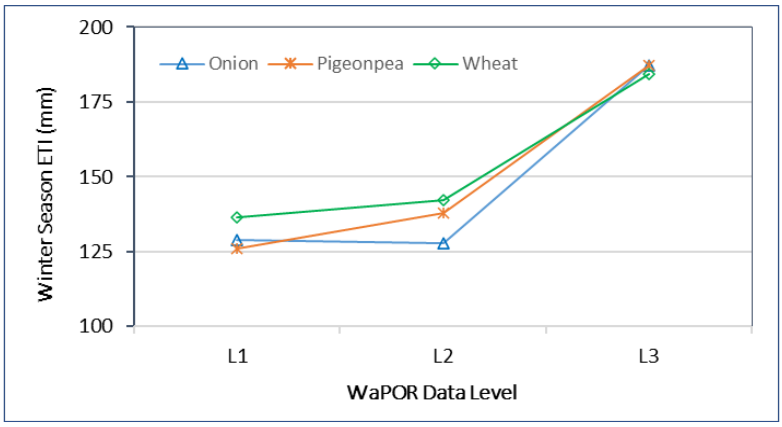

Figure 4-7: Standard deviation of ETI calculated from WaPOR L1, L2 and L3 in winter season.

Figure 4.8 shows that winter season average ETI of Onion, Pigeonpea, and Wheat from all three level datasets for the period of 2009 to 2019. WaPOR L1, L2, and L3 derived ETI follows a similar trend for all crops, although WaPOR L2 generated ETI is slightly lower than others. Calculated average ETI

consumption derived from WaPOR L2 results in always smaller ETI than WaPOR L1 and L3. Calculated seasonal average ETI of Onion was 444mm, 423mm, and 441mm from WaPOR L1, L2, and L3, respectively. For Onion, ETI from L1and L3 is almost the same, whereas L2 ETI was a little lower compared to L1 and L3. Pigeonpea and Wheat ETI from WaPOR L1, L2, and L3 are almost similar though L2 ETI slightly lower than other levels. Wheat ETI from WaPOR L1, L2, and L3 always results in lower consumption than the similar type of studies. Cai & Sharma (2010) calculated Wheat average ET value 416mm in India, Li et al. (2008) estimated values range from 424mm to 475mm in North China. Steduto et al. (2012) also reported that Wheat evapotranspiration varies from 200mm to 500mm, and values may reach 600mm to 800mm under well irrigated and semi-arid areas.

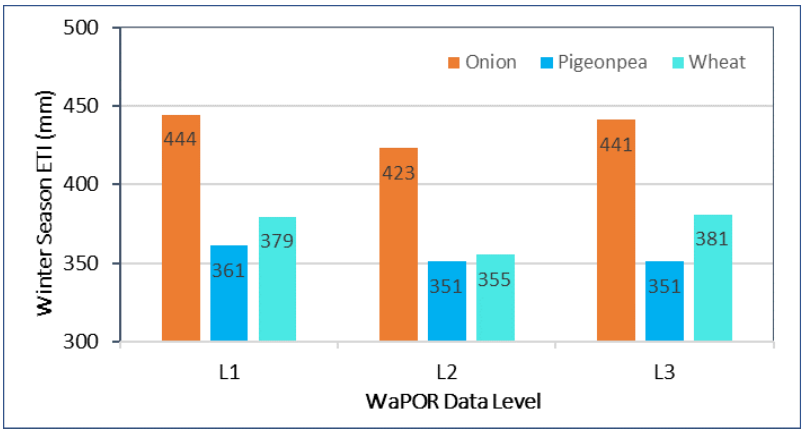

Figure 4-8: Winter season yearly average ETI of Onion, Pigeonpea, and Wheat from WaPOR L1, L2 and L3.

4.3. Total Biomass Production

The total biomass production is the sum of total dry matter production during the growing season, usually expressed as kgDMha^{-1}. TBP gradually increases from the start of the season to the end of the season. TBP is one of the main components for the quantification of the water productivity assessment process. Dekadal TBP calculated from net primary production, which is available in the WaPOR open-access portal and FRAME project. In this study, dekadal basis TBP calculated for all three levels from the first dekad of 2009 to the 9th dekad of 2020. The calculated dekadal values then summarized on a summer and winter season basis. Three main crops from each summer season and winter season are used in TBP calculation.

4.3.1. Summer Season TBP

Analysis of TBP and yearly variation, TBP of the year 2009 of all three levels, is used as a base level. Figure 4-9 shows the yearly average TBP production and yearly total biomass production for the Cotton. From 2009 to 2014, there is a gradual increase in TBP. A sharp decrease in TBP observed in 2015 from 2014 then gradually increase again till 2019. The figure also shows in 2015 and 2016, TBP of Cotton was below the base production for all WaPOR L1, L2, and L3.

Figure 4-9: TBP of Cotton and yearly changes in TBP of WaPOR L1, L2, and L3 in summer season.

Figure 4-10 shows the yearly average TBP and changes in TBP for the Groundnut for the period 2009 to 2019. It shows that from 2009 to 2014, there is a gradual increase in TBP. A sudden decrease in TBP is observed in 2015, then it again gradually increases till 2019. From 2015 to 2017, TBP of Groundnut was below the base production for all WaPOR L1, L2, and L3. The L2 derived Groundnut TBP results in a higher decrease in TBP compared to L1 and L3 TBP.

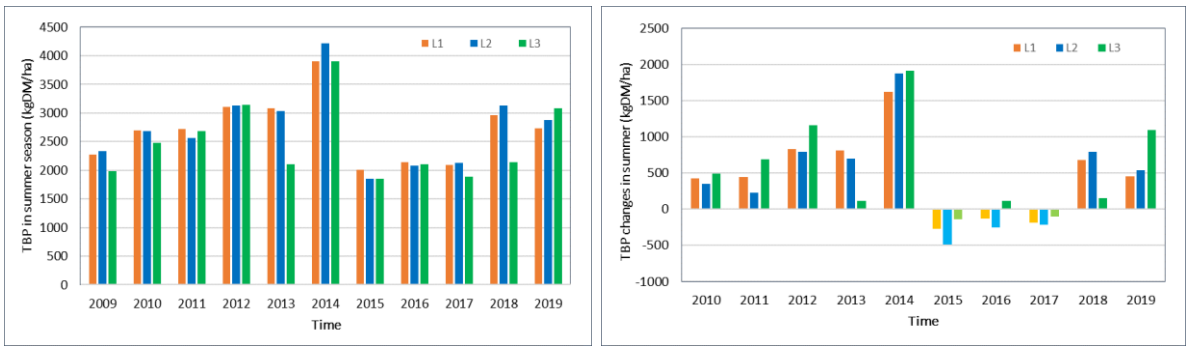

Figure 4-10: TBP of Groundnut and yearly changes in TBP of WaPOR L1, L2, and L3 in summer season.

Figure 4-11 shows the yearly average TBP and changes in TBP for Sorghum for the period 2009 to 2019. A similar trend as Groundnut also observed for Sorghum, showing an increase in TBP from 2010 to 2014, then followed an abrupt decrease in TBP in 2015, then increases again till 2019. In 2015 and 2017, TBP of Sorghum was well below the base production for all L1, L2, and L3. In 2018, L1 and L2 generated TBP slightly increased; however, L3 derived TBP was below the base level. In 2019, a similar trend as Cotton, Groundnut, and Sorghum was observed with a significant increase in TBP compared to the base production of 2009.

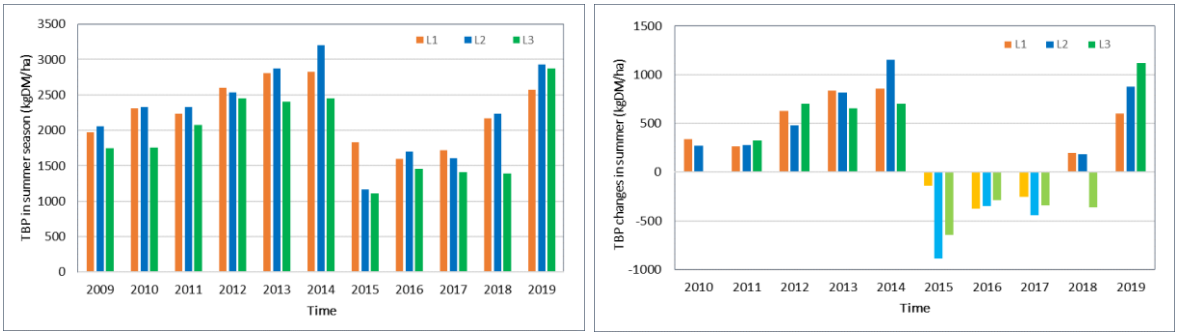

Figure 4-11: TBP of Sorghum and yearly changes in TBP of WaPOR L1, L2, and L3 in summer season.

Total biomass production of WaPOR L1, L2, and L3 were computed on a dekadal basis. Every year 36 dekadal maps of each level were generated and used in TBP calculation from 2009 to 2020. Figures 4-12 represents a sample of temporal variations of WaPOR L2 TBP of the summer season (26th dekad-left column images) of the year of 2009, 2014, and 2019 and in the winter season (4th dekad-right side column images) of the year 2010, 2015, and 2020, respectively. The figure shows that more area was cultivated during the summer season compared to the winter season. Rainfall with supplement irrigation facilities might encourage farmers to cultivate more areas in the summer season. Water shortage or rational water budgeting might be the limiting factor for potential coverage of cultivable land.

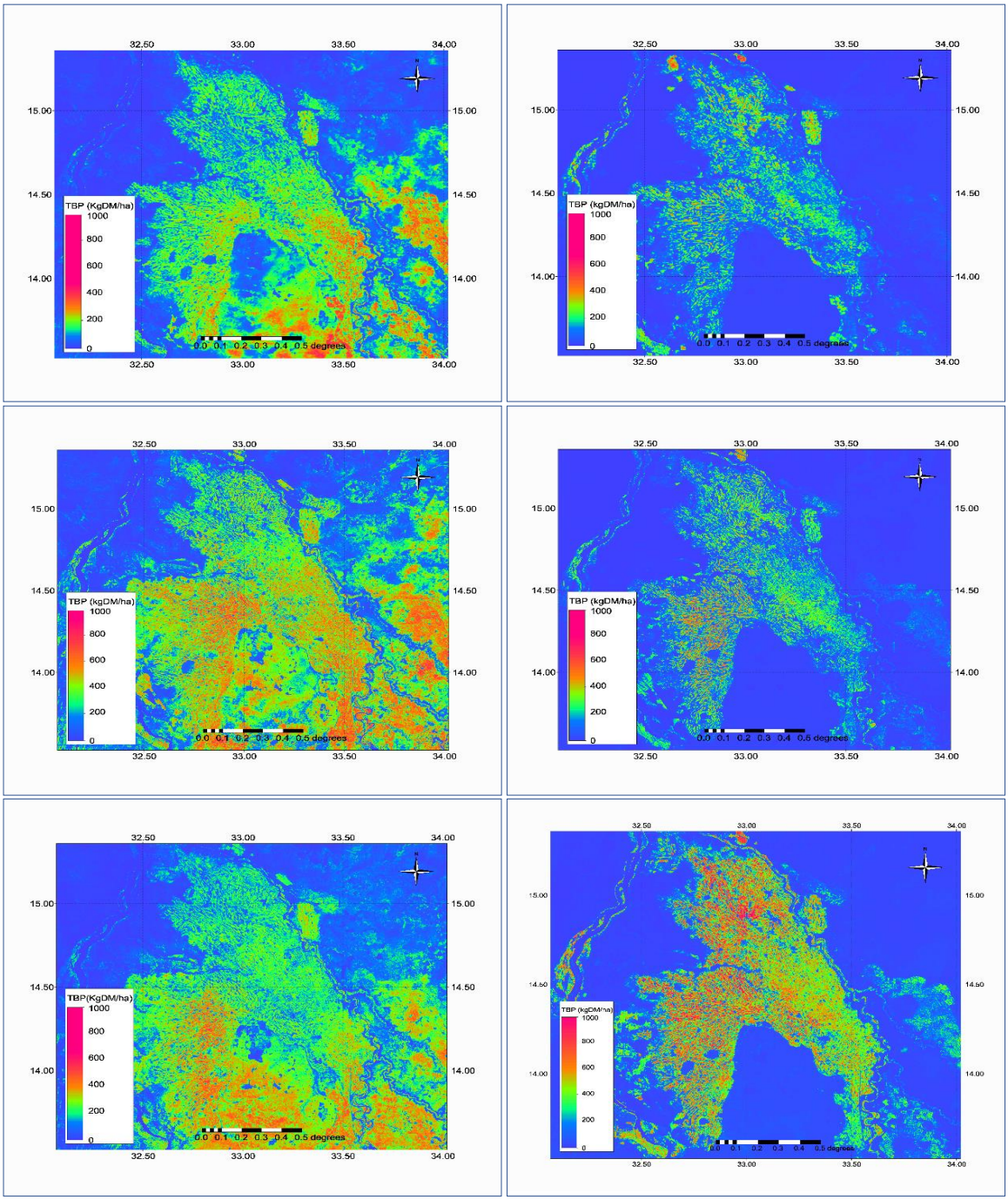

Figure 4-12: Temporal variations of summer season TBP at 26th dekad of 2009, 2014 and 2019 (left column) and winter season TBP of 4th dekad of 2010, 2015 and 2020 (right column).

4.3.2. Winter Season TBP

In winter season analysis of TBP and yearly variation, TBP of the year 2010 of all three levels, is used as a base level. Figure 4-13 shows the yearly average TBP and yearly changes in production for Onion. From 2009 to 2016, a gradual increase in TBP observed with an exception for L3 in 2013 and 2015. For the period 2016 to 2019, a slight and steady decrease in TBP of Onion was observed. The Onion TBP was well above the base TBP for all WaPOR L1, L2, and L3 except for the L3 in 2013 and 2015.

Figure 4-13: TBP of Onion and yearly changes in TBP of WaPOR L1, L2, and L3 in winter season.

Figure 4.14 represents the yearly average TBP and yearly change of Pigeonpea for the period 2010 to 2019. After a small increase in 2011, TBP decreases over the next two years then steadily increase to reach a peak in 2016 and gradually decreases again till 2019. For Pigeonpea, it is noticeable that TBP calculated from WaPOR L1, and L2 continuously results in higher TBP over WaPOR L3 generated TBP. For the period 2012 to 2015, WaPOR L3 generated TBP of Pigeonpea was significantly lower than the base production.

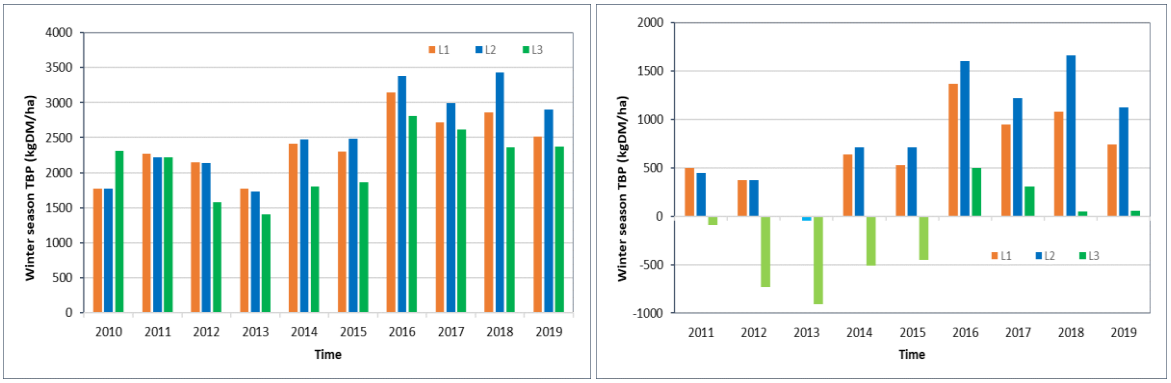

Figure 4-14: TBP of Pigeonpea and yearly changes in TBP of WaPOR L1, L2, and L3 in winter season.

Figure 4.15 shows the yearly average TBP and yearly change over 2010 of Wheat for the period 2010 to 2019. A steady and gradual increase of all level derived Wheat TBP observed from 2010 to 2017 with an exception for the year 2013. From 2017, a decrease in TBP for the next two years is observed. In 2013, TBP of all three levels was well below the base production, but a sharp decrease is observed for L3

generated TBP. A moderate increased TBP is observed in 2011-2015, whereas a considerable increase in TBP is observed from 2016-2019 compared to the base TBP in 2010.

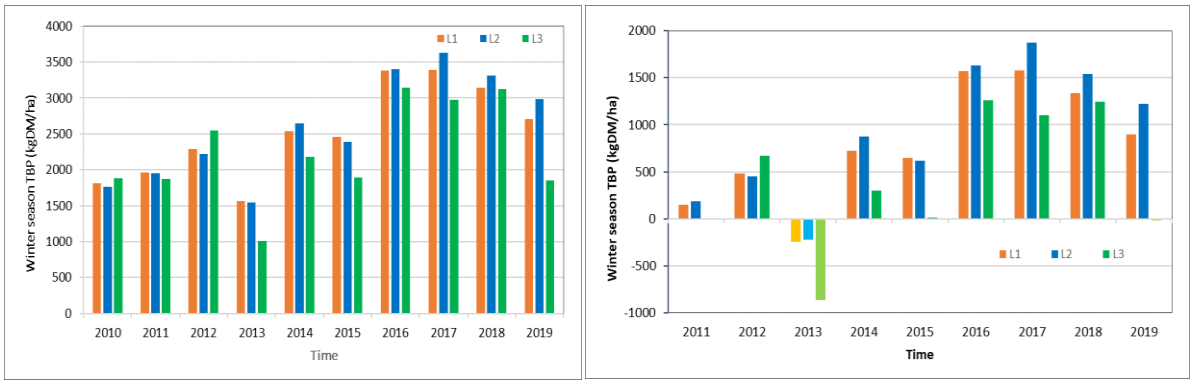

Figure 4-15: TBP of Wheat and yearly changes in TBP of WaPOR L1, L2, and L3 in winter season.

4.4. Gross Biomass Water Productivity

Gross biomass water productivity calculates in the relation between total biomass production to the total water consumption known as ETI, which is explained in section 3.5.6. Figure 3-2 shows the study area observed peak precipitation in August. Mul & Bastiaanssen (2019) reported that the average GBWP value for the Africa continent is 0.66 kgm^{-3}. In this study, dekadal GBWP was calculated for both the summer and winter season for the period 2009 to 2020.

4.4.1. Summer season GBWP_TBP

Summer season GBWP_TBP is calculated using equation 3.9. Figure 4.16 illustrates the time series of summer season GBWP_TBP of WaPOR L1, L2, and L3 for Cotton, Groundnut, and Sorghum. The results showed that from 2009 to 2014, there is a steady and gradual increase in water productivity of all three crops. These gradual increase in GBWP prevails for WaPOR L1, L2, and L3 and reaches a peak in 2014. It is noticeable that peak GBWP_TBP follows precipitation peak after 2-3 dekads for the period 2009 to 2014 and 2019. A reverse trend is observed for the period 2015 to 2018, where the GBWP_TBP peak is observed a dekad earlier for all crops. The GBWP_TBP average value of Cotton, Groundnut, and Sorghum from WaPOR L1, L2, and L3 was 0.50 km^{-3}, 0.56 kgm^{-3}, and 0.48 kgm^{-3} with a standard deviation of 0.25 kgm^{-3}, 0.28 kgm^{-3}, and 0.25 kgm^{-3}, respectively. The summer season average GBWP value of WaPOR L1, L2, and L3 are well below the continental average of 0.66 kgm^{-3}. It is noticeable that the seasonal precipitation also gradually increases over the period 2009 to 2014. In 2015, a sudden decrease was observed in GBWP and onwards. It is noticeable that in 2015, the observed precipitation was also substantially low compared to the previous years. From 2016 to 2019, the average precipitation was the same and well above from the 2015 value. From 2016 to 2018, the GBWP was remained low though the precipitation was stable over the period. In 2019, we observed a slight increase of GBWP of WaPOR L1, L2, and L3 for all Cotton, Groundnut, and Sorghum.

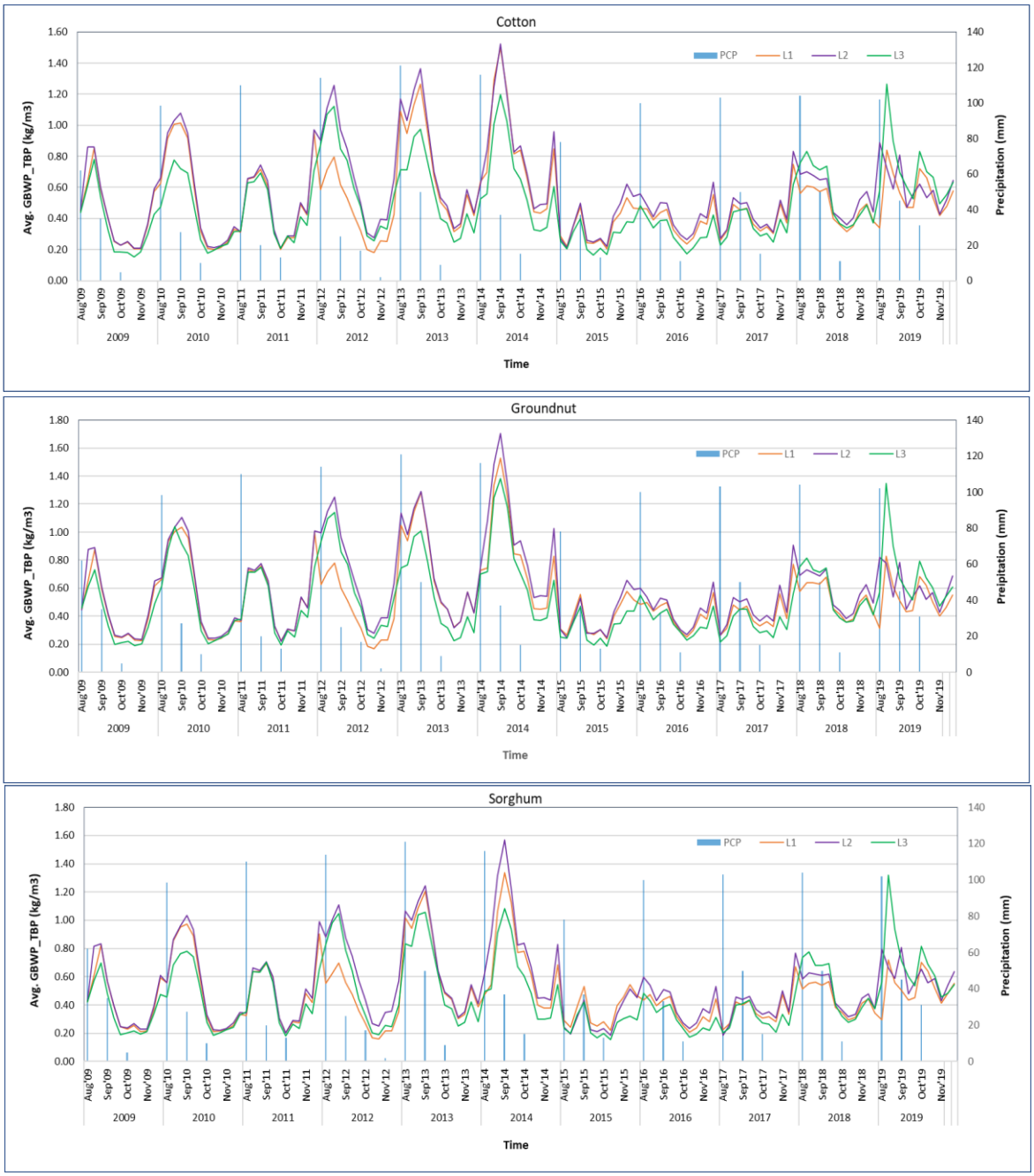

Figure 4-16: Dekadal average GBWP_TBP of WaPOR L1, L2, and L3 and monthly precipitation time series for Cotton, Groundnut, and Sorghum.

Figures 4.17 represent the sample temporal variation of WaPOR L3 GBWP_TBP of 26th dekad (left column images) of the year of 2009, 2014, & 2019 in the summer season and 4th dekad (right column images) of the year 2010, 2015, & 2020 in the winter season. Figures showed a significant spatial variation of GBWP_TBP was observed in the study area over the period. In the summer season, GBWP_TBP of the 26th dekadal of 2009 & 2014 was similar, whereas significant changes are observed in 2019. In the winter season, 4th dekad GBWP_TBP values also changed remarkably greatly from 2010 to 2020.

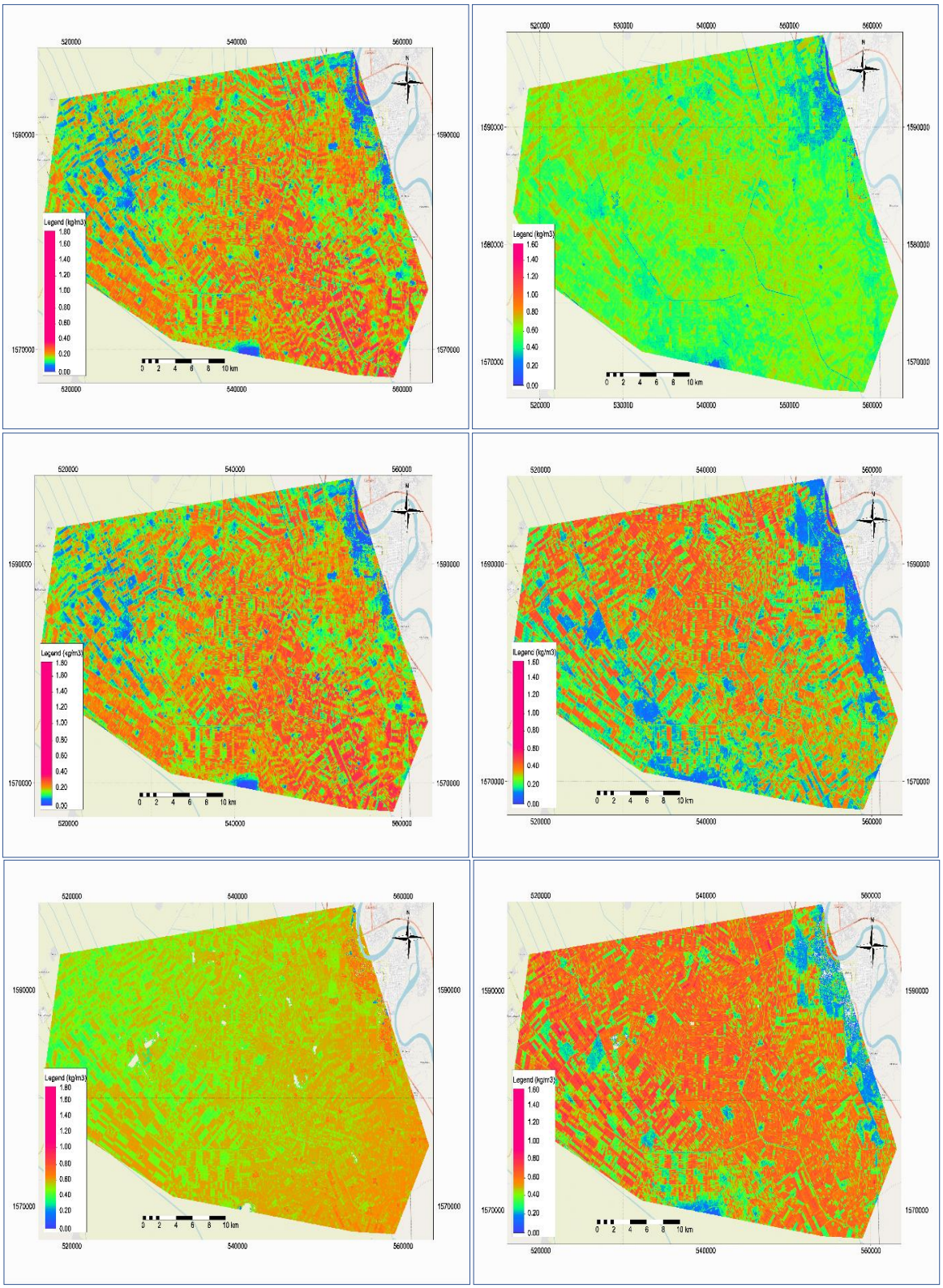

Figure 4-17: Temporal variations GBWP_TBP at 26th dekad of 2009, 2014 & 2019 (left column) in summer season and 4th dekad of 2010, 2015 & 2020 (right column) in winter season.

4.4.2. Winter Season GBWP_TBP

Figure 4.18 illustrates the time series of winter season GBWP_TBP of WaPOR L1, L2, and L3 for Onion, Pigeonpea, and Wheat for the period 2010 to 2020. The result shows from 2010 to 2014, almost the same pattern observed in GBWP_TBP of all three crops. From 2015 to 2019, WaPOR L1, L2, and L3 derived GBWP_TBP observed a slight increase for all three crops, although a trough in 2019 for L2 and L3. Winter season average GBWP_TBP values of Onion, Pigeonpea, and Wheat from WaPOR L1, L2, and L3 was 0.60 kgm^{-3}, 0.59 kgm^{-3}, and 0.52 kgm^{-3} with a standard deviation 0.28 kgm^{-3}, 0.34 kgm^{-3}, and 0.26 kgm^{-3}, respectively. The winter season average GBWP value of WaPOR L1, L2, and L3 are well below the continental average of 0.66 kgm^{-3}. It is noticeable, from 2010 to 2014, GBWP_TBP of all three levels was close to each other. However, from 2015 to onwards, considerable variations of GBWP_TBP values are observed for WaPOR L1, L2, and L3.

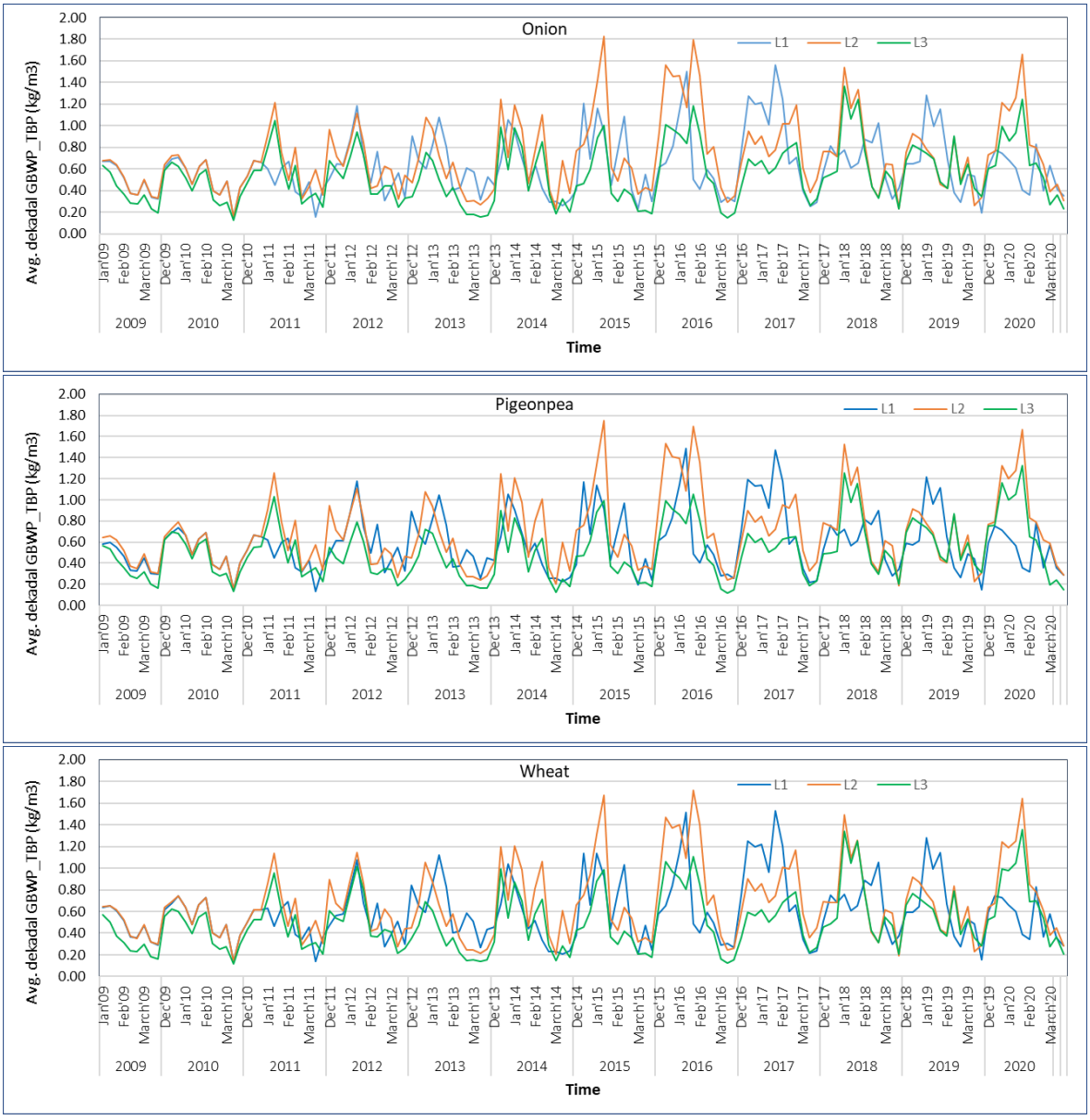

Figure 4-18: WaPOR L1, L2, and L3 dekadal GBWP_TBP time series for Onion, Pigeonpea, and Wheat.

4.5. Net Biomass Water Productivity

Net biomass water productivity calculates the relation between Above-ground biomass production to transpirational water consumption, which is explained in section 3.5.7. Equation 3-12 is used to calculate NBWP_AGBP. Figure 3-2 shows that most of the precipitation observed in the summer season, while winter season experience almost zero precipitation study area. All water requirements for crop production comes through irrigation. Mul & Bastiaanssen (2019) reported that the average NBWP value for the Africa continent is 1.20 kgm^{-3}. In this study, dekadal NBWP_AGBP is derived in the summer and winter season for the period 2009 to 2020 described in the following sections.

4.5.1. Summer Season NBWP_AGBP

NBWP_AGBP during the summer season calculated using equation 3.12. Figure 4-19 illustrates the time series of summer season NBWP_AGBP of WaPOR L1, L2, and L3 for Cotton, Groundnut, and Sorghum. The results show for 2009 to 2014, a steady and gradual increase in water productivity of all three crops with an exception in 2011. This gradual increase in NBWP prevails for all WaPOR L1, L2, and L3 and reaches a peak in 2014. It is noticeable that the peak of NBWP_AGBP follows the precipitation peak after 2-3 dekads in the period 2009 to 2014 and 2019. A reverse trend is observed for the period 2015 to 2018, where NBWP_AGBP and precipitation peak coincides or a dekad earlier than the precipitation peak for all crops. The NBWP_AGBP average value of Cotton, Groundnut, and Sorghum from WaPOR L1, L2, and L3 was 0.48 km^{-3}, 0.54 kgm^{-3}, and 0.43 kgm^{-3} with standard deviation of 0.24 kgm^{-3}, 0.28 kgm^{-3}, and 0.23 kgm^{-3}, respectively. The observed summer season average NBWP value of WaPOR L1, L2, and L3 are well below the continental average of 1.20 kgm^{-3}. It is noticeable that the seasonal precipitation also gradually increase over the period 2009 to 2014. In 2015, a sudden drop was observed in NBWP and onwards. It is also noticeable that in 2015 the observed precipitation is also substantially lower compared to the previous year. From 2016 to 2019, the average precipitation was the same and well above the 2015 value. Despite considerable precipitation for the period 2016 to 2018, the NBWP remained low. In 2019, we observed a slight increase of NBWP of WaPOR L1, L2, and L3 for all Cotton, Groundnut, and Sorghum.

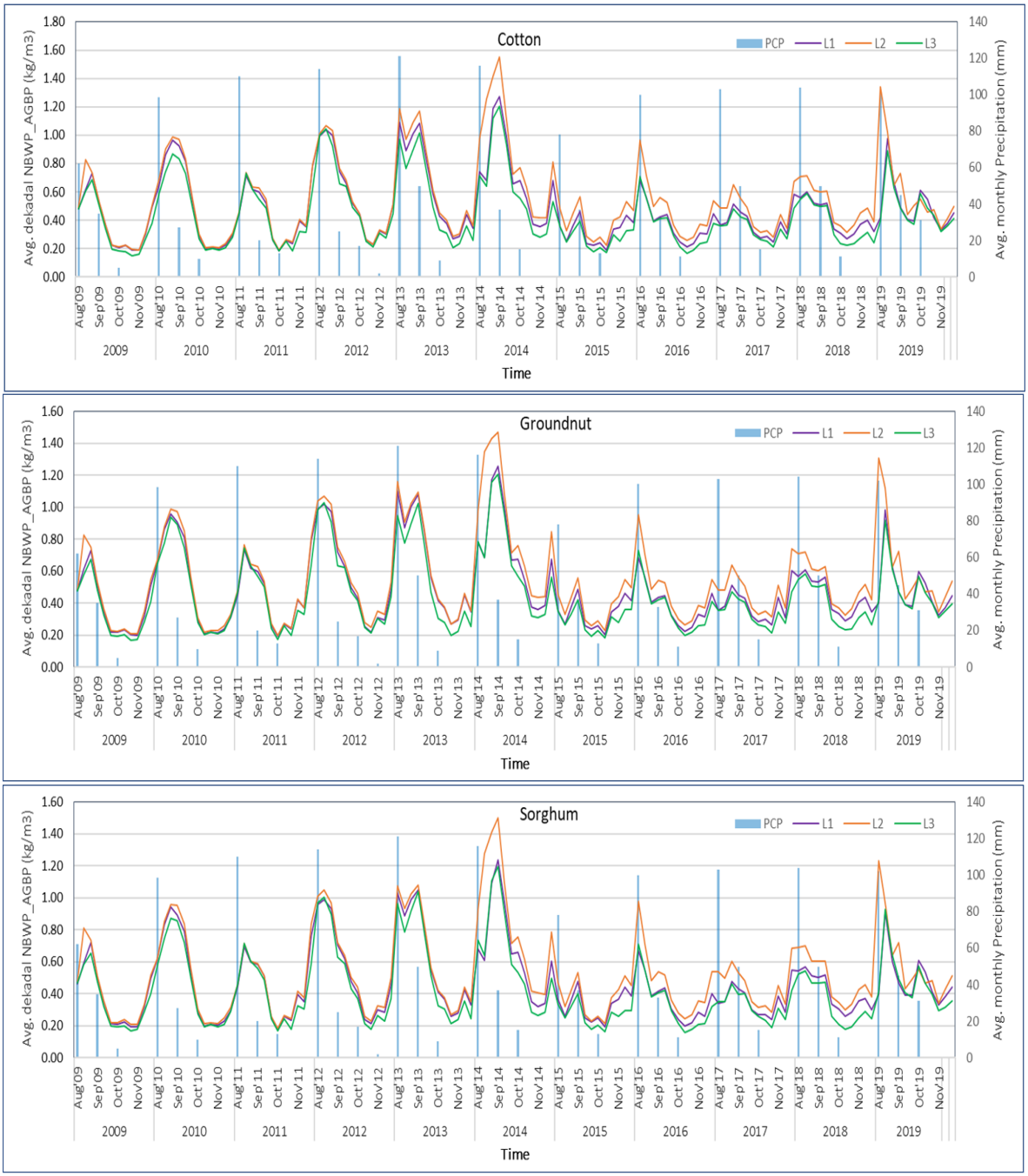

Figure 4-19: WaPOR L1, L2, and L3 dekadal NBWP_AGBP and monthly precipitation time series for Cotton, Groundnut, and Sorghum.

Figures 4-20 represent the sample temporal variation of WaPOR L3 NBWP_AGBP of 26th dekad (left column images) of the year 2009, 2014, & 2019 in the summer season and 4th dekad (Right column images) of the year 2010, 2015, & 2020 in the winter season. Figures show, over time, significant variation of spatial NBWP_AGBP in the study area. In the summer season, the 26th dekadal values of 2009 & 2019 are significantly different from 2014. In the winter season, 4th dekad GBWP_TBP values are almost similar for 2009, 2014 and 2020.

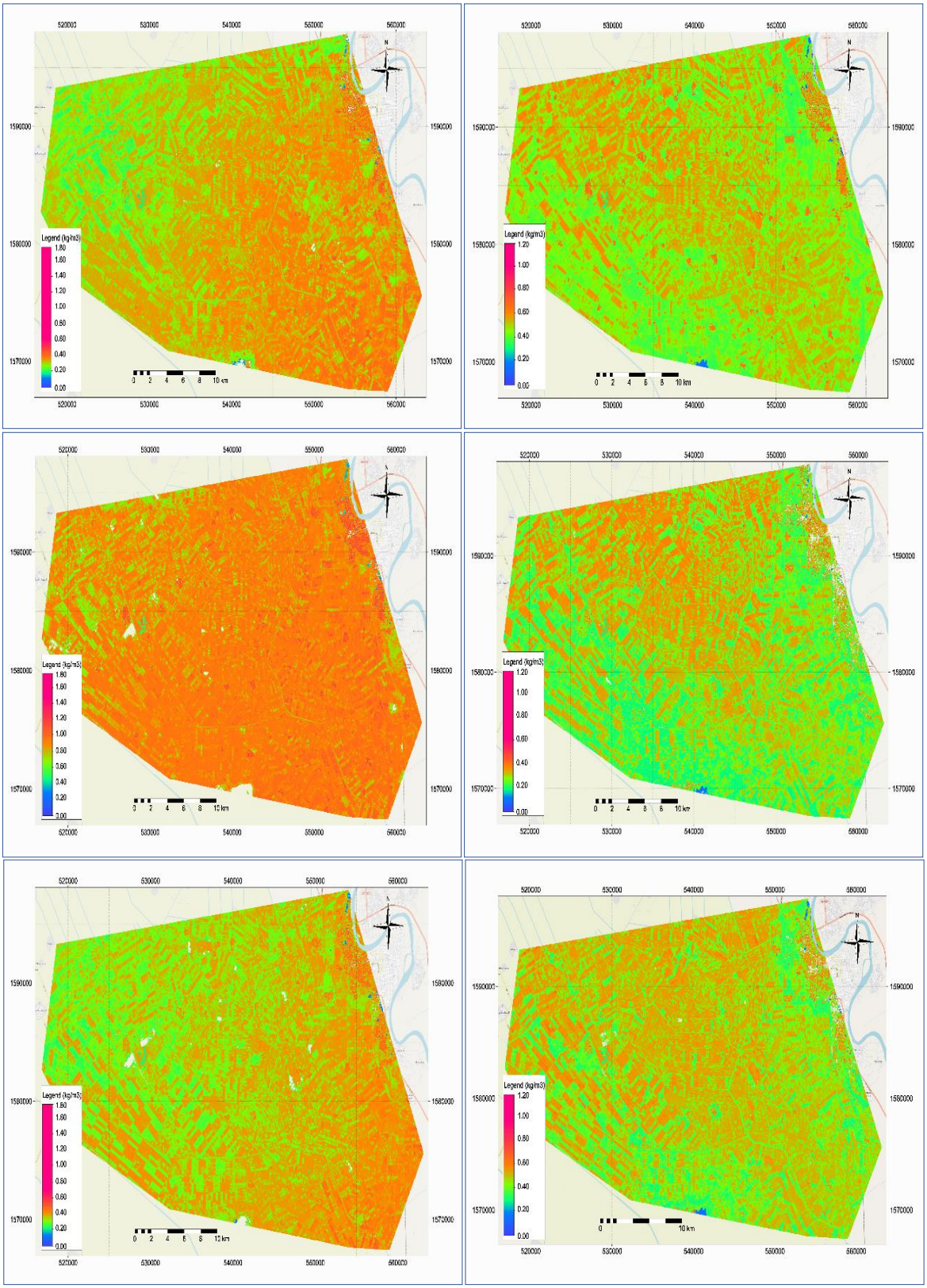

Figure 4-20: Temporal variations NBWP_AGBP at 26th dekad of 2009, 2014 & 2019 (left column) in summer season and 4th dekad of 2010, 2015 & 2020 (right column) in winter season.

4.5.2. Winter Season NBWP_AGBP

Figure 4-21 illustrates the time series of winter season NBWP_AGBP calculated from WaPOR L1, L2, and L3 for Onion, Pigeonpea, and Wheat. The result shows from 2010 to 2014, almost a similar pattern observed in NBWP_AGBP of all three crops. From 2015 to 2020, WaPOR L1, L2, and L3 derived NBWP_AGBP observed a slight increase for all crops, although a trough in 2019 for all levels. Winter season NBWP_AGBP average value of WaPOR L1, L2, and L3 is 0.51 kgm^{-3}, 0.59 kgm^{-3}, and 0.53 kgm^{-3}, with standard deviation of 0.21 kgm^{-3}, 0.26 kgm^{-3}, and 0.19 kgm^{-3}, respectively. In the winter season, the average NBWP value of WaPOR L1, L2, and L3 results are lower than half of the continental average of 1.20 kgm^{-3}. It is noticeable, from 2010 to 2014, WaPOR L1, L2, L3 measured NBWP_AGBP values are close to each other. However, from 2015 to onwards, considerable variations of NBWP_AGBP values are observed for WaPOR L1, L2, and L3.

Figure 4-21: WaPOR L1, L2, and L3 dekadal NBWP_AGBP time series for Onion, Pigeonpea, and Wheat.

4.6. Validation of Evapotranspiration

4.6.1. Summer Season ET

WaPOR L1, L2, and L3 derived dekadal ETI, and LSA SAF daily evapotranspiration DMET aggregated to the dekadal basis and used in the study. Summer and winter, two crop seasons of 2019-20, are used in the analysis. The distribution of dekadal ETI from WaPOR L1, L2, & L3 and LSA SAF ET DMET of Cotton is illustrated in Figure 4-22. All WaPOR L1, L2, & L3 and DMET followed a similar pattern upto the mid-season. After mid-season, DMET results in lower values compare to WaPOR measured ETI. The correlation between WaPOR L1, L2, & L3, and DMET was further investigated through regression analysis. The results showed a weak relation between WaPOR and DMET though WaPOR L1 results in better relation (R^2=0.40) compared to L2 (R^2=0.21) and L3 (R^2=0.18).

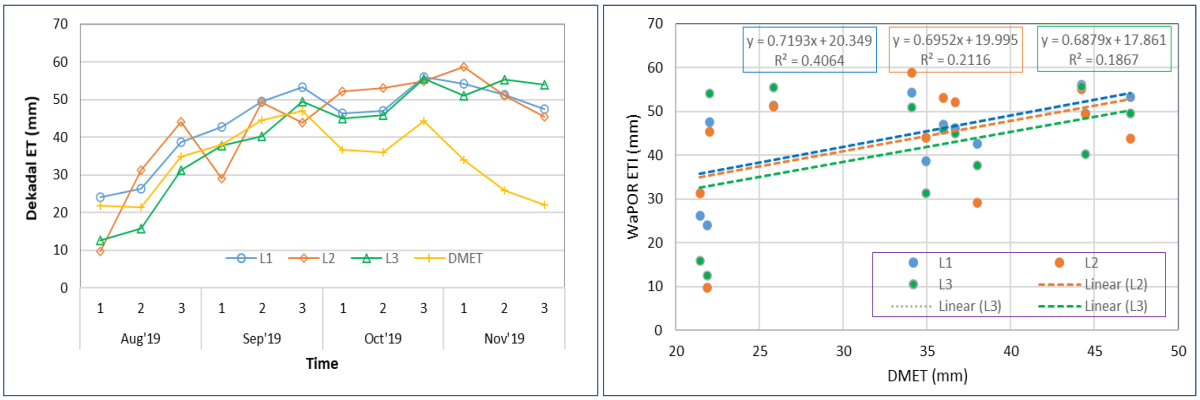

Figure 4-22: Summer season dekadal variation (left) and regression (right) of ETI of WaPOR L1, L2, & L3, and DMET of Cotton.

Figure 4-23 illustrates the distribution of dekadal ETI from WaPOR L1, L2, & L3 and LSA SAF ET DMET of Groundnut. Both Groundnut followed a similar pattern as Cotton. However, regression analysis shows that correlation between WaPOR L1, L2, & L3, and DMET was much better than Cotton. The results showed a moderate relation between WaPOR L1 and DMET with R^2 of 0.63. However, the relationship was poor and almost the same for L2 (R^2=0.37), and L3 (R^2=0.42).

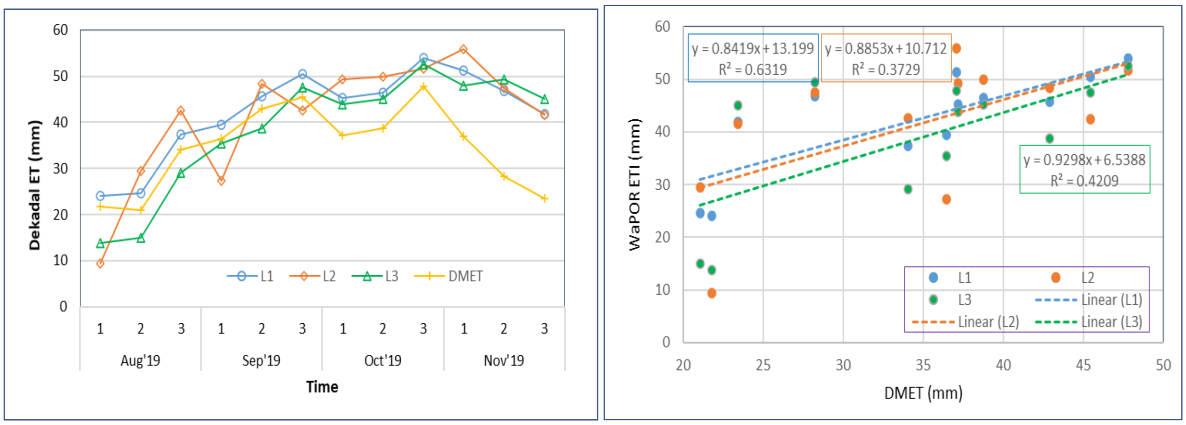

Figure 4-23: Summer season dekadal variation (left) and regression (right) of ETI of WaPOR L1, L2, & L3, and DMET of Groundnut.

Figure 4-24 illustrates the distribution of dekadal ETI from WaPOR L1, L2, & L3 and LSA SAF ET DMET of Sorghum. Results show that all the datasets followed a similar pattern, but DMET always results in lower ET than WaPOR. The regression analysis shows that the overall correlation between WaPOR L1, L2, & L3, and DMET was weak for Sorghum. The regression results of the relation between WaPOR L1, L2, & L3 with DMET was R^2 of 0.43, 0.42, and 0.56, respectively.

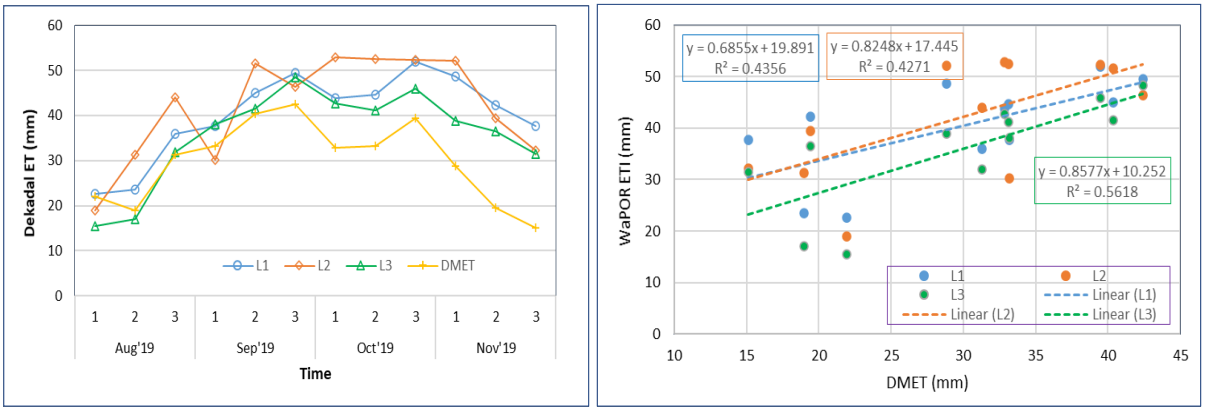

Figure 4-24: Summer season dekadal variation (left) and regression (right) of ETI of WaPOR L1, L2, & L3, and DMET of Sorghum.

4.6.2. Winter Season ET

Dekadal ETI from WaPOR L1, L2, and L3, and daily DMET LSA SAF aggregated on dekadal basis for the 2019-20 winter season of Onion, Pigeonpea, and Wheat are used in the analysis. The distribution of dekadal ETI from WaPOR L1, L2, & L3 and LSA SAF ET DMET of Onion, Pigeonpea, and Wheat are illustrated in Figure 4-25, and 4-26, respectively. WaPOR L1, L2, and L3 followed a similar pattern for Onion and Wheat, whereas L3 generated always results in a higher ET for the whole season. For Pigeonpea, WaPOR L1 and L2 followed a similar pattern, whereas L2 results in higher values upto mid-season and lower ET rest of the season. For all three crops, LSA SAF generated DMET results in low values, which followed almost a flat line with a tiny peak in the middle of the mid-season. The illustrated figures show that there is no noticeable relation between WaPOR ETI and DMET in the winter season in the study area.

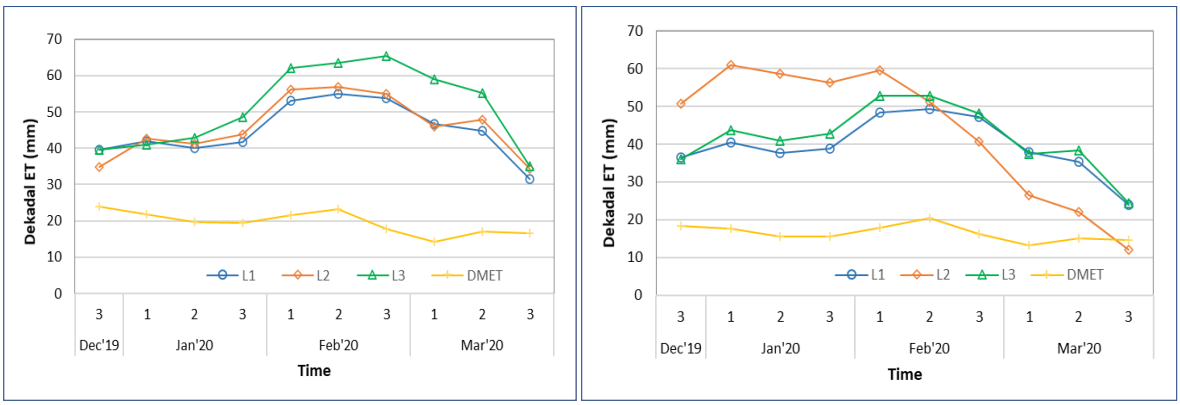

Figure 4-25: Winter season dekadal variation of ETI of WaPOR L1, L2, & L3, and DMET for Onion (left), and Pigeonpea (right).

There might be two reasons behind the low values of LSA SAF generated ET in the winter season. Since LSA SAF used a spatial resolution of 3km and there are some pocket built-up areas within the irrigation scheme at the study area. In the winter season, there is no precipitation, so LSA SAF averages the ET values from the crop and with the zero values from the built-up areas that result in very low ET. Another reason might be LSA SAF uses the Slob-de Bruin formula (De Bruin, 1987) that uses very few parameters and does not consider local irrigation and micro-climate effects on their ET estimation.

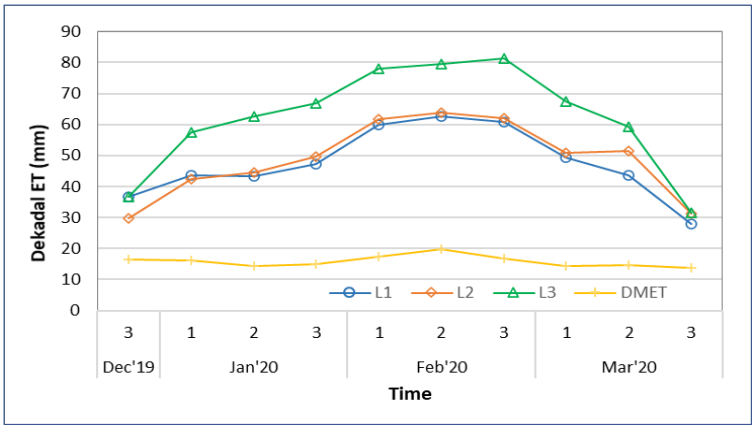

Figure 4-26: Winter season dekadal variation of ETI of WaPOR L1, L2, & L3, and DMET for Wheat.

4.6.3. Comparison of Water Productivity

WaPOR data derived L1, L2, and L3 GBWP_TBP and NBWP_AGBP values retrieved for Cotton, Groundnut, and Sorghum selected point of the summer season for the period 2009 to 2019. Yearly seasonal average GBWP_TBP and NBWP_AGBP of each crop on SOS, MOS, and EOS are computed for WaPOR L1, L2, and L3 separately. Similarly, winter seasonal average GBWP_TBP and NBWP_AGBP of Onion, Pigeonpea, and Wheat on SOS, MOS, and EOS are computed independently of WaPOR L1, L2, and L3 for the period 2009-10 to 2019-20. A comparative analysis is carried out for WaPOR L1, L2, and L3 as the water productivity retrieval point was fixed. The purpose of the study is to find how different spatial resolution represents water productivity in the study area.

4.6.4. Gross Biomass Water Productivity

Figure 4-27 illustrates the WaPOR L1, L2, and L3 derived average dekadal GBWP_TBP of summer and winter season for different crops. The results show that WaPOR L2 derived GBWP_TBP always higher compare to WaPOR L1 and L3. For all temporal region of SOS, MOS, and EOS, WaPOR L2 measured average GBWP_TBP was higher, and the pattern prevailed for all the crops in both summer and winter season. Average GBWP_TBP values in the SOS are higher than the EOS, which is expected as in the earlier season, biomass production occurred more efficiently. The amplitude of average GBWP_TBP was higher in the MOS, which is expected.

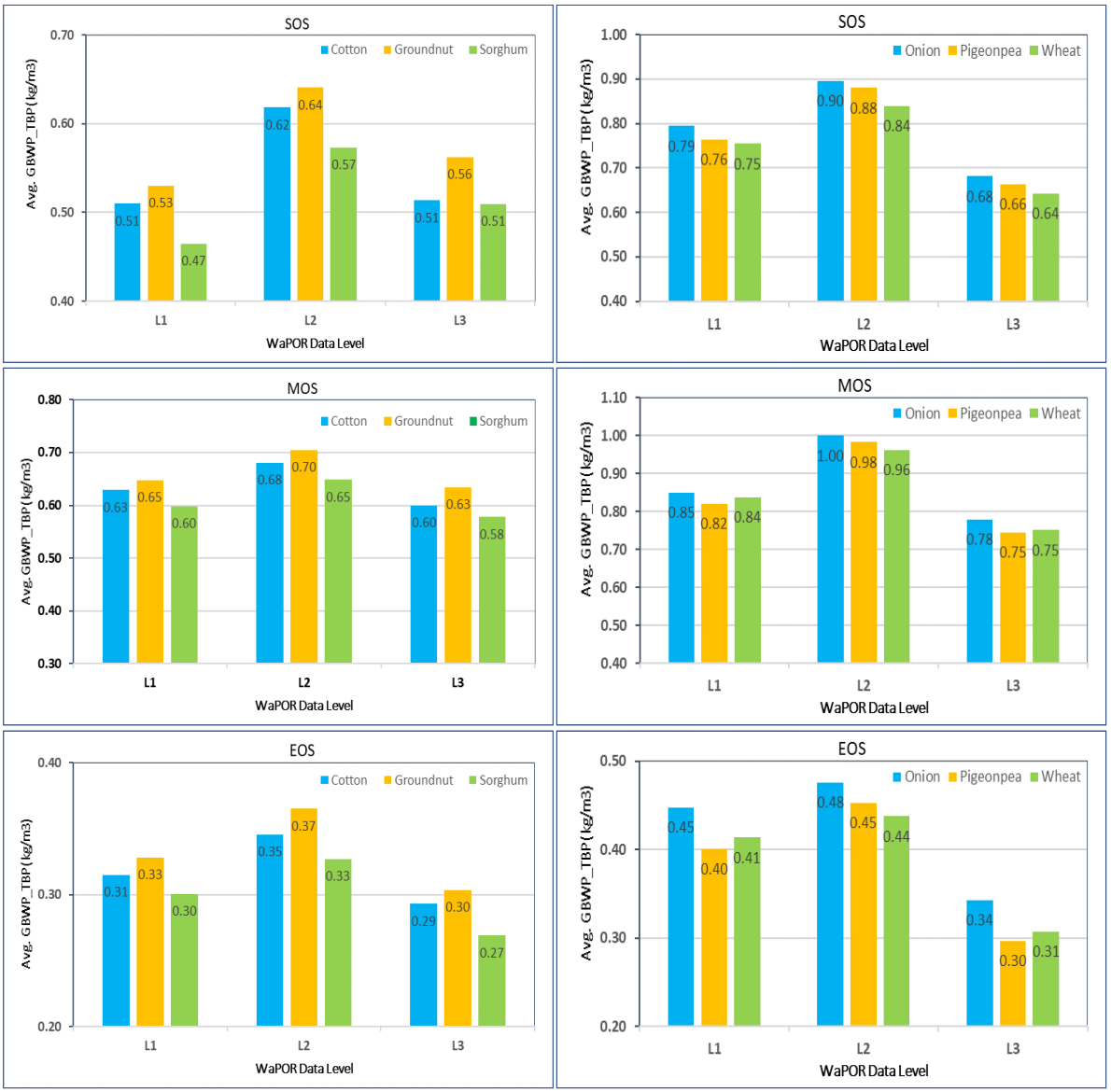

Figure 4-27: Average dekadal GBWP_TBP from WaPOR L1, L2, and L3 at SOS, MOS, and EOS of summer (Left) and winter (Right) season crops.

4.6.5. Net Biomass Water Productivity

Figure 4.28 illustrates the WaPOR L1, L2, and L3 derived average dekadal NBWP_AGBP of summer and winter season for Onion, Pigeonpea, and Wheat. The results show that WaPOR L2 derived NBWP_AGBP always higher compare to WaPOR L1 and L3. For all temporal region of SOS, MOS, and EOS, WaPOR L2 measured average dekadal NBWP_AGBP was higher, and the pattern prevailed for all the crops in both summer and winter season. Average NBWP_AGBP values in the SOS are higher than the EOS, which is expected as in the earlier season biomass produced more efficiently. The amplitude of average dekadal NBWP_AGBP was higher in the MOS, which is expected.

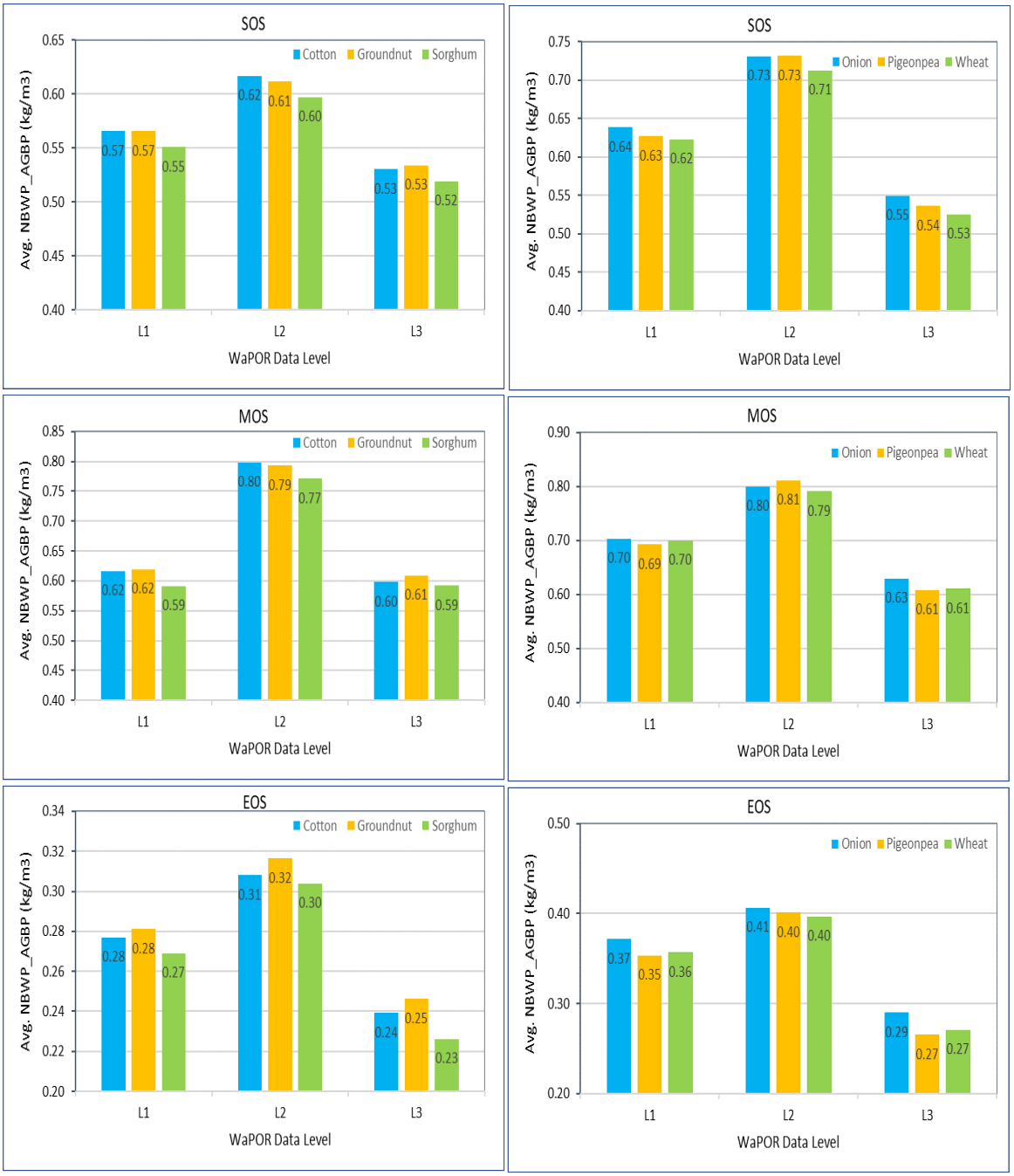

Figure 4-28: Average dekadal NBWP_AGBP from WaPOR L1, L2, and L3 at SOS, MOS, and EOS of summer (Left) and winter (Right) season crops.

5. LIMITATIONS AND OPPORTUNITIES

5.1. Limitations

One of the objectives of the study was to the validation of WaPOR L3 measured water productivity with in-situ measurement. Due to Sudan's political instability and global pandemic COVID-19, not all required in-situ measurements were available for the study. Validation of indirect measurement like remote sensing-based measurement reliability largely depends on its correlation with the ground measurements. Since satellite measures earth systems with its specific sensors that need further analysis and interpretation based on local environments and climates. Local environments and climatology on earth are spatially highly diversified. The results showed that water productivity assessment in the Gezira irrigation scheme needs further detailed study. It was a challenging task to conduct most of the research without face to face communication with peers, colleagues and friends.

5.2. Opportunities

To fulfill the objectives, openly accessible datasets such as LSA SAF DMET, ECMWF ERA5 precipitation are used in the study. Overall remote sensing offers tremendous opportunities to scientists, agronomists, engineers, policymakers and large farmer communities, and they will directly be benefited from the outputs of the study.

6. CONCLUSIONS AND RECOMMENDATIONS

The study is designed to evaluate WaPOR L1, L2, and L3 measured agricultural water productivity in the Gezira irrigation scheme in Sudan for the period 2009 to 2020. The analysis was carried out for the summer and winter seasons of the period. The seasonal average water consumption (ETI) computed from WaPOR and FRAME datasets for the whole period and retrieved value for pre-selected specific points. The seasonal average ETI of Cotton, Groundnut, and Sorghum was found 455mm, 485mm, 423mm, respectively. The values are within the range compared to other studies, Cotton, 317mm to 534mm, Singh et al. (2013), Groundnut 500mm to 700mm, and Sorghum 450mm to 750mm, respectively (Steduto et al., 2012). The average ETI for that period of Onion, Pigeonpea, and Wheat was 436mm, 354mm, and 372mm, respectively. Total biomass production varies significantly over the period; however, it followed a similar pattern of all the crops in the summer season. TBP increases from 2010 to 2014 and 2019, while the other year, TBP decreases compared to 2009 production for all three crops in the summer season. In the winter season, TBP increases from 2011 to 2019, with an exception in 2013 for all three crops compared to 2010 production. WaPOR L2 derived TBP results are always higher values compared to L1 and L3.

GBWP and NBWP time series almost follow a similar trend over the period. A gradual increase in water productivity is observed from 2009 to 2014, and in the next four years, a sharp decrease in productivity was observed for all crops in the summer season. However, the NDVI response to the precipitation was almost the same over the period. The seasonal average NDVI response followed the peak precipitation after 2-3 dekads throughout the period 2009 to 2019. The average GBWP_TBP and NBWP_AGBP of Cotton, Groundnut, and Sorghum in summer season was 0.51, 0.56, & 0.48 kgm^{-3} and 0.48, 0.54, & 0.43 kgm^{-3}, respectively. In addition, the average GBWP_TBP and NBWP_AGBP of Onion, Pigeonpea, and Wheat in winter season was 0.60, 0.59, & 0.52 kgm^{-3}, and 0.51, 0.59, & 0.53 kgm^{-3}, respectively. WaPOR estimated GBWP_TBP and NBWP_AGBP values for both summer and winter season are below the continental average of 0.66 kgm^{-3} and 1.20 kgm^{-3} respectively (Mul & Bastiaanssen, 2019). There are several possible reasons or combination of reasons for the low average GBWP and NBWP values found within the study area. The first one might be the overestimation of water consumption (ETI) because ETI estimation in WaPOR uses CHIRPS v2 precipitation data as input. A comparison between CHIRPS v2 with another independent precipitation dataset (ERA5 from ECMWF) shows that over the period, CHIRPS v2 estimates higher precipitation in the study area (Figure 4-2). In the summer season, comparison between WaPOR measured ETI and DMET showed that at the end of the season, all WaPOR L1, L2, and L3 results in considerably higher evapotranspiration. The second possible cause might be due to changes in the inputs, e.g., related to the use of other sensors overtime of the datasets. There is a major change in input elements, such as from 2014, WaPOR L2 used PROBA-V sensor derived data instead of MODIS resampled data. Besides, the MERRA model also replaced by the GEOS-5

atmospheric circulation model at the same time for the downscaling and retrieving of meteorological data components for WaPOR L1, L2, and L3. This transformation from MERRA to GEOS-5 might have a significant influence on water productivity assessment because this change is applied to all levels. There also some reasons that are Gezira scheme oriented. The occurrence of some fallow or sparse vegetation fields adjacent to the main crop fields in both summer and winter season could result in low aggregate WP. The local expert also confirmed that some cultivable land remained fallow in both seasons. Moreover, long-term political instability in Sudan might be another crucial factor that farmers might be afraid of insecurity in the farming business. The political instability might affect the management and operation & maintenance of the Gezira irrigation scheme.

Validation of ET with an independent data set, like DMET, results in moderate to poor correlation between the two datasets in the summer season. From the SOS to MOS, both WaPOR L1, L2, & L3 and DMET followed a similar trend. After MOS, DMET sharply decreased to the end of the season, whereas WaPOR L1, L2, and L3 ET were significantly higher during the remainder of the season for all crops. In the Winter season, DMET results in very low ET, and there is no relation between DMET and WaPOR L1, L2, and L3 measured ET. The spatial resolution of DMET might play a crucial role because, in the Gezira scheme, there are some dispersedly distributed built-up and bare areas within the irrigation scheme. As the DMET spatial resolution is 3*3 KM, each pixel might contain some built-up and bare areas, and subsequently, the aggregate ET value becomes lower.

Comparative analysis among the WaPOR l1, L2, and L3 shows that WaPOR L2 measured water productivity is always higher than L1 and L3 for all crops in both summer and winter season. The water productivity in the MOS always shows higher productivity compared to SOS and EOS as expected for all crops in both the summer and winter season. This observation and results indicate that the overall water productivity in the Gezira irrigation scheme is rated low. There is sufficient scope to improve water productivity in the scheme. To obtain a better insight into these discrepancies, as mentioned above, further detailed study is required.

LIST OF REFERENCES

Abbott, B. W., Bishop, K., Zarnetske, J. P., Minaudo, C., Chapin, F. S., Krause, S., … Pinay, G. (2019). Human domination of the global water cycle absent from depictions and perceptions. *Nature Geoscience*, *12*(7), 533–540. https://doi.org/10.1038/s41561-019-0374-y

Al Zayed, I. S., Elagib, N. A., Ribbe, L., & Heinrich, J. (2016). Satellite-based evapotranspiration over Gezira Irrigation Scheme, Sudan: A comparative study. *Agricultural Water Management*, *177*, 66–76. https://doi.org/10.1016/j.agwat.2016.06.027

Alexandratos, N., & Bruinsma, J. (2012). *World Agriculture Towards 2030 / 2050: The 2012 revision* (ESA Working paper No. 12-03). Rome, FAO.

Ali, M. H., & Talukder, M. S. U. (2008). Increasing water productivity in crop production-A synthesis. *Agricultural Water Management*, *95*(11), 1201–1213. https://doi.org/10.1016/j.agwat.2008.06.008

Allen, R. G., Pereira, L. S., Howell, T. A., & Jensen, M. E. (2011). Evapotranspiration information reporting: I. Factors governing measurement accuracy. *Agricultural Water Management*, *98*(6), 899–920. https://doi.org/10.1016/j.agwat.2010.12.015

Allen, R. G., Pereira, L. S., Raes, D., & Smith, M. (1998). *Crop evapotranspiration-Guidelines for computing crop water requirements. FAO Irrigation and Drainage Paper No. 56,*. Rome, FAO. https://doi.org/10.1016/j.eja.2010.12.001

Allen, R. G., Pereira, L. S., Raes, D., & Smith, M. (2005). Penman-Monteith Equation. *Encyclopedia of Soils in the Environment. Elsevier/Academic Press, Oxford/Boston*, 180–188.

Bastiaanssen, W G M, Cheema, M. J. M., Immerzeel, W. W., & Miltenburg, I. J. (2012). Surface energy balance and actual evapotranspiration of the transboundary Indus Basin estimated from satellite measurements and the ETLook model, *48*, 1–16. https://doi.org/10.1029/2011WR010482

Bastiaanssen, Wim G.M., Molden, D. J., & Makin, I. W. (2000). Remote sensing for irrigated agriculture: Examples from research and possible applications. *Agricultural Water Management*, *46*(2), 137–155. https://doi.org/10.1016/S0378-3774(00)00080-9

Biradar, C. M., Thenkabail, P. S., Platonov, A., Xiao, X., Geerken, R., Noojipady, P., … Vithanage, J. (2008). Water productivity mapping methods using remote sensing. *Journal of Applied Remote Sensing*, *2*. https://doi.org/10.1117/1.3033753

Blatchford, M. L., Mannaerts, C. M., Njuki, S. M., Nouri, H., Zeng, Y., Pelgrum, H., … Karimi, P. (2020). Evaluation of WaPOR V2 evapotranspiration products across Africa. *Hydrological Processes*, 1–24. https://doi.org/10.1002/hyp.13791

Blatchford, M. L., Mannaerts, C. M., Zeng, Y., Nouri, H., & Karimi, P. (2019). Status of accuracy in remotely sensed and in-situ agricultural water productivity estimates: A review. *Remote Sensing of Environment*, *234*(September 2018), 111413. https://doi.org/10.1016/j.rse.2019.111413

Bruinsma, J. (2009). The resources outlook: by how much do land, water and crop yields need To increase by 2050? (pp. 233–278).

Bushara, M., & Ahmed, A. (2016). Economic Analysis of Cotton Production in the Gezira Scheme: 19 70-2004. *Journal of Business & Financial Affairs*, *5*(2). https://doi.org/10.4172/2167-0234.1000191

Cai, X. M., & Rosegrant, M. W. (2009). World water productivity: current situation and future options. *Water Productivity in Agriculture: Limits and Opportunities for Improvement*, 163–178. https://doi.org/10.1079/9780851996691.0163

Cai, X., & Sharma, B. (2009). Remote sensing and census based assessment and scope for improvement of rice and wheat water productivity in the Indo-Gangetic Basin. *Science in China, Series E: Technological Sciences*, *52*(11), 3300–3308. https://doi.org/10.1007/s11431-009-0346-3

Choudhury, I., & Bhattacharya, B. (2018). An assessment of satellite-based agricultural water productivity over the Indian region. *International Journal of Remote Sensing*, *39*(8), 2294–2311.

https://doi.org/10.1080/01431161.2017.1421792

Christy, C. D. (2008). Real-time measurement of soil attributes using on-the-go near-infrared reflectance spectroscopy. *Computers and Electronics in Agriculture*, *61*(1), 10–19. https://doi.org/10.1016/j.compag.2007.02.010

Clay, D. E., Kim, K. I., Chang, J., Clay, S. A., & Dalsted, K. (2006). Characterizing water and nitrogen stress in corn using remote sensing. *Agronomy Journal*, *98*(3), 579–587. https://doi.org/10.2134/agronj2005.0204

Cohen, Y., Alchanatis, V., Meron, M., Saranga, Y., & Tsipris, J. (2005). Estimation of leaf water potential by thermal imagery and spatial analysis. *Journal of Experimental Botany*, *56*(417), 1843–1852. https://doi.org/10.1093/jxb/eri174

Conrad, C., Dech, S. W., Hafeez, M., Lamers, J., Martius, C., & Strunz, G. (2007). Mapping and assessing water use in a Central Asian irrigation system by utilizing MODIS remote sensing products. *Irrigation and Drainage Systems*, *21*(3–4), 197–218. https://doi.org/10.1007/s10795-007-9029-z

Corwin, D. L., & Lesch, S. M. (2003). Application of soil electrical conductivity to precision agriculture: Theory, principles, and guidelines. *Agronomy Journal*, *95*(3), 455–471. https://doi.org/10.2134/agronj2003.0455

Courault, D., Seguin, B., & Olioso, A. (2005). Review on estimation of evapotranspiration from remote sensing data: From empirical to numerical modeling approaches. *Irrigation and Drainage Systems*, *19*(3–4), 223–249. https://doi.org/10.1007/s10795-005-5186-0

De Bruin, H. A. R. (1987). From Penman to Makkink. In J. Hooghart (Ed.), *Evaporation and Weather* (pp. 5–31). Ede, The Netherlands.

de Fraiture, C., & Wichelns, D. (2010). Satisfying future water demands for agriculture. *Agricultural Water Management*, *97*(4), 502–511. https://doi.org/10.1016/j.agwat.2009.08.008

Doorebos, J., & Kassam, A. H. (1979). *Yield response to water. FAO Irrigation and Drainage Paper No. 33*. FAO, Rome.

Elshaikh, A. E., Yang, S. H., Jiao, X., & Elbashier, M. M. (2018). Impacts of legal and institutional changes on irrigation management performance: A case of the Gezira irrigation scheme, Sudan. *Water (Switzerland)*, *10*(11). https://doi.org/10.3390/w10111579

FAO. (2011a). *The State of Food and Agriculture: Women in agriculture*. Rome, FAO. https://doi.org/10.1109/PVSC.2008.4922754

FAO. (2011b). *The state of the world's land and water resources for food and agriculture (SOLAW) – Managing systems at risk*. FAO, Rome and Earthscan, London. https://doi.org/10.1007/978-3-319-92049-8_31

FAO. (2012). *Coping with water scarcity: An action framework for agriculture and food security*. *FAO Water Reports* (Vol. 38). https://doi.org/http://www.fao. org/docrep/016/i3015e/i3015e.pdf

FAO. (2015). Towards a water critical perspectives for policy-makers. *Food and Agriculture Organization of the United Nations.*, 8–9. Retrieved from http://www.fao.org/3/a-i4560e.pdf

FAO. (2016). *Water accounting and Auditing: A sourcebook*. FAO, Rome. Retrieved from http://www.fao.org/publications/card/en/c/d43dad58-d587-48dd-ad0e-7c4a7397a175/

FAO. (2018a). *WaPOR Database Methodology: Level 1 Data Using Remote Sensing in Support of Solutions To Reduce Agricultural Water Productivity Gaps. Food and Agriculture Organization of the United Nations (FAO)*. Rome. Retrieved from http://www.fao.org/3/i7315en/i7315en.pdf

FAO. (2018b). *WaPOR Database Methodology: Level 2 Data Using Remote Sensing in Support of Solutions To Reduce Agricultural Water Productivity Gaps. Food and Agriculture Organization of the United Nations (FAO)*. Rome. Retrieved from http://www.fao.org/3/i7315en/i7315en.pdf

FAO. (2018c). *WaPOR Database Methodology: Level 3 Data Using Remote Sensing in Support of Solutions To Reduce Agricultural Water Productivity Gaps. Food and Agriculture Organization of the United Nations (FAO)*. Rome. Retrieved from http://www.fao.org/3/i7315en/i7315en.pdf

Ge, Y., Li, X., Hu, M. G., Wang, J. H., Jin, R., Wang. J. F., & Zhang, R. H. (2013). Technical specification for the validation of remote sensing products. *International Archives of the Photogrammetry, Remote Sensing and Spatial Information Sciences*, *XL-2/W1*(June), 13–17.

Ghilain, N., Arboleda, A., & Gellens-Meulenberghs, F. (2011). Evapotranspiration modelling at large scale using near-real time MSG SEVIRI derived data. *Hydrology and Earth System Sciences*, *15*(3), 771–786. https://doi.org/10.5194/hess-15-771-2011

Kijne, J. W., Barker, R., & Molden, D. (2003). Improving Water Productivity in Agriculture: Editors' Overview, in Jacob Kijne and others (Eds.) Water Productivity in Agriculture: Limits and Opportunities for Improvement, Comprehensive Assessment of Water Management in Agriculture. *UK: CABI Publishing*. Colombo, Sri Lanka.

Lamb, D. W., & Brown, R. B. (2001). Remote-sensing and mapping of weeds in crops. *Journal of Agricultural and Engineering Research*, *78*(2), 117–125. https://doi.org/10.1006/jaer.2000.0630

Li, H., Zheng, L., Lei, Y., Li, C., Liu, Z., & Zhang, S. (2008). Estimation of water consumption and crop water productivity of winter wheat in North China Plain using remote sensing technology. *Agricultural Water Management*, *95*(11), 1271–1278. https://doi.org/10.1016/j.agwat.2008.05.003

Lipper, L., Thornton, P., Campbell, B. M., Baedeker, T., Braimoh, A., Bwalya, M., … Torquebiau, E. F. (2014). Climate-smart agriculture for food security. *Nature Climate Change*, *4*(12), 1068–1072. https://doi.org/10.1038/nclimate2437

Molden, D., Oweis, T., Steduto, P., Bindraban, P., Hanjra, M. A., & Kijne, J. (2010). Improving agricultural water productivity: Between optimism and caution. *Agricultural Water Management*, *97*(4), 528–535. https://doi.org/10.1016/j.agwat.2009.03.023

Monteith, J. L. (1965). Evaporation and Environment. *Symposia of the Society for Experimental Biology*, (19), 205–234.

Monteith, J. L. (1972). Solar Radiation and Productivity in Tropical Ecosystems. *The Journal of Applied Ecology*, *9*(3), 747. https://doi.org/10.2307/2401901

Mu, Q., Zhao, M., & Running, S. W. (2011). Improvements to a MODIS global terrestrial evapotranspiration algorithm. *Remote Sensing of Environment*, *115*(8), 1781–1800. https://doi.org/10.1016/j.rse.2011.02.019

Mul, M., & Bastiaanssen, W. (2019). WaPOR quality assessment: Technical report on the data quality of the WaPOR FAO database version 1.0, (April), 117.

Mulla, D. J. (2013). Twenty five years of remote sensing in precision agriculture: Key advances and remaining knowledge gaps. *Biosystems Engineering*, *114*(4), 358–371. https://doi.org/10.1016/j.biosystemseng.2012.08.009

Patil, V. C., Al-Gaadi, K. A., Madugundu, R., Tola, E. H. M., Marey, S., Aldosari, A., … Gowda, P. H. (2015). Assessing agricultural water productivity in desert farming system of Saudi Arabia. *IEEE Journal of Selected Topics in Applied Earth Observations and Remote Sensing*, *8*(1), 284–297. https://doi.org/10.1109/JSTARS.2014.2320592

Platonov, A., Thenkabail, P. S., Biradar, C. M., Cai, X., Gumma, M., Dheeravath, V., … Isaev, S. (2008). Water productivity mapping (WPM) using landsat ETM+ data for the irrigated croplands of the Syrdarya river basin in Central Asia. *Sensors*, *8*(12), 8156–8180. https://doi.org/10.3390/s8128156

Ramankutty, N., Sheehan, J., Siebert, S., Mueller, N. D., Monfreda, C., Brauman, K. A., … Zaks, D. P. M. M. (2011). Solutions for a cultivated planet. *Nature*, *478*(7369), 337–342. https://doi.org/10.1038/nature10452

Russo, T., Alfredo, K., & Fisher, J. (2014). Sustainable water management in urban, agricultural, and natural systems. *Water (Switzerland)*, *6*(12), 3934–3956. https://doi.org/10.3390/w6123934

Seelan, S. K., Laguette, S., Casady, G. M., & Seielstad, G. A. (2003). Remote sensing applications for precision agriculture: A learning community approach. *Remote Sensing of Environment*, *88*(1–2), 157–169. https://doi.org/10.1016/j.rse.2003.04.007

Shanahan, J. F., Schepers, J. S., Francis, D. D., Varvel, G. E., Wilhelm, W. W., Tringe, J. M., … Major, D. J. (2001). Use of remote-sensing imagery to estimate corn grain yield. *Agronomy Journal*, *93*(3), 583–589. https://doi.org/10.2134/agronj2001.933583x

Singh, S. K., Datta, S., & Dharaiya, N. (2013). Estimation of crop evapotranspiration of cotton using remote sensing technique. *International Journal of Environmental Engineering and Management*, *4*(1), 523–528.

Steduto, P., Raes, D., Hsiao, T. C., Fereres, E. (2012). Crop yield response to water. *FAO Irrigation and Drainage Paper 66*.

Sun, H. Y., Liu, C. M., Zhang, X. Y., Shen, Y. J., & Zhang, Y. Q. (2006). Effects of irrigation on water balance, yield and WUE of winter wheat in the North China Plain. *Agricultural Water Management*, *85*(1–2), 211–218. https://doi.org/10.1016/j.agwat.2006.04.008

Sun, Z., Gebremichael, M., Ardö, J., Nickless, A., Caquet, B., Merboldh, L., & Kutschi, W. (2012). Estimation of daily evapotranspiration over Africa using MODIS/Terra and SEVIRI/MSG data. *Atmospheric Research*, *112*, 35–44. https://doi.org/10.1016/j.atmosres.2012.04.005

Tasumi, M., Trezza, R., Allen, R. G., & Wright, J. L. (2005). Operational aspects of satellite-based energy balance models for irrigated crops in the semi-arid U.S. *Irrigation and Drainage Systems*, *19*(3–4), 355–376. https://doi.org/10.1007/s10795-005-8138-9

Teixeira, A. H. d. C., Bastiaanssen, W. G. M., Ahmad, M. D., & Bos, M. G. (2009). Reviewing SEBAL input parameters for assessing evapotranspiration and water productivity for the Low-Middle São Francisco River basin, Brazil. Part A: Calibration and validation. *Agricultural and Forest Meteorology*, *149*(3–4), 462–476. https://doi.org/10.1016/j.agrformet.2008.09.016

Thorp, K. R., & Tian, L. F. (2004). A review on remote sensing of weeds in agriculture. *Precision Agriculture*, *5*(5), 477–508. https://doi.org/10.1007/s11119-004-5321-1

Tilling, A. K., O'Leary, G. J., Ferwerda, J. G., Jones, S. D., Fitzgerald, G. J., Rodriguez, D., & Belford, R. (2007). Remote sensing of nitrogen and water stress in wheat. *Field Crops Research*, *104*(1–3), 77–85. https://doi.org/10.1016/j.fcr.2007.03.023

Trigo, I. F., & DeBruin, H. (2016). Validation report Reference Evapotranspiration METREF (LSA-303), (I), 1–38. Retrieved from https://landsaf.ipma.pt/en/products/evapotranspiration-energy-flxs/metref/

United Nations. (2014). WWAP (United Nations World Water Assessment Programme). 2014. The United Nations World Water Development Report 2014: *Water and Energy.* (Vol. 1). Paris. https://doi.org/10.18356/c7830fe1-en

United Nations. (2016). About the Sustainable Development Goals - United Nations Sustainable Development. Retrieved July 4, 2019, from https://www.un.org/sustainabledevelopment/sustainable-development-goals/

Veroustraete, F., Sabbe, H., & Eerens, H. (2002). Estimation of carbon mass fluxes over Europe using the C-Fix model and Euroflux data. *Remote Sensing of Environment*, *83*(3), 376–399. https://doi.org/10.1016/S0034-4257(02)00043-3

Wada, Y., Flörke, M., Hanasaki, N., Eisner, S., Fischer, G., Tramberend, S., … Wiberg, D. (2016). Modeling global water use for the 21st century: The Water Futures and Solutions (WFaS) initiative and its approaches. *Geoscientific Model Development*, *9*(1), 175–222. https://doi.org/10.5194/gmd-9-175-2016

Xiong, Y. J., Qiu, G. Y., Yin, J., Zhao, S. H., Wu, X. Q., Wang, P., & Zeng, S. (2008). Estimation of daily evapotranspiration by three-temperatures model at large catchment scale. *International Archives of the Photogrammetry, Remote Sensing and Spatial Information Sciences - ISPRS Archives*, *37*, 767–774.

Yang, C., Everitt, J. H., Bradford, J. M., & Escobar, D. E. (2000). Information & Electrical Technologies Division of ASAE, *43*(6), 1927–1938.

Zwart. (2010). *Benchmarking water productivity in agriculture and the scope for improvement: remote sensing modelling from field to global scale*. https://doi.org/ISBN: 978-90-6562-237-2

Zwart, S. J., & Bastiaanssen, W. G. M. (2004). Review of measured crop water productivity values for irrigated wheat, rice, cotton and maize. *Agricultural Water Management*, *69*(2), 115–133. https://doi.org/10.1016/j.agwat.2004.04.007

Zwart, S. J., Bastiaanssen, W. G. M., de Fraiture, C., & Molden, D. J. (2010). A global benchmark map of water productivity for rainfed and irrigated wheat. *Agricultural Water Management*, *97*(10), 1617–1627. https://doi.org/10.1016/j.agwat.2010.05.018

APPENDICES

A. Data Description (L1&L2)

Data Level	Data Component	Input Data Components	Sensor	Data Product	Remarks
L1 & L2	Evaporation, Transpiration, Interception	Precipitation		CHIRPS v2, CHIRP	
		Surface albedo	MODIS/ PROBA-V	MOD09GA, MOD09GQ	MODIS for L1, For L2, MODIS MOD09GA, MOD09GQ data resampled to 100m until PROBA-V data available from March 2014.
		NDVI	MODIS/ PROBA-V	MOD09GQ	MODIS for L1, For L2, MODIS MOD09GA, MOD09GQ data resampled to 100m until PROBA-V data available from March 2014.
		Soil moisture stress	MODIS	MOD11A1, MYD11A1	Land Surface Temperature
		Solar radiation		SRTM	DEM
			MSG		Transmissivity
		Land Cover		WaPOR LCC Product	
		Weather data (Temp., Sp. humidity, wind speed, air pressure)	MERRA/ GEOS-5		MERRA used up to 21-2-2014
L1 & L2	Net Primary Products (NPP)	Solar radiation		SRTM	DEM
			MSG		Transmissivity
		Soil moisture stress	MODIS	MOD11A1, MYD11A1	Land Surface Temperature
		fAPAR	MODIS/ PROBA-V	MOD09GQ	MODIS for L1, For L2, MODIS MOD09GQ data resampled to 100m until PROBA-V data available from March 2014.
		Precipitation		CHIRPS v2, CHIRP	
		Land Cover		WaPOR LCC Product	
		Weather data (Temp., Sp. humidity, wind speed, air pres.)	MERRA/ GEOS-5		MERRA used up to 21-2-2014

B. Data Description (L3)

Data Level	Data Component	Input Data Components	Sensor	Data Product	Remarks
L3	Evaporation, Transpiration, Interception	Precipitation		CHIRPS v2	
		Surface albedo	LANDSAT (5, 6 and 7)		
		NDVI	LANDSAT (5, 6 and 7)		
		Soil moisture stress	LANDSAT (5, 6 and 7)		Land Surface Temperature
			MERRA/ GEOS-5		MERRA used up to 21-2-2014
		Solar radiation		SRTM	DEM
			MSG		Transmissivity
		Land Cover	LANDSAT (5, 6 and 7)		
		Weather data (Temperature, Specific humidity, wind speed, air pressure)	MERRA/ GEOS-5		MERRA used up to 21-2-2014
L3	Net Primary Products (NPP)	Solar radiation		SRTM	DEM
			MSG		Transmissivity
			MERRA/ GEOS-5		MERRA used up to 21-2-2014
		Soil moisture stress	LANDSAT (5, 6 and 7)		Land Surface Temperature
		fAPAR	LANDSAT (5, 6 and 7)		
		Precipitation		CHIRPS v2	
		Land Cover	LANDSAT (5, 6 and 7)		
		Weather data (Temperature, Specific humidity, wind speed, air pressure)	MERRA/GEOS-5		MERRA used up to 21-2-2014

C. Summer Crop Information

Serial No	Crop Name	Start of the Season (SOS)	End of the Season (EOS)	No. of irrigations	Farm Area (ha)	Yield (ton/ha)
1	Cotton1	Mid-Jul.	Begin Dec.	5	3.36	1.169
2	Cotton2	Begin Jul.	Mid Nov.	3	1.68	1.063
3	Cotton3	Begin Jul.	Mid Nov.	4	1.68	1.382
4	Cotton4	Begin Jul.	Mid Nov.	4	1.68	1.169
5	Cotton5	Begin Jul.	Mid Nov.	5	1.68	1.275
6	Cotton6	Begin Jul.	Begin Nov.	4	0.84	1.488
7	Cotton7	Begin Jul.	Begin Nov.	4	1.68	1.594
8	Cotton8	Begin Jul.	Mid Nov.	4	1.68	1.063
9	Cotton9	Begin Aug.	End Nov.	4	1.26	1.063
10	Cotton10	Mid-Jul.	End Nov.	4	5.04	1.488
11	Cotton11	Begin Jul.	Mid Nov.	4	2.52	1.275
12	Cotton12	Begin Jul.	End Nov.	4	0.84	0.531
13	Groundnut1	Begin Jul.	End Nov.	4	1.68	1.179
14	Groundnut2	Begin Jun.	Mid Nov.	4	1.68	1.607
15	Groundnut3	Mid Jun.	Mid Nov.	3	1.68	2.143
16	Groundnut4	Mid Jun.	Mid Nov.	5	1.68	1.179
17	Groundnut5	Begin Jul.	End Nov.	4	1.68	1.286
18	Groundnut6	Begin Jul.	Mid Nov.	4	1.68	3.274
19	Groundnut7	Begin Jul.	Begin Nov.	4	1.68	1.286
20	Groundnut8	Begin Jul.	Mid Nov.	4	0.84	1.071
21	Groundnut9	Begin Jul.	Mid Nov.	4	2.1	2.357
22	Groundnut10	Begin Jul.	End Nov.	4	29.4	1.393
23	Groundnut11	Begin Jul.	Mid Nov.	4	0.84	1.071
24	Groundnut12	Begin Jul.	Mid Nov.	4	2.94	1.071
25	Sorghum1	Begin Jul.	Mid Nov.	2	1.68	1.429
26	Sorghum2	Begin Jul.	Mid Nov.	3	2.52	3.571
27	Sorghum3	Begin Jul.	Mid Nov.	3	1.68	3.333
28	Sorghum4	Begin Jul.	End Oct.	3	1.68	3.571
29	Sorghum5	Begin Jul.	Mid Nov.	3	1.68	2.857
30	Sorghum6	Begin Jul.	End Oct.	3	0.84	3.095
31	Sorghum7	Begin Jul.	Mid Nov.	3	0.84	2.857
32	Sorghum8	Begin Jul.	Begin Nov.	4	37.8	2.381
33	Sorghum9	Begin Aug.	Mid Nov.	4	37.8	3.571
34	Sorghum10	Begin Jul.	Mid Nov.	3	37.8	3.571
35	Sorghum11	Begin Jul.	End Nov.	3	2.1	2.381

D. Winter Crop Information

Serial No	Crop	Start of the Season (SOS)	End of the Season (EOS)	No. of irrigations	Farm Area (ha)	Yield (ton/ha)
1	Onion1	Begin Dec.	Mid-April	5		20.000
2	Onion2	Begin Dec.	Begin April	5	12.60	22.857
3	Onion3	Begin Dec.	Begin April	5	12.60	22.857
4	Onion4	Begin Nov.	Begin March	7	4.20	28.571
5	Onion5	Begin Dec.	Mid-April	5		22.857
6	Onion6	Begin Dec.	Begin March	6	8.40	28.571
7	Onion7	Begin Nov.	Begin March	7	1.26	28.571
8	Onion8	Begin Dec.	Mid April	5	0.84	17.143
9	Onion9	Mid Nov.	Begin April	6	4.20	14.286
10	Onion10	Mid Nov.	Begin April	6	2.10	15.714
11	Onion11	Begin Dec.	Begin March	5	1.68	15.714
12	Onion12	Begin Nov.	Begin March	7	1.26	30.286
13	Onion13	Mid Nov.	Mid March	4	1.26	22.857
14	Onion14	Mid Nov.	Mid March	6	6.30	28.571
15	Onion15	Mid-Oct.	End Feb.	8		24.286
16	Onion16	Mid-Oct.	End Feb.	8		14.286
17	Onion17	Begin Nov.	Mid-March	7		17.143
18	Pigeonpea1	Mid-Aug.	Mid-Feb.	10	5.04	2.083
19	Pigeonpea2	Mid-Aug.	Mid-Feb.	10	12.60	1.786
20	Pigeonpea3	Mid-Sep.	Mid-March	8	18.90	2.083
21	Pigeonpea4	Mid-Aug.	Mid-Feb.	10		2.381
22	Pigeonpea5	Mid-Aug.	Mid-Feb.	10	12.60	2.083
23	Pigeonpea6	Mid-Aug.	Begin March	10	18.90	1.786
24	Pigeonpea7	Mid-Aug.	Mid-Feb.	7	12.60	2.083
25	Pigeonpea8	Mid-Aug.	Mid-Feb.	7	12.60	2.679
26	Pigeonpea9	Begin Sep.	Begin March	10	1.68	2.083
27	Pigeonpea10	Mid-Aug.	Mid-Feb.	10	2.10	2.381
28	Pigeonpea11	Mid-Aug.	Mid-Feb.	10	2.10	1.786
29	Pigeonpea12	Mid-Aug.	Mid-Feb.	8	1.68	1.488
30	Pigeonpea13	Mid-Aug.	Mid-Feb.	10	2.10	2.083
31	Pigeonpea14	Mid-Aug.	Mid-Feb.	10	2.10	2.083
32	Pigeonpea15	Begin Aug.	Mid-Feb.	9	2.10	2.381
33	Pigeonpea16	Mid-Aug.	Mid-Feb.	10	4.20	2.679
34	Pigeonpea17	Mid-Aug.	Mid-Feb.	10	37.80	2.083
35	Wheat1	Mid Nov.	Mid March	6	12.60	3.571
36	Wheat2	Mid Dec.	Begin March	4	8.40	3.095
37	Wheat3	Begin Dec.	Begin March	4	37.80	3.571
38	Wheat4	Mid Nov.	Mid March	6	37.80	4.762
39	Wheat5	Mid Nov.	Mid-March	5	18.90	4.762
40	Wheat6	End Dec.	Mid-March	3	4.20	1.905

Serial No	Crop	Start of the Season (SOS)	End of the Season (EOS)	No. of irrigations	Farm Area (ha)	Yield (ton/ha)
41	Wheat7	Begin Dec.	Begin March	5	4.20	3.571
42	Wheat8	Begin Dec.	Begin April	5	2.94	4.286
43	Wheat9	Mid Dec.	Mid-April	4	4.20	2.381
44	Wheat10	Begin Jan.	End April	3	6.30	1.190
45	Wheat11	Begin Dec.	End March	5	37.80	1.429
46	Wheat12	Begin Dec.	End March	5	37.80	4.762
47	Wheat13	Begin Dec.	Mid-March	5	37.80	4.524
48	Wheat14	Mid Nov.	Mid March	6	1.68	4.762
49	Wheat15	Begin Jan.	Mid April	3	0.84	1.190
50	Wheat16	Begin Dec.	Mid March	5	8.40	3.095
51	Wheat17	Begin Dec.	Mid-March	7	4.20	4.524

E. Summer Season Ground Truthing Information

Sl. No.	Sample point	Longitude	Latitude		Sl. No.	Sample point	Longitude	Latitude
1	Bare/grass1	33.27418	14.31758		44	Cotton1	33.406458	14.197046
2	Bare/grass10	33.33677	14.35939		45	Cotton10	33.341375	14.362838
3	Bare/grass11	33.50402	14.36991		46	Cotton11	33.450988	14.41598
4	Bare/grass12	33.50222	14.37149		47	Cotton12	33.300731	14.360245
5	Bare/grass13	33.40145	14.27963		48	Cotton2	33.372667	14.221507
6	Bare/grass14	33.36236	14.27469		49	Cotton3	33.562695	14.223076
7	Bare/grass15	33.39164	14.22403		50	Cotton4	33.562746	14.228534
8	Bare/grass16	33.30383	14.26087		51	Cotton5	33.382817	14.271762
9	Bare/grass2	33.27533	14.31324		52	Cotton6	33.384395	14.280594
10	Bare/grass3	33.27791	14.31636		53	Cotton7	33.430568	14.296818
11	Bare/grass4	33.27905	14.31910		54	Cotton8	33.522196	14.325944
12	Bare/grass5	33.24627	14.33581		55	Cotton9	33.228576	14.32976
13	Bare/grass6	33.24604	14.32293		56	Depression1	33.45595	14.23634
14	Bare/grass7	33.21288	14.33248		57	Depression2	33.26435	14.32596
15	Bare/grass8	33.30768	14.35679		58	Depression3	33.27795	14.33240
16	Bare/grass9	33.31642	14.36038		59	Depression4	33.55153	14.26057
17	Builtup1	33.53070	14.31441		60	Depression5	33.43701	14.31381
18	Builtup10	33.39156	14.28364		61	Depression6	33.35047	14.29243
19	Builtup11	33.39813	14.27953		62	Depression7	33.33983	14.40959
20	Builtup12	33.33497	14.29015		63	Depression8	33.46747	14.33443
21	Builtup13	33.25240	14.33185		64	Groundnut1	33.405909	14.243359
22	Builtup14	33.31231	14.35801		65	Groundnut10	33.383589	14.416387
23	Builtup15	33.43226	14.26866		66	Groundnut11	33.396412	14.41103
24	Builtup2	33.53234	14.31220		67	Groundnut12	33.419907	14.39807
25	Builtup3	33.52748	14.31806		68	Groundnut2	33.354405	14.272353
26	Builtup4	33.52701	14.31745		69	Groundnut3	33.319402	14.283344
27	Builtup5	33.52734	14.31612		70	Groundnut4	33.495061	14.309447
28	Builtup6	33.50978	14.40442		71	Groundnut5	33.507113	14.318593
29	Builtup7	33.51627	14.40195		72	Groundnut6	33.290412	14.361346
30	Builtup8	33.51603	14.40039		73	Groundnut7	33.36633	14.365249
31	Builtup9	33.50702	14.38909		74	Groundnut8	33.339523	14.369456
32	Canal1	33.41178	14.30104		75	Groundnut9	33.359289	14.395778
33	Canal10	33.42946	14.41109		76	Onion1	33.436978	14.352282
34	Canal11	33.38480	14.41792		77	Onion2	33.419003	14.319333
35	Canal12	33.27495	14.30448		78	Onion3	33.402112	14.268842
36	Canal2	33.41604	14.31000		79	Onion4	33.345607	14.274877
37	Canal3	33.42501	14.32934		80	Onion5	33.262234	14.354603
38	Canal4	33.41239	14.33487		81	Onion6	33.431115	14.41049
39	Canal5	33.38878	14.24941		82	Pigeonpea1	33.399886	14.208874
40	Canal6	33.48533	14.23071		83	Pigeonpea2	33.331864	14.235715
41	Canal7	33.49855	14.20600		84	Pigeonpea3	33.439351	14.367516
42	Canal8	33.54394	14.23039		85	Pigeonpea4	33.397667	14.256468
43	Canal9	33.32440	14.25347		86	Pigeonpea5	33.434157	14.409278

Sl. No.	Sample point	Longitude	Latitude
87	Pigeonpea6	33.454808	14.417286
88	Sorghum1	33.334663	14.245802
89	Sorghum10	33.364302	14.403221
90	Sorghum11	33.441641	14.409935
91	Sorghum2	33.563005	14.246092
92	Sorghum3	33.563615	14.268597
93	Sorghum4	33.395592	14.256861
94	Sorghum5	33.355728	14.274822

Sl. No.	Sample point	Longitude	Latitude
95	Sorghum6	33.314976	14.288015
96	Sorghum7	33.338353	14.284338
97	Sorghum8	33.214244	14.323585
98	Sorghum9	33.251152	14.349949
99	Water1	33.50680	14.43429
100	Water2	33.50751	14.42575
101	Water3	33.51030	14.41773
102	Water4	33.51732	14.40861

F. Winter Season Ground Truthing Information

Sl. No.	Sample point	Longitude	Latitude		Sl. No.	Sample point	Longitude	Latitude
1	Bare/grass1	33.2742	14.3176		41	Canal8	33.5439	14.2304
2	Bare/grass10	33.3368	14.3594		42	Canal9	33.3244	14.2535
3	Bare/grass11	33.5040	14.3699		43	Depression1	33.4559	14.2363
4	Bare/grass12	33.5022	14.3715		44	Depression2	33.2644	14.3260
5	Bare/grass13	33.4014	14.2796		45	Depression3	33.2779	14.3324
6	Bare/grass14	33.3624	14.2747		46	Depression4	33.5515	14.2606
7	Bare/grass15	33.3916	14.2240		47	Depression5	33.4370	14.3138
8	Bare/grass16	33.3038	14.2609		48	Depression6	33.3505	14.2924
9	Bare/grass2	33.2753	14.3132		49	Onion1	33.2608	14.3538
10	Bare/grass3	33.2779	14.3164		50	Onion10	33.4166	14.2886
11	Bare/grass4	33.2791	14.3191		51	Onion11	33.4255	14.2745
12	Bare/grass5	33.2463	14.3358		52	Onion12	33.4404	14.2702
13	Bare/grass6	33.2460	14.3229		53	Onion13	33.4431	14.2836
14	Bare/grass7	33.2129	14.3325		54	Onion14	33.4423	14.2942
15	Bare/grass8	33.3077	14.3568		55	Onion15	33.4782	14.3102
16	Bare/grass9	33.3164	14.3604		56	Onion16	33.4965	14.3115
17	Builtup1	33.5307	14.3144		57	Onion17	33.5053	14.3179
18	Builtup10	33.3916	14.2836		58	Onion2	33.2785	14.3612
19	Builtup11	33.3981	14.2795		59	Onion3	33.3212	14.3662
20	Builtup12	33.3350	14.2902		60	Onion4	33.3777	14.4144
21	Builtup13	33.2524	14.3319		61	Onion5	33.4506	14.3879
22	Builtup14	33.3123	14.3580		62	Onion6	33.4517	14.4027
23	Builtup15	33.4323	14.2687		63	Onion7	33.5635	14.2264
24	Builtup2	33.5323	14.3122		64	Onion8	33.4018	14.2687
25	Builtup3	33.5275	14.3181		65	Onion9	33.4053	14.2852
26	Builtup4	33.5270	14.3175		66	P Trees1	33.3501	14.4080
27	Builtup5	33.5273	14.3161		67	Pigeonpea1	33.2114	14.3203
28	Builtup6	33.5098	14.4044		68	Pigeonpea10	33.4110	14.1791
29	Builtup7	33.5163	14.4019		69	Pigeonpea11	33.4032	14.2023
30	Builtup8	33.5160	14.4004		70	Pigeonpea12	33.3836	14.2148
31	Builtup9	33.5070	14.3891		71	Pigeonpea13	33.3681	14.2338
32	Canal1	33.4118	14.3010		72	Pigeonpea14	33.3699	14.2774
33	Canal10	33.4295	14.4111		73	Pigeonpea15	33.4235	14.2801
34	Canal11	33.3848	14.4179		74	Pigeonpea16	33.4532	14.3115
35	Canal2	33.4160	14.3100		75	Pigeonpea17	33.4680	14.3142
36	Canal3	33.4250	14.3293		76	Pigeonpea2	33.2489	14.3468
37	Canal4	33.4124	14.3349		77	Pigeonpea3	33.2973	14.3600
38	Canal5	33.3888	14.2494		78	Pigeonpea4	33.3305	14.3732
39	Canal6	33.4853	14.2307		79	Pigeonpea5	33.3646	14.4076
40	Canal7	33.4985	14.2060		80	Pigeonpea6	33.3824	14.4162

Continuation of Winter Season Ground Truthing Information

Sl. No.	**Sample point**	**Longitude**	**Latitude**		Sl. No.	**Sample point**	**Longitude**	**Latitude**
81	Pigeonpea7	33.4330	14.4065		93	Wheat14	33.3234	14.2876
82	Pigeonpea8	33.4522	14.3981		94	Wheat15	33.4307	14.2624
83	Pigeonpea9	33.5626	14.2474		95	Wheat16	33.4461	14.2898
84	Water1	33.5068	14.4343		96	Wheat17	33.4830	14.3062
85	Water2	33.5075	14.4257		97	Wheat2	33.2385	14.3329
86	Water3	33.5103	14.4177		98	Wheat3	33.3411	14.3833
87	Water4	33.5173	14.4086		99	Wheat4	33.3503	14.3874
88	Wheat1	33.2055	14.3160		100	Wheat5	33.3600	14.3965
89	Wheat10	33.3728	14.2226		101	Wheat6	33.4104	14.4037
90	Wheat11	33.3592	14.2362		102	Wheat7	33.4540	14.4075
91	Wheat12	33.3357	14.2345		103	Wheat8	33.4013	14.2095
92	Wheat13	33.3343	14.2505		104	Wheat9	33.3869	14.2160

G. Land Cover Classification Confusion Matrix in Summer Season

Reference data

Classified data	Bare/ Grass	Cotton	Groundnut	Onion	Depression	Builtup	Canal	Pigeonpea	Sorghum	Water	Total
Bare/ Grass	14	0	0	0	0	2	0	0	0	0	16
Cotton	0	10	1	0	0	0	0	0	1	0	12
Groundnut	0	1	10	0	0	0	0	0	1	0	12
Onion	0	0	1	4	0	0	0	1	0	0	6
Depression	0	0	0	0	6	0	1	0	0	1	8
Builtup	2	0	0	0	0	13	0	0	0	0	15
Canal	0	0	0	0	2	0	9	0	0	1	12
Pigeonpea	0	0	0	1	0	0	0	5	0	0	6
Sorghum	0	1	0	0	0	0	0	0	10	0	11
Water	0	0	0	0	0	0	0	0	0	4	4
Total	16	12	12	5	8	15	10	6	12	6	85

ACCURACY TOTALS:

	Reference Totals	Classified Totals	Number Correct	Producer Accuracy (%)	User Accuracy (%)
Bare/ Grass	16	16	14	87.50	87.50
Cotton	12	12	11	91.67	91.67
Groundnut	12	12	10	83.33	83.33
Onion	6	5	4	66.67	80.00
Depression	8	8	5	62.50	62.50
Builtup	15	15	13	86.67	86.67
Canal	12	10	9	75.00	90.00
Pigeonpea	6	6	5	83.33	83.33
Sorghum	11	12	10	90.91	83.33
Water	4	6	4	100.00	66.67
Total	102	102	85		

Overall classification accuracy (%)= 83.33

Overall Kappa (K^) coefficient =0.817

H. Land Cover Classification Confusion Matrix in Winter Season

Reference data

Classified data	Bare/ grass	Pigeonpea	Wheat	Onion	Depression	Builtup	Canal	Water	Total
Bare/ grass	13	1	0	1	0	1	0	0	16
Pigeonpea	0	12	2	2	0	0	1	0	17
Wheat	0	2	13	2	0	0	0	0	17
Onion	0	1	1	15	0	0	0	0	17
Depression	0	0	0	0	6	0	0	0	6
Builtup	2	0	0	0	0	14	0	0	16
Canal	1	0	0	0	0	0	10	0	11
Water	0	0	0	0	0	0	0	4	4
Total	16	16	16	20	6	16	11	4	88

ACCURACY TOTALS:

	Reference Totals	Classified Totals	Number Correct	Producer Accuracy (%)	User Accuracy (%)
Bare/ grass	16	15	13	81.25	86.67
Pigeonpea	17	16	12	70.59	75.00
Wheat	17	16	13	76.47	81.25
Onion	17	20	15	88.24	75.00
Depression	6	6	6	100.00	100.00
Builtup	16	16	15	93.75	93.75
Canal	11	11	10	90.91	90.91
Water	4	4	4	100.00	100.00
Total	104	104	88		

Overall classification accuracy (%)= 84.62

Overall Kappa (K^) coefficient =0.821

I. Precipitation Extract Sample Point in the Gezira Scheme.

Precipitation comparison CHIRPS-V2 and ERA-5
Table: Sample point locations

Sample Point	Longitude	Latitude
Cotton10	33.341375	14.362838
Groundnut5	33.507113	14.318593
Onion1	33.436978	14.352282
Sorghum11	33.441641	14.409935
Sorghum5	33.355728	14.274822
Wheat2	33.238512	14.332855
Wheat10	33.372814	14.222618
Onion6	33.451734	14.402671
Onion16	33.496454	14.311456
Pigeonpea15	33.42349	14.280098

J. Script to Extract Precipitation from Google Earth Engine

Script to Extract CHIRPS-V2 from GEE

Example for cotton 10:

```
// Example script to load and visualize CHIRPS-V2 daily precipitation in Google Earth Engine
var dataset = ee.ImageCollection('UCSB-CHG/CHIRPS/DAILY')
                .filter(ee.Filter.date('2009-01-01', '2020-01-01'));
var precipitation = dataset.select('precipitation');
var precipitationVis = {
 min: 1.0,
  max: 17.0,
  palette: ['001137', '0aab1e', 'e7eb05', 'ff4a2d', 'e90000'],
};
Map.setCenter(33.5, 14.2);
Map.addLayer(precipitation, precipitationVis, 'Precipitation');

// point location in lon - lat
var testPoint = ee.Geometry.Point(33.341375,14.362838);
print (testPoint);
Map.addLayer(testPoint, {}, 'default display');

print(ui.Chart.image.series(precipitation, testPoint));
```

Script to Extract ERA-5 from GEE

Example for cotton 10:

```
// Example script to load and visualize ERA5 climate reanalysis parameters in Google Earth Engine
// Daily total precipitation sums
var era5_tp = ee.ImageCollection('ECMWF/ERA5/DAILY')
   .select('total_precipitation')
   .filter(ee.Filter.date('2009-01-01', '2020-01-01'));
print(era5_tp);

// Visualization palette for total precipitation
var visTp = {
  min: 0,
  max: 0.1,
  palette: ['#FFFFFF', '#00FFFF', '#0080FF', '#DA00FF', '#FFA400', '#FF0000']
};

// Add a layer to map
Map.addLayer(
 era5_tp.filter(ee.Filter.date('2019-07-15')), visTp,
  'Daily total precipitation sums');

// point location in lon - lat
var testPoint = ee.Geometry.Point(33.341375,14.362838);
print (testPoint);
Map.addLayer(testPoint, {}, 'default display');

print(ui.Chart.image.series(era5_tp, testPoint));
```

K. Seasonal average ETI derived from WaPOR for the major crop in the summer season.

			2009	2010	2011	2012	2013	2014	2015	2016	2017	2018	2019	Avg
Cotton	L1	Min	314	295	219	299	305	261	300	320	293	306	375	299
		Max	737	574	626	703	582	573	685	631	631	760	709	656
		Mean	480	418	472	506	445	455	440	497	489	522	537	478
		Std	120	88	118	110	90	90	115	94	114	114	100	105
	L2	Min	340	299	219	293	304	217	237	241	230	298	329	273
		Max	653	567	620	646	565	610	677	595	678	689	686	635
		Mean	469	417	466	493	431	390	385	438	450	502	523	451
		Std	94	79	112	95	85	112	128	103	154	115	110	108
	L3	Min	262	252	196	248	162	183	144	242	165	108	283	204
		Max	734	662	775	736	693	639	858	717	805	727	794	740
		Mean	434	412	473	524	361	393	420	438	515	326	494	435
		Std	161	126	177	152	175	142	246	151	219	183	143	170
Groundnut	L1	Min	349	344	354	305	349	334	357	365	358	406	345	351
		Max	730	602	692	634	599	594	668	693	638	694	645	653
		Mean	541	478	537	497	458	454	512	523	490	564	507	506
		Std	112	76	99	106	74	76	105	97	84	85	93	91
	L2	Min	345	338	365	298	326	308	251	307	308	342	305	317
		Max	718	574	674	613	562	613	670	662	622	737	636	644
		Mean	528	463	506	480	444	440	441	459	439	536	495	476
		Std	110	68	92	105	73	88	135	107	93	108	99	98
	L3	Min	283	361	254	282	171	203	234	264	228	117	177	234
		Max	836	681	816	733	662	707	930	866	832	671	702	767
		Mean	507	489	542	531	352	474	512	528	485	350	464	476
		Std	197	107	181	140	161	153	248	190	197	194	171	176
Sorghum	L1	Min	254	258	240	246	214	265	215	282	242	323	334	261
		Max	643	599	644	614	568	500	667	597	601	662	575	606
		Mean	489	434	475	442	420	381	477	441	442	471	483	450
		Std	124	111	125	125	105	69	150	98	117	115	83	111
	L2	Min	254	256	239	246	213	203	185	235	228	254	331	240
		Max	636	581	643	573	563	477	578	594	564	657	615	589
		Mean	484	424	478	418	416	361	340	402	382	434	494	421
		Std	122	105	127	109	103	95	131	119	108	138	87	113
	L3	Min	202	274	223	219	156	134	156	182	252	57	245	191
		Max	715	620	767	745	651	575	694	765	671	577	631	674
		Mean	473	420	457	403	385	358	391	405	422	227	429	397
		Std	172	104	168	153	165	151	178	175	133	174	118	154

L. Seasonal average ETI derived from WaPOR for the major crop in the winter season.

			2009	2010	2011	2012	2013	2014	2015	2016	2017	2018	2019	Avg
Onion	L1	Min	149	177	183	192	200	229	194	287	313	314	224	149
		Max	637	610	624	640	677	652	689	727	679	721	666	637
		Mean	384	373	395	393	441	425	445	515	526	546	444	384
		Std	134	129	121	139	150	128	140	127	106	115	129	134
	L2	Min	149	177	179	192	185	244	203	260	255	312	215	149
		Max	569	574	554	603	668	682	683	733	713	876	665	569
		Mean	372	358	379	369	433	400	400	499	487	533	423	372
		Std	125	116	104	122	145	123	135	140	114	153	128	125
	L3	Min	180	216	119	134	112	155	127	219	172	89	152	180
		Max	737	615	910	741	883	729	877	906	774	677	785	737
		Mean	433	406	452	336	479	389	486	569	451	409	441	433
		Std	161	123	210	182	238	175	210	210	182	181	187	161
Wheat	L1	Min	154	138	168	133	145	188	135	187	212	290	175	154
		Max	584	620	621	544	577	677	657	782	712	750	652	584
		Mean	333	313	337	281	361	375	363	483	463	485	379	333
		Std	117	141	135	118	136	147	136	169	133	133	136	117
	L2	Min	147	151	114	130	165	154	105	174	174	232	154	147
		Max	533	588	612	517	573	683	551	841	797	833	653	533
		Mean	317	304	319	272	360	320	311	453	426	469	355	317
		Std	106	128	139	109	128	155	131	182	168	178	142	106
	L3	Min	193	184	130	103	121	158	122	140	97	78	133	193
		Max	762	632	718	528	825	773	876	989	814	842	776	762
		Mean	400	347	419	253	375	370	431	493	426	294	381	400
		Std	165	132	172	119	208	184	212	244	195	211	184	165
Pigeonpea	L1	Min	167	187	150	178	193	210	189	240	265	254	203	167
		Max	558	571	631	526	593	663	655	697	677	779	635	558
		Mean	323	337	317	303	343	354	340	412	431	451	361	323
		Std	125	128	136	99	119	113	142	135	123	138	126	125
	L2	Min	170	175	150	178	205	172	161	188	197	242	184	170
		Max	550	563	595	525	588	688	743	826	713	889	668	550
		Mean	317	322	310	294	342	328	316	390	431	459	351	317
		Std	118	129	128	96	114	142	167	168	146	170	138	118
	L3	Min	190	227	123	100	103	149	115	129	81	90	131	190
		Max	768	709	643	715	862	674	804	933	688	763	756	768
		Mean	446	387	308	306	321	364	388	439	334	364	366	446
		Std	177	150	156	160	217	170	221	239	188	194	187	177